
Marine Physical Laboratory

MDA AEL Error Analysis

**E.D. Wolin, D.E. Ensberg, S. Escher, J.
Murray, and W.S. Hodgkiss**

Supported by the
Office of Naval Research
Contract N00014-89-D-0142(DO#1)

19950310 042



MPL Technical Memorandum 438

**MPL-U-15/94
January 1994**

Approved for public release; distribution is unlimited.



University of California, San Diego
Scripps Institution of Oceanography

MDA AEL Error Analysis

E. D. Wolin, D. E. Ensberg, S. Escher, J. Murray, and W. S. Hodgkiss

Marine Physical Laboratory
Scripps Institution of Oceanography
San Diego, CA 92152-6400

ABSTRACT

The following report summarizes the types and effects of errors in navigating the tripod array deployed in the Northwest Atlantic in July 1991. We argue that the overall root mean squared error (RMSE) in navigating array element positions is less than 2 m (one and two leg data) and 4 m (three leg data).

Accession For	
NTIS	CRA&I <input checked="" type="checkbox"/>
DTIC	TAB <input type="checkbox"/>
Unannounced	<input type="checkbox"/>
Justification _____	
By _____	
Distribution / _____	
Availability Codes	
Dist	Avail and/or Special
A-1	

REPORT DOCUMENTATION PAGE

Form Approved
OMB No. 0704-0188

Public reporting burden for this collection of information is estimated to average 1 hour per response, including the time for reviewing instructions, searching existing data sources, gathering and maintaining the data needed, and completing and reviewing the collection of information. Send comments regarding this burden estimate or any other aspect of this collection of information, including suggestions for reducing this burden, to Washington Headquarters Services, Directorate for Information Operations and Reports, 1215 Jefferson Davis Highway, Suite 1204, Arlington, VA 22202-4302, and to the Office of Management and Budget, Paperwork Reduction Project (0704-0188), Washington, DC 20503.

1. Agency Use Only (Leave Blank).		2. Report Date. January 1994	3. Report Type and Dates Covered. MPL Technical Memorandum	
4. Title and Subtitle. MDA AEL Error Analysis			5. Funding Numbers. N00014-89-D-0142 (D0#1)	
6. Author(s). E.D. Wolin, D.E. Ensberg, S. Escher, J. Murray, and W.S. Hodgkiss			Project No. Task No.	
7. Performing Monitoring Agency Name(s) and Address(es). University of California, San Diego Marine Physical Laboratory Scripps Institution of Oceanography San Diego, California 92152-5000			8. Performing Organization Report Number. MPL TM-438 MPL-U-15/94	
9. Sponsoring/Monitoring Agency Name(s) and Address(es). Chief of Naval Research Ballston Tower One 800 North Quincy Street Arlington, VA 22217-5660 (Code 321)			10. Sponsoring/Monitoring Agency Report Number.	
11. Supplementary Notes.				
12a. Distribution/Availability Statement. Approved for public release; distribution is unlimited.			12b. Distribution Code.	
13. Abstract (Maximum 200 words). The following report summarizes the types and effects of errors in navigating the tripod array deployed in the Northwest Atlantic in July 1991. We argue that the overall root mean squared error (RMSE) in navigating array element positions is less than 2 m (one and two leg data) and 4 m (three leg data).				
14. Subject Terms. Array navigation, transponder navigation, tripod array, RMSE, signal processing.			15. Number of Pages. 88	
			16. Price Code.	
17. Security Classification of Report. Unclassified	18. Security Classification of This Page. Unclassified	19. Security Classification of Abstract. Unclassified		20. Limitation of Abstract. None

Table of Contents

I. Introduction

- a) Purpose
- b) Survey and Array Geometry

II. Transponder Survey Error

- a) How transponder navigation was done
- b) Sources of errors
- c) Decomposition of error into random and bias components

III. Array Navigation Error

- a) How array navigation was done
- b) Sources of errors
- c) Decomposition of error into random and bias components

III. Conclusions

- a) Estimates of array element bias and random error

IV. Present/ Future Considerations

Appendix A - MDA-I transponder navigation bias error

Appendix B - Raw slant range plots

Appendix C - Bias correction plots

Appendix D - How ray trace corrections affect transponder positioning

Figures

Figure 1	Navigation of the '91 MDA-I array elements
Figure 2	MDA-I transponder survey
Figure 3	MDA-I navigation errors
Figure 4	AEL simulations
Figure 5	Why bias correction works
Figures 6 A->C	Standard deviations of highpassed X,Y,Z AEL data
Figures 7 A->E	Standard deviations of highpassed transponder slant ranges
Figure 8	High pass filter used in figures 6, 7
Figures 9 A->I	How perturbed transponder positions affect array positions
Figure 10	Slant range error decomposition into bias and random components
Appendix A	Sound speed profile plot, one perturbed by +0.9 m/s
Appendix B	Raw slant range plots for all days and transponders
Appendix C	Bias correction plots
Appendix D	How ray trace corrections move transponders radially outward

Introduction

The purpose of this report is to estimate how much navigational error there is in the MPL '91 MDA-1 tripod array positions. Sources and types of errors are summarized and their magnitudes estimated. How array positions were influenced by these errors is then discussed.

The geometry of the array and the surrounding transponder net is shown in Figures 1 and 2. The navigation of the array was done in two steps. First the transponders were surveyed in. Then in a second step these "known" transponder positions were used to navigate in the array elements. Figure 3 provides a summary of error sources for each.

Figure 1 shows how the tripod array was navigated using known transponder positions. The geometric picture of how the transponder survey was done is similar to Figure 1, but without the tripod array and with two more transponders (which subsequently failed). For both the ship interrogated the various transponders in a round robin fashion and recorded the transponder replies back at the ship.

I. Transponder Survey Error

In the transponder survey the ship moved slowly along the course described by the dots in Figure 2. A transponder was interrogated every ten seconds, an entire ping sequence occurring every two minutes. The following procedure was used to navigate the transponders:

1. The recorded round trip travel times were interpolated to align the different transponders on two minute boundaries.
2. The transponder turn around time and receiver recognition time were subtracted.
3. These round trip travel times were halved to yield one way travel times.
4. These one way travel times were multiplied by their appropriate harmonic mean sound speeds and a small time delay added to account for ray bending. (See Appendix D for an explanation of how corrections were made to account for ray bending.)
5. These data were input into a non-linear least squares (Marquardt) algorithm where the various ship transducer positions (X and Y only as transducer depth was known) and seven (assumed fixed) transponder (X,Y,Z) locations were estimated.

It is not possible to decompose or estimate the random or deterministic components of the transponder positional error directly from the data. This is because the ship is not stationary hence neither are the slant ranges from the ship to the transponders.

Random slant range errors during the transponder survey are estimated to be less than two meters RMS. This estimate was obtained from physical considerations, the components of which are discussed in Figure 3.

These random slant range errors propagate as much smaller errors ($< 1/2$ meter RMS) when estimating transponder positions, see Figure 4A. This simulation demonstrates that most of the random slant range errors cancel themselves rather than contaminating the transponder position estimates due to the many ship positions each derived via triangulation from the various transponders.

Bias errors are the largest source of transponder navigation error. Furthermore, there is no known reference, say a known transponder depth with which to calibrate the bias. Hence these bias errors have been bounded using physical considerations. It is possible however to remove much of the bulk bias in the transponder positions when navigating the array elements. Viewing Figure 1, the transponders are shown to have a lensing effect where moving them outward radially has the same effect as if the transponders were held fixed and the slant ranges shortened roughly equally. This shortening of the slant ranges would cause the array to be translated, primarily downward due to the roughly symmetric transponder placement. The bias errors are caused primarily by error in estimating sound speed precisely combined with any unknown system bias error. The system bias error is a second order concern as the Sonatech system was carefully calibrated. Error due to ray bending is also a second order concern as this was estimated and corrected for via table lookup (see Appendix D).

As sound speed error is the primary source of error an upper bound was estimated as well as the effect this upper bound would have on transponder navigation.

This upper bound caused less than one meter/second error in the harmonic means used to convert the travel times into slant ranges. A one meter/second error in harmonic mean causes less than 1.2 meters of differential slant range error; that is error that isn't radially the same for all transponders and hence correctable when navigating array elements (see Appendix A). There is much more bias in a common/bulk bias due to the symmetric way that the survey was done. In fact this bulk bias is estimated to be about seven meters of primarily radial transponder motion. However, this is corrected when the transponder positions are used to navigate array elements as discussed below.

An attempt was also made to estimate unknown system bias error by varying bias numbers as is done below when navigating array elements. Unfortunately this attempt at bias cancellation failed for the transponder survey as the ship was not stationary and reducing slant ranges continually reduces the RMS error. However as is discussed below most of the bulk bias (the portion propagated by the incorrect common radial motion of the transponders) was eliminated during array navigation.

II. Array Navigation Error

In order to localize the array elements the following procedure was used:

1. To get slant range travel times from the transponders to the array elements the travel time from the ship to a transponder was subtracted from the "round trip" travel time from the ship to a transponder to an array element (the travel time recorded at the array element).

2. The ship to transponder time was computed from the round trip travel time collected at the ship by $ST = (SRTT - TAT - SRR)/2$, where SRTT is the round trip travel time from the ship to the transponder and then to the array, TAT is the transponder turn around time delay and SRR the ship receiver recognition time delay.
3. Then $(RTT - ST - TAT - ARR)$, where ARR is the array receiver recognition time, was used to compute the travel times from transponder to array element.
4. This transponder to array element travel time was multiplied by its harmonic mean sound speed and a small travel time was added to correct for ray bending.
5. These data were then input into a non-linear least squares (Marquardt) algorithm where the various AEL (X,Y,Z) positions were estimated using the slant ranges and the previously derived transponder positions.

AEL (Array Element Localization) error consists of a combination of errors from both the transponder positioning and then the array positioning based on these transponder positions. Both sources of error may be decomposed into random and deterministic (bias) components.

Unlike the slant range error in the transponder survey the error in the slant ranges from the transponders to the array elements is easy to view and analyze since the array motion is quite stationary. This error is similarly decomposed into random and deterministic components and both bounded by empirical and practical considerations. Furthermore, much of the deterministic component may be removed. The portion of the deterministic component that may be removed is the combination/ sum of the common radial bias in the transponder positions with the common slant range bias.

The random slant range error was bounded by trend removal (high pass filtering) then the resulting high frequency "jitter" examined. Some of this "jitter" was caused by actual array motion; still this provides an upper bound. This random error in the transponder to array element slant ranges is estimated to be one to two meters RMS. This is plotted across time in the "Standard deviations of slant ranges" plots (Figures 7A - 7E). A bound based on physical considerations is also given in Figure 3. Studying the description above as to how the slant ranges are calculated, the random slant range error consists of only 1/2 the random error in the transponder turn-around-time and 1/2 the random receiver recognition error at the ship as well as the random receiver recognition error at the array.

Simulations show that AEL positions are affected by random slant range error (error in all slant ranges) by roughly the magnitude of the error. For example adding random errors of one meter RMS to all five slant ranges move an array element on average about one meter RMS, see Figure 4B. Figures 9A-9I describe how any transponder's X, Y or Z motion would affect AEL positioning. In particular they suggest that an incorrect transponder position affect the array by less than two-thirds of the magnitude of the error. Figure 4C examines how random error in all the transponder positions affects array navigation. It demonstrates that array navigation errors are approximately on the order of the random transponder position error. Figure 4D suggests that bias error in slant ranges affects AEL on about the order of the slant range error. Note that most of the error is in incorrectly estimating the depth due to the roughly symmetrical transponder positions.

The AEL bias error consists of error produced by having incorrect transponder positions combined with errors caused by an incorrect sound speed when computing harmonic means/ray trace corrections (from the transponders to the array elements) as well as any unknown system delay in either the ship recognition circuit (negligible) or the array recognition circuit. Incorrect transponder positions are shown in Appendix A to contribute about 1.2 meters of differential slant range error. The different transponder (to a fixed array element) slant ranges are over very similar depths, hence incorrect sound speed bias is almost exactly the same for the different slant ranges. The system delay is also a bulk bias that is identical for all transponder slant ranges.

By averaging over long sequences, slant range random error was removed, and aggregate AEL bias error estimated. The bias error in the slant ranges was estimated by subtracting a constant from all slant ranges and looking for a "best" least squares fit over different such constants. Using this technique most of the common/bulk bias was removed. This common bias is the combination of the aggregate bias in slant ranges that is common for all five slant ranges, combined with the common radial bias in the placement of the transponders. This could be done as there was redundancy (i.e. five transponders ranged to each element requiring three estimated parameters: X, Y, and Z) and the geometry consisted of a roughly vertical/upward slant range combined with four more horizontal (35-60 degrees from vertical) slant ranges (see Figure 5). This bulk bias was estimated to be seven to nine meters depending on array configuration; these lengths were subtracted from all slant ranges.

Remaining uncorrected aggregate bias (in slant ranges and incorrect transponder positions) is estimated to be less than three meters and by simulation to affect array navigation by less than two meters (absolute). This number was derived heuristically by adding the worst-case array positioning errors from the two sources of AEL bias error: the differential transponder positions and the differential bias errors in the slant ranges.

There are also several additional errors which are of second order importance:

1) Transponder (conical) motion may translate the array slightly over time (since local currents should be very similar for the 5 transponders). With an estimated bottom current of 10 cm/sec and a 30 m tether length these discussions are estimated to be on the order of < 1 m.

2) Sound speed variability (primarily in upper 50-100m) may cause slight bias error. All array navigation elements are below this upper level; hence the only time this upper region is used is for navigating the transponders where the travel path was from the ship's transducer (7m) to transponders which were approximately 5000 meters deep. Due to the very long travel paths the effect of the upper region variability is negligible.

3) Both additive and multiplicative biases exist. For example sound speed errors multiply whereas system delays add. Further these are measured as a sum hence we don't know how large each component is. However due to the geometry, the slant ranges are all of similar length, hence error due to correcting one way rather than the other is a second order effect.

Conclusions

AEL random errors appear to be on the order of one to two meters RMS, probably larger (estimated at twice this or three to four meters RMS) for the three legged data. The random component of the three legged data is difficult to estimate due to the low signal-to-noise ratio and the ten minute on/ twenty minute off ping cycle which produced inconsistent transponder reply detections (see Appendix B).

AEL bias error is estimated to be on the order of two meters (absolute). This was primarily caused by combined uncorrectable differential bias in transponder positions and slant ranges.

Present/Future Considerations

It is desirable to have a symmetrical transponder survey, that is to have ship positions symmetrically located about the transponders. Symmetric ship survey positions assure that the unknown bias (caused by inaccurately measured sound speed and any unknown hardware delays) will push the transponders radially in or out symmetrically. It is also important to collect slant ranges both when the ship is directly above the transponders and when the ship is far away (horizontally) from the transponders. Ship positions directly above a transponder yield depth information, while ship positions far from a transponder will yield information about the transponder in the X-Y plane to the extent that the slant ranges are horizontal (e.g. a 45 degree downward slant range would yield about the same information in Z as in X-Y).

Placing the transponders symmetrically about the array is also important. Having opposing pairs of transponders spaced equally in angle about the array assures that the bias will cause primarily depth errors which may be reduced via a central (upward or downward) transponder. This symmetry combined with an accurate array element depth estimate (say from a calibrated engineering depth sensor) pinpoints array depth, without having to rely on additive constants yielding a minimum mean square error (averaged over long time intervals to eliminate the random component). Knowing transponder depths accurately also simplifies the problem. Note that in MDA-I two of the transponders failed and the tripod array was placed slightly off center. Both of these changes adversely affected the symmetry.

Having redundant transponders is also desirable for two reasons. Navigation error caused by random slant range errors is reduced on the order of the number of transponders. Also having extra transponders allows for successful navigation if transponders fail (as two did in MDA-I). In general it is very desirable to have at least four transponders as these are used to estimate three parameters, each array element's (X,Y,Z) position. In MDA-I five transponders were used to navigate the array elements.

Jitter reduction, as was used in MDA-I, is also beneficial. Jitter reduction uses two interrogation frequencies which enhances a transponder's ability to more accurately detect the leading edge of the interrogation pulse. By using jitter reduction the largest source of random error, transponder turn-around-time, is significantly

reduced.

A known transceiver depth reduces by one the number of parameters to estimate in all least squares calculations. In MDA-I, this was achieved by using the hull mounted transducer on the USNS Lynch.

Acknowledgements

Dick Harriss and David Ensberg drew several of the descriptive figures. James Murray did the computer simulations in Figures 4A-E, David Ensberg in Figures 6-8 and Appendix C, and was also responsible for navigating much of the array. Sharon Escher was responsible for computing ray trace corrections, as well as the figures in Appendices C and D. This work was supported by the Office of Naval Technology under ONR contract #N000-14-89-D-0142.

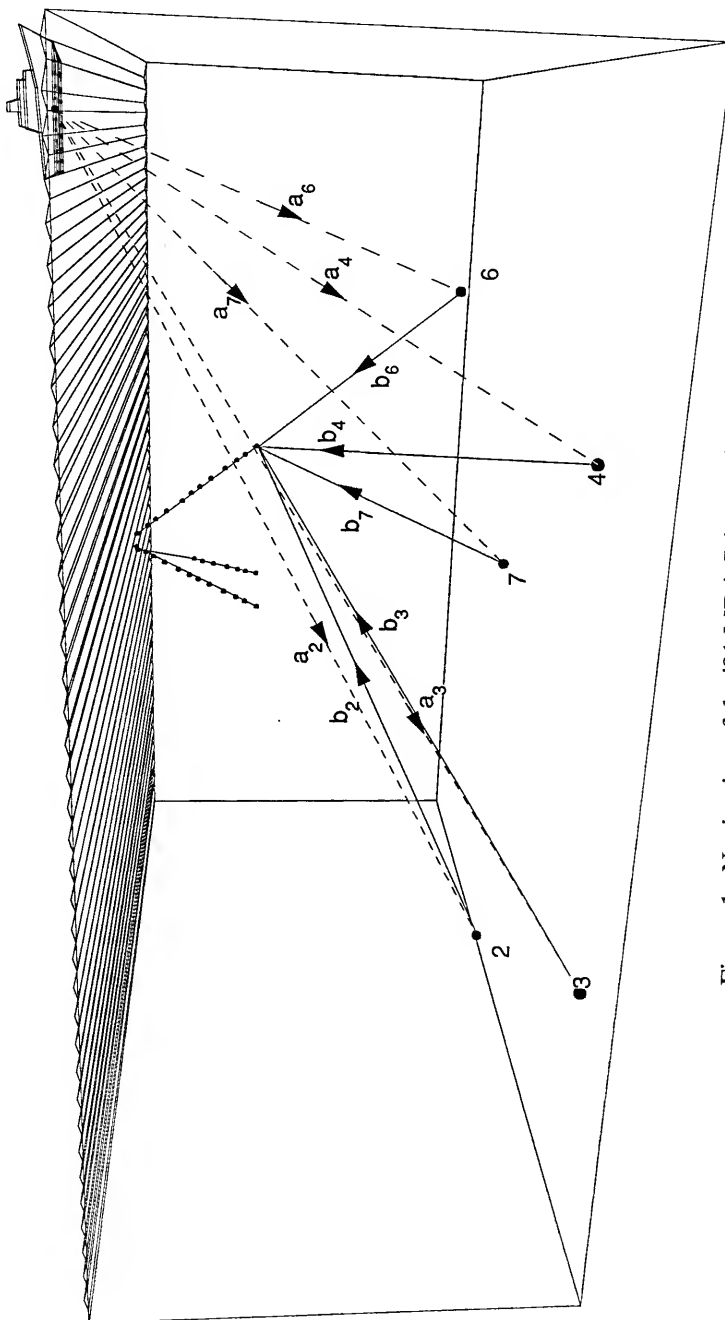


Figure 1 Navigation of the '91 MDA-I Array Elements

A ship (the USNS Lynch) pinged in a round robin to five transponders, denoted 2,3,4,6 and 7. The transponder replies were recorded both at the array and at the ship.

Figure 2

Transponder Survey MDA-I

Ship track and final transponder positions

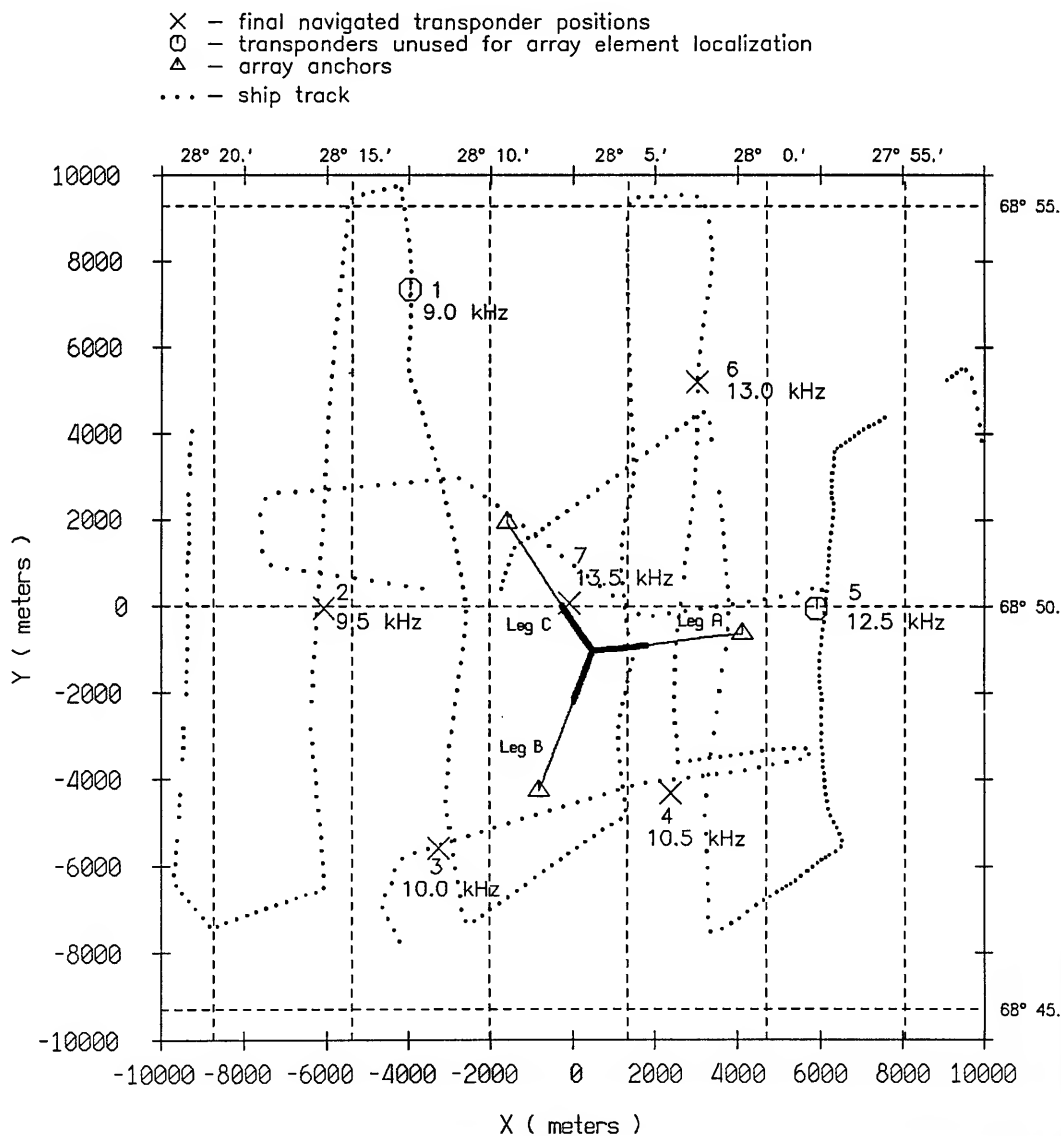
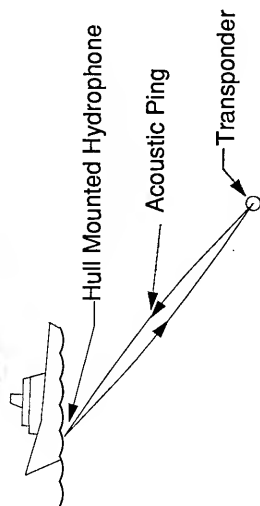


Figure 3 MDA-I Navigation Errors

TRANSPONDER SURVEY ERRORS



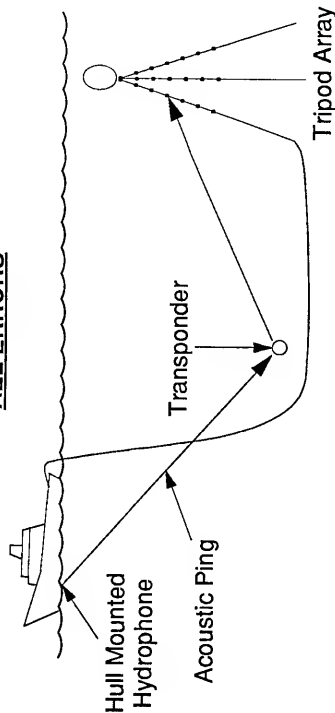
Random Errors

<u>Source of Error</u>	<u>Estimated Error</u>
Transponder Turn-Around-Time/2	= .2 ms
Ship Receiver Recognition Time/2	< .5 ms
Total:	$\frac{< .7 \text{ ms}}{\text{(worst case } \sigma < 2 \text{ m)}}$

Bias Errors

<u>Source of Error</u>	<u>Estimated Error</u>
Sound Speed	.8 m/s
Refraction + Hardware	< .1 m/s
A 1m/s error yields < 1.2 m differential slant range error for all array elements.	

AEL ERRORS



Random Errors

<u>Source of Error</u>	<u>Estimated Error</u>
Transponder Turn-Around-Time/2	= .2 ms
Array Receiver Recognition Time	< 1.5 ms
Ship Receiver Recognition Time/2	< .5 ms
Total	$\frac{< 2.2 \text{ ms}}{\text{(worst case } \sigma \approx 3 \text{ m)}}$

Bias Errors

<u>Source of Error</u>	<u>Estimated Error</u>
Incorrect transponder positions	< 1.2 m differential
Sound Speed	.8 m/s
Refraction	< .1 m/s
Hardware	< 3 m

Figures 4 A-E AEL Simulations

In the following simulations a geometry was used that matched the average geometry of the MDA-I transponders and tripod array. Ideal slant ranges were computed using these transponder and array positions. The array positions used were an average top, middle, and bottom element from each leg. The different lines on these plots correspond to results from these different elements. The specific element positions used were as follows:

Element Positions		X	Y	Z
Leg A:	element 1	519.4	-1009.1	158.9
	element 24	1143.5	-961.1	941.7
	element 48	1769.7	-894.7	1791.8
Leg B:	element 49	455.6	-1056.4	157.7
	element 72	222.7	-1644.2	939.6
	element 96	-4.0	-2213.8	1795.4
Leg C:	element 97	445.5	-976.7	160.0
	element 120	75.7	-479.3	962.9
	element 144	-281.0	28.3	1812.1

Figure 4A How Slant Range Errors Affect Transponder Positions

This simulation used the same ship positions and available slant ranges as the survey used to navigate in the MDA-I transponders. White Gaussian noise with variance specified on the X axis of this plot was added to all slant ranges. Input noise is reduced by a factor of nearly ten across all elements. This large reduction of error was due to cancellation of the noise due to the many ship positions, each of which was derived via pings from available transponders (up to seven since much of the survey occurred prior to transponders failing).

Figure 4B How Slant Range Errors Affect Array Locations

White Gaussian noise with the variance specified on the X axis was added to all slant ranges. The output array positional error is about the same as the input error across all elements. Errors in slant ranges are equally likely to either add constructively or cancel each other hence the array is moved by about the magnitude of the input noise.

Figure 4C How Random Transponder Positions Affect Array Locations

White Gaussian noise with the variance specified on the X axis was added to all transponder X,Y,Z's. The output Array positional error is about the same as the input error across all elements. Errors in transponder positions are equally likely to add constructively or cancel each other.

Figure 4D How Radial Noise Affects Array Locations

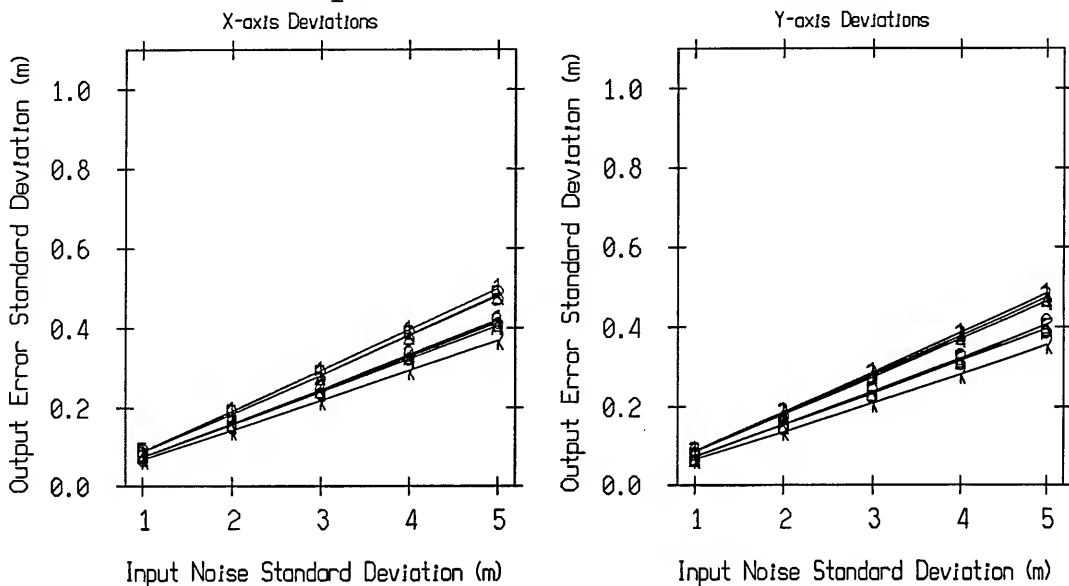
White Gaussian noise with the variance specified on the X axis was added in a radial direction to the transponder locations. Input noise is reduced by a factor of four in X and eight in Y, but Z errors are not reduced. This is reasonable due to the approximate symmetry of the transponders which causes cancellation of error in X and Y but not in Z. Since all transponders are located beneath the array, pushing the transponders up or down radially moves the array primarily up or down. Larger error propagation in X (compared to Y) is due to the somewhat asymmetrical transponder placement caused by the death of two transponders as well as the decision to place the array slightly off center and in a different configuration than originally intended (due to changes in the surface current direction as well as to avoid tangling the umbilical cable on a previously used anchor).

Figure 4E Sample Output Distribution Plot

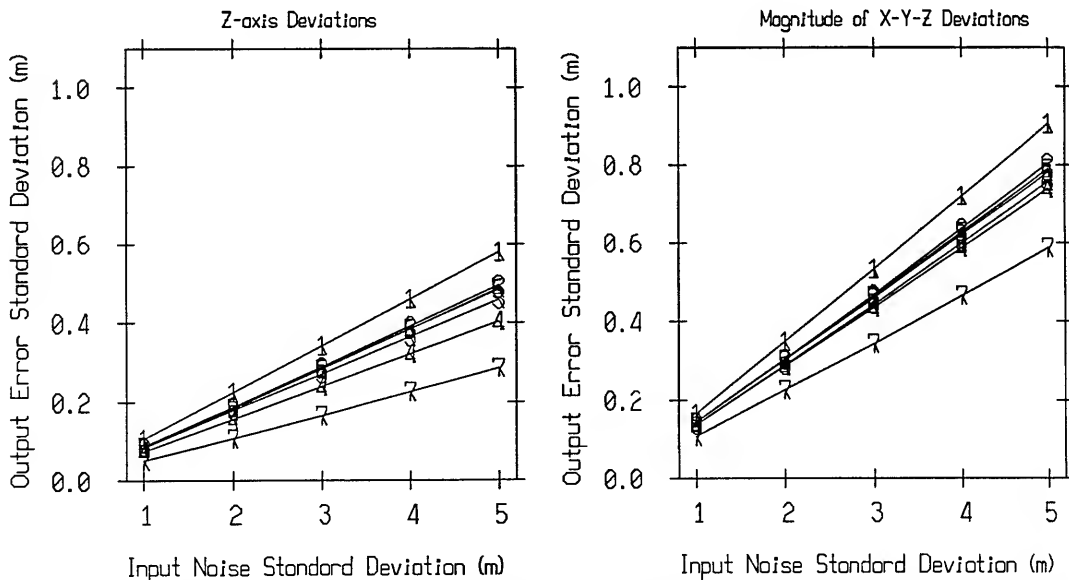
While many of these plots were generated only one is included in this report as the summary plots above more readily summarize the results. This is a sample of the output error distribution showing how an independent identically distributed Gaussian input distribution with a variance of one added to all five slant ranges influenced the positioning of element #1 (top element of leg A). Note this output distribution appears Gaussian with a variance of about one. The Gaussian nature is typical of all of the output distribution plots in these simulations although for some the output variance is more reduced than others.

Figure 4A

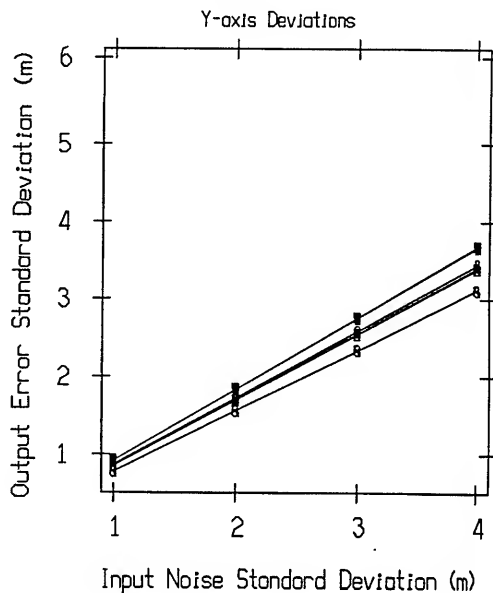
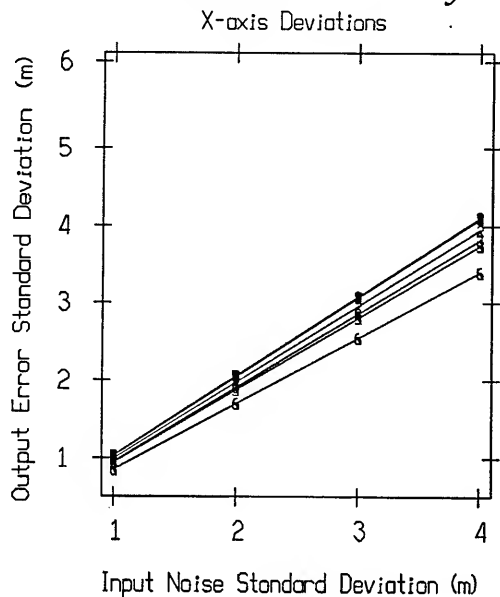
How Slant Ranges + Noise Affect Transponder Position Error



*Numbers on Graphs Represent Transponder Numbers
(See Figure 2 for Transponder Locations)*



How Slant Ranges + Noise Affect Array Position Error



#1: Top Leg A #4: Top Leg B #7: Top Leg C
 #2: Middle Leg A #5: Middle Leg B #8: Middle Leg C
 #3: Bottom Leg A #6: Bottom Leg B #9: Bottom Leg C

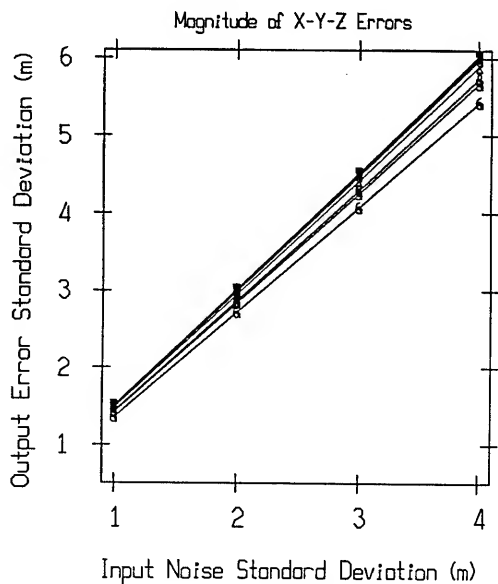
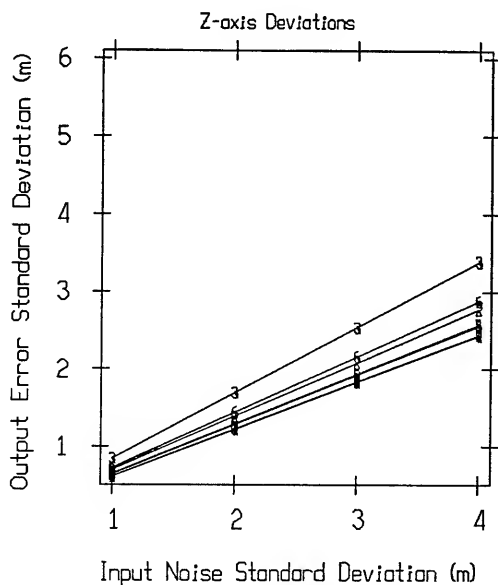
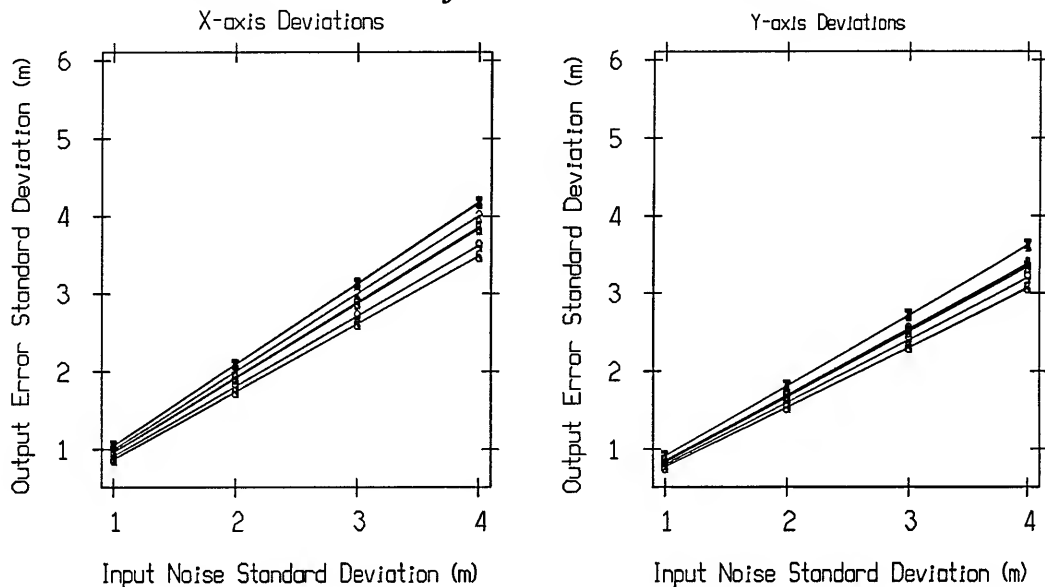
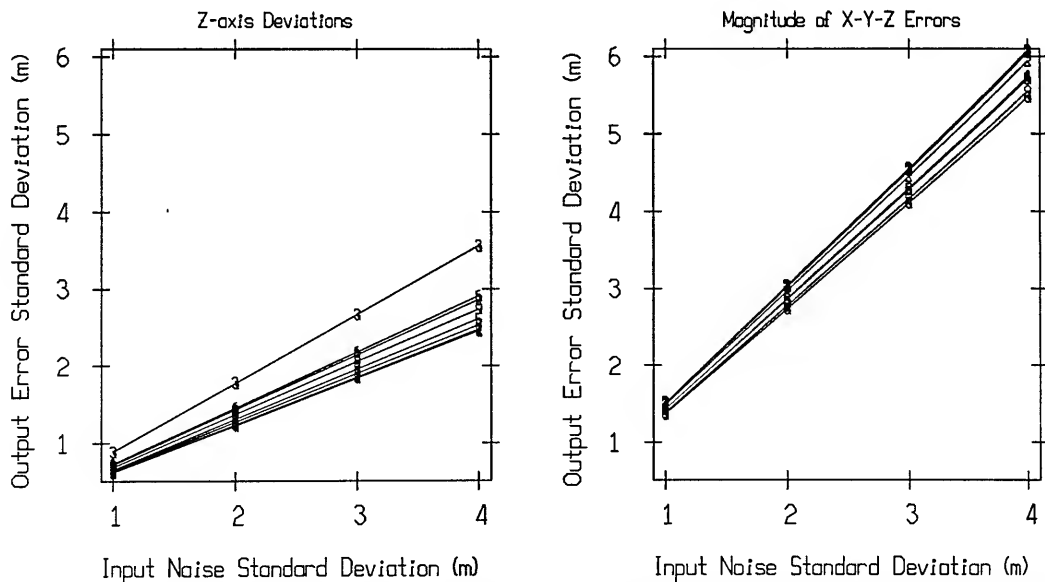


Figure 4C

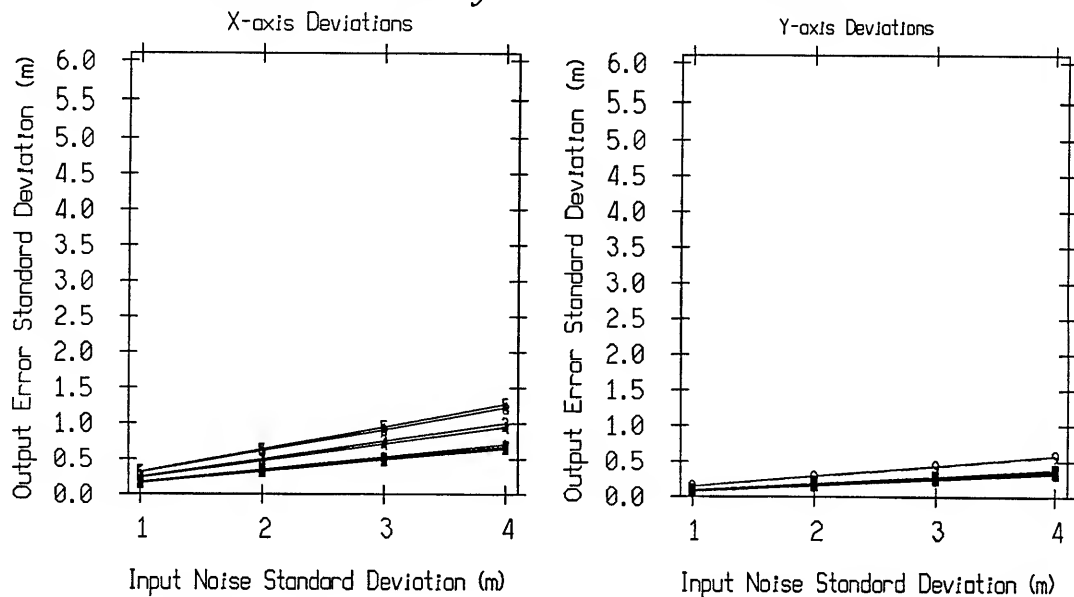
How Random Transponder Positions Affect Array Position Error



#1: Top Leg A #4: Top Leg B #7: Top Leg C
 #2: Middle Leg A #5: Middle Leg B #8: Middle Leg C
 #3: Bottom Leg A #6: Bottom Leg B #9: Bottom Leg C



How Radial Noise Affect Array Position Error



#1: Top Leg A #4: Top Leg B #7: Top Leg C
 #2: Middle Leg A #5: Middle Leg B #8: Middle Leg C
 #3: Bottom Leg A #6: Bottom Leg B #9: Bottom Leg C

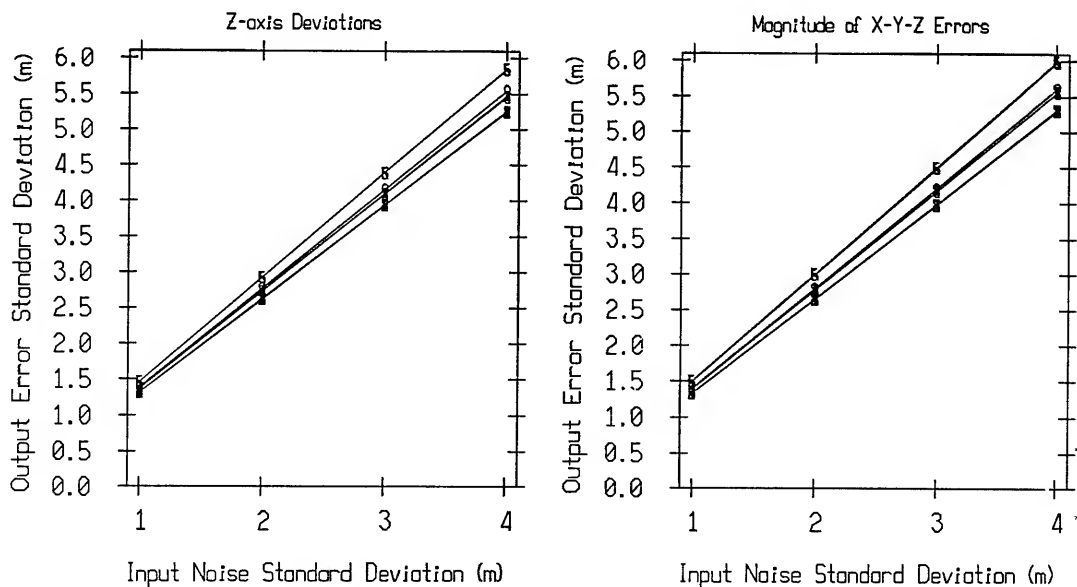


Figure 4E

Slant Ranges + Noise [N(0,1)]
Element #1 (3 leg mean)

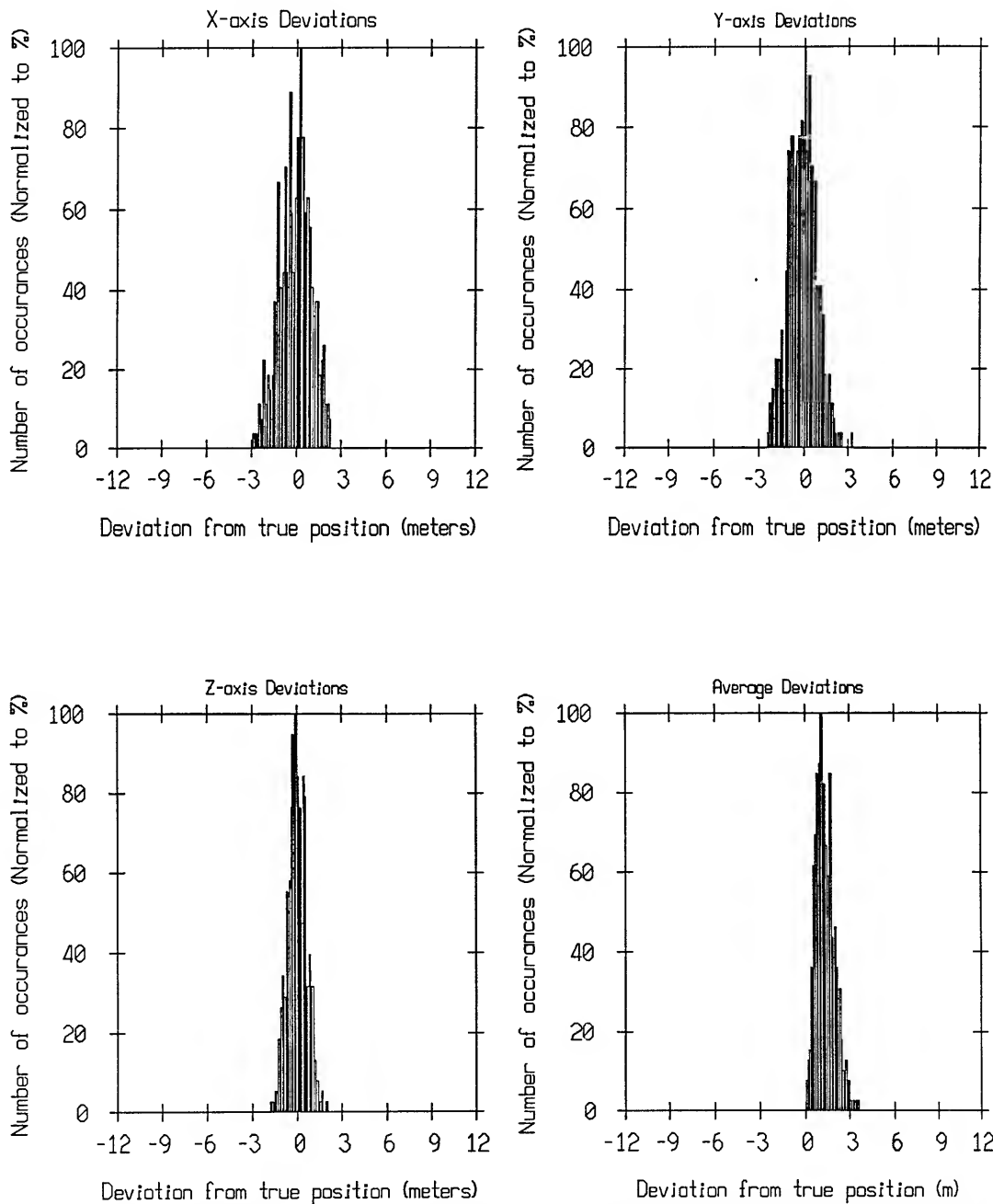
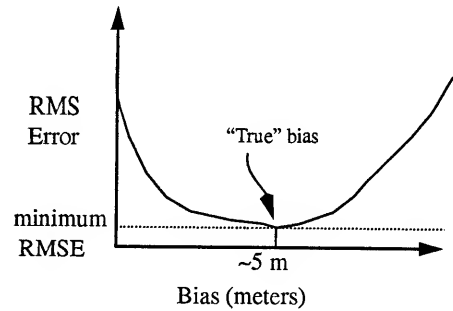
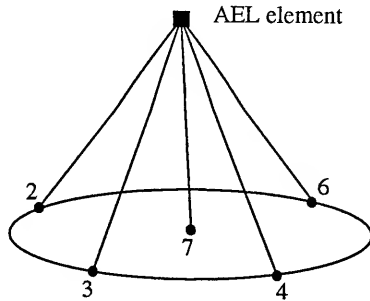
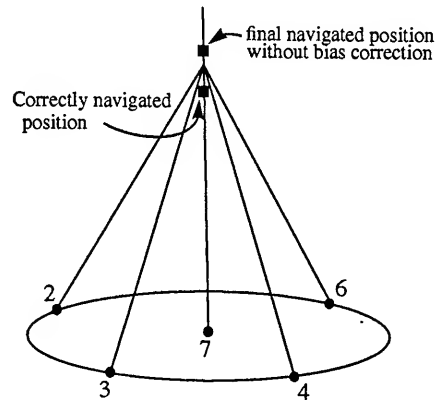
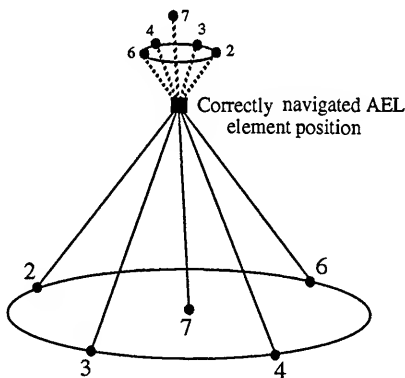


Figure 5



The ray paths from transponders 2,3,4 and 6 to an AEL element are roughly in opposing pairs and ~35 - 60 degrees from vertical, whereas the ray path from transponder 7 (beneath the array) to the AEL element is nearly vertical. Note the geometry has been idealized to better illustrate the effects of bias.

Because of this geometry it is possible to estimate the bulk bias (i.e. bias common to all slant ranges) by reducing the slant ranges by a common amount until the RMSE is minimized. This required subtracting ~ 5 meters of correction.



For example given a correctly navigated array element and slant ranges that are all artificially extended by 5 m, the above figure shows where the true navigated position should be along with an exaggerated 5 m bias added to each slant range. Note the geometry has been idealized to better illustrate the effects of bias.

When the bias is not corrected for, the ray paths no longer intersect at a point. Four of the five rays converge to (roughly) the same place, now above the correctly navigated array element. The fifth ray due to the geometry extends further above the other rays, thus causing the larger RMSE and raising the element depth incorrectly. Note that the bias is exaggerated and the geometry has been idealized to better illustrate the effects of bias.

Figures 6 A-C

These figures are time series of the standard deviations of highpassed AEL data for the X, Y and Z axis respectively. They were generated by taking the corresponding time series of X, Y, or Z for each navigated array element, convolving it with the high pass filter shown in Figure 8 and then taking the standard deviation of the result.

Figures 7 A-E

These figures are time series of the standard deviations of highpassed AEL data for the five working transponders. They were generated by taking the corresponding time series (slant range from each transponder to navigated array element), convolving it with the high pass filter shown in Figure 8 and then taking the standard deviation of the result.

Figure 8

This is a figure of the frequency response of the high pass filter used in creating figures 6 A-C and 7 A-E.

Figure 6A

Standard Deviation of (highpassed) AEL
1, 2, and 3 leg cases x axis

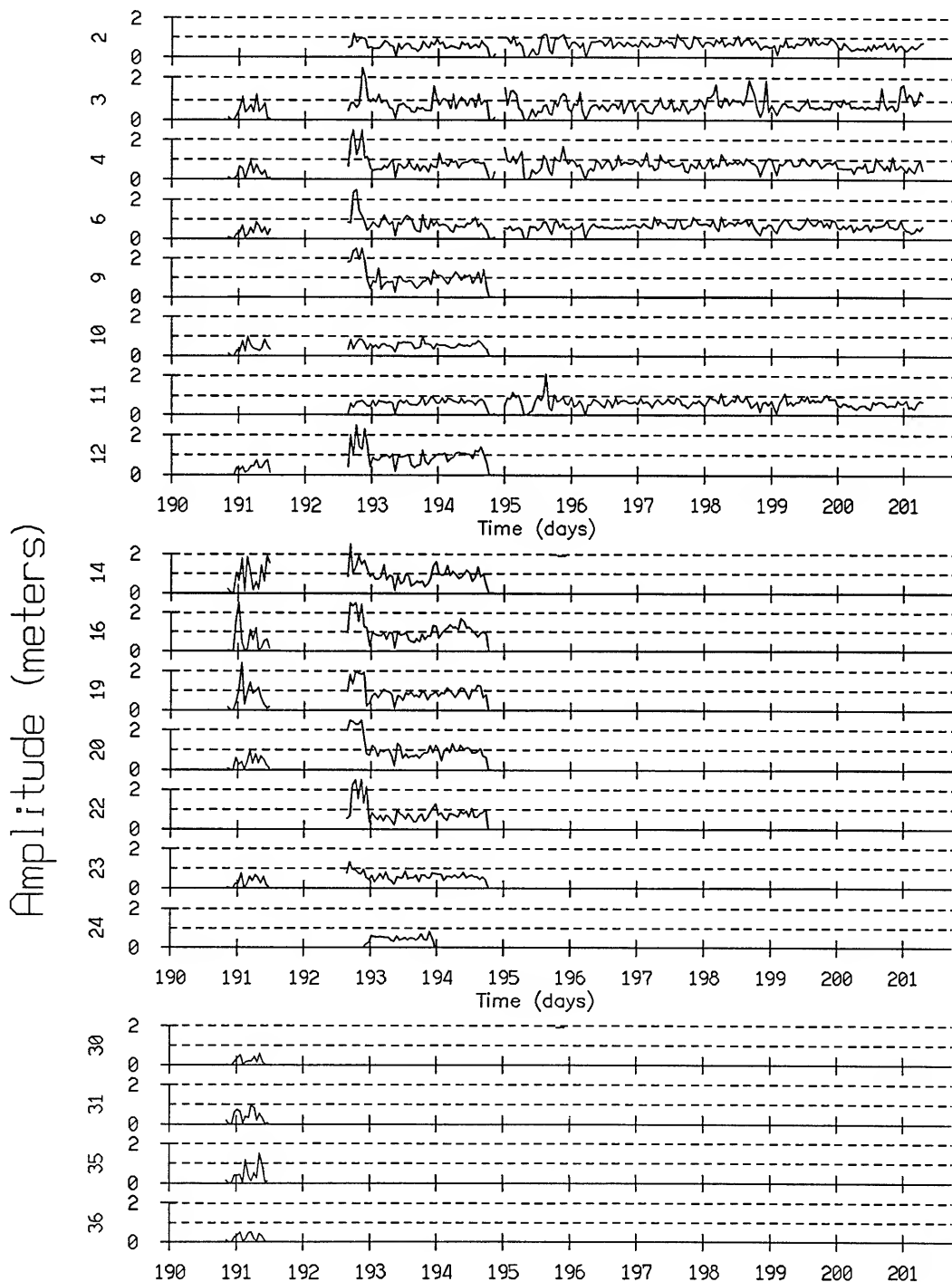


Figure 6B

Standard Deviation of (highpassed) AEL
1, 2, and 3 leg cases y axis

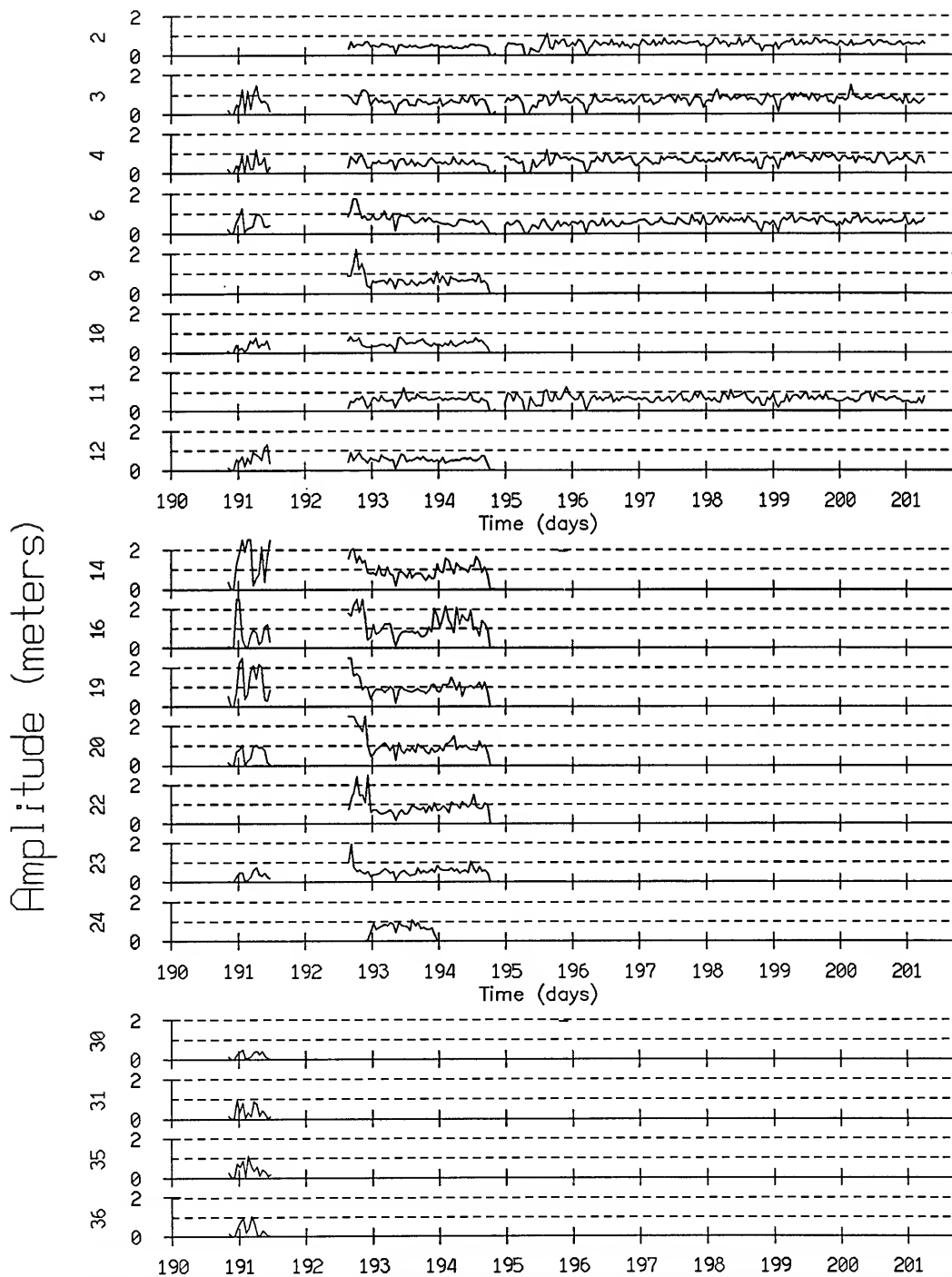


Figure 6C

Standard Deviation of (highpassed) AEL
1, 2, and 3 leg cases z axis

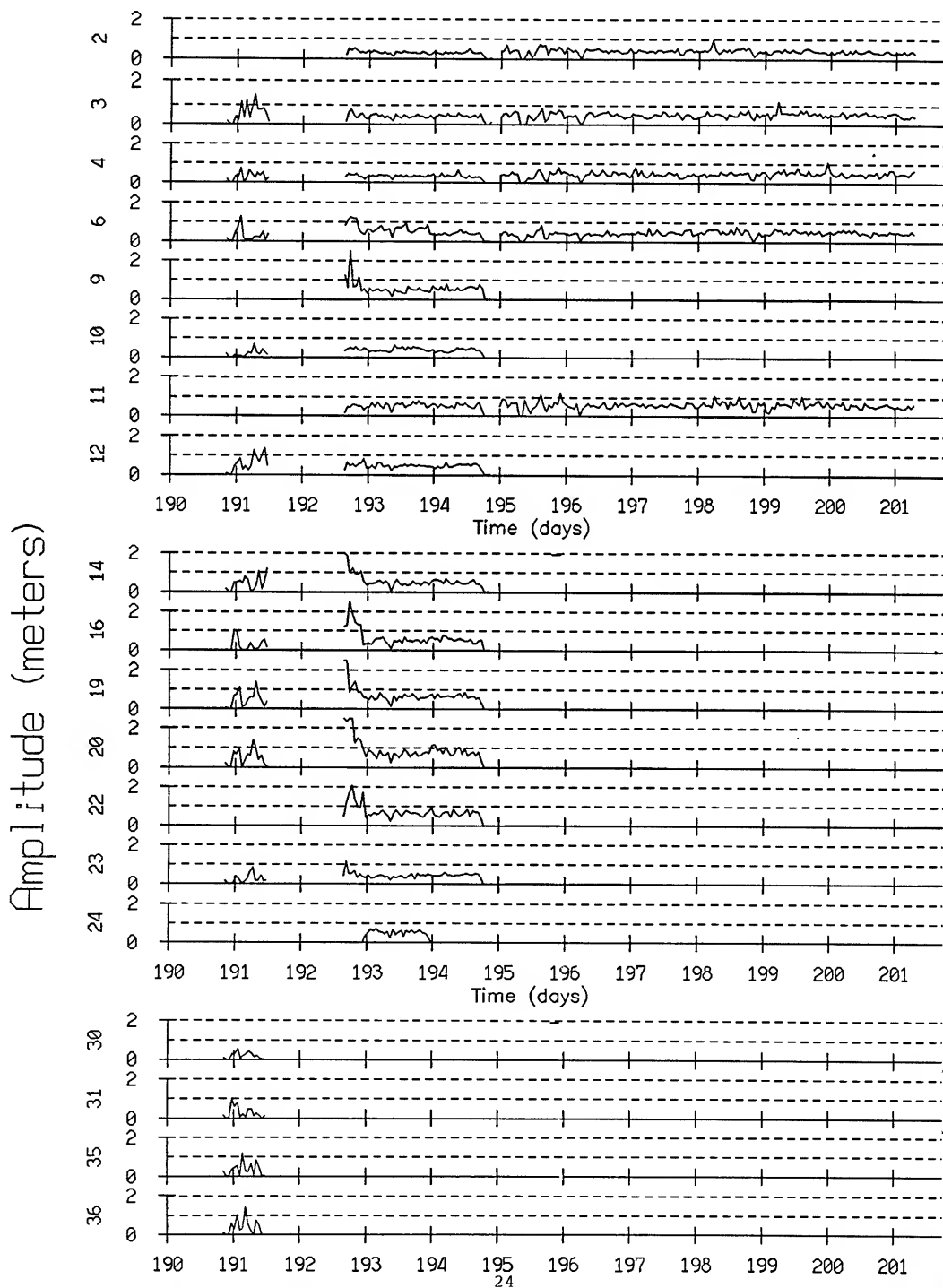


Figure 7A

Standard Deviation of (highpassed) 9500 Hz Slant Ranges
Each sample represents a 1 hr. average, $f_s = 2$ min.

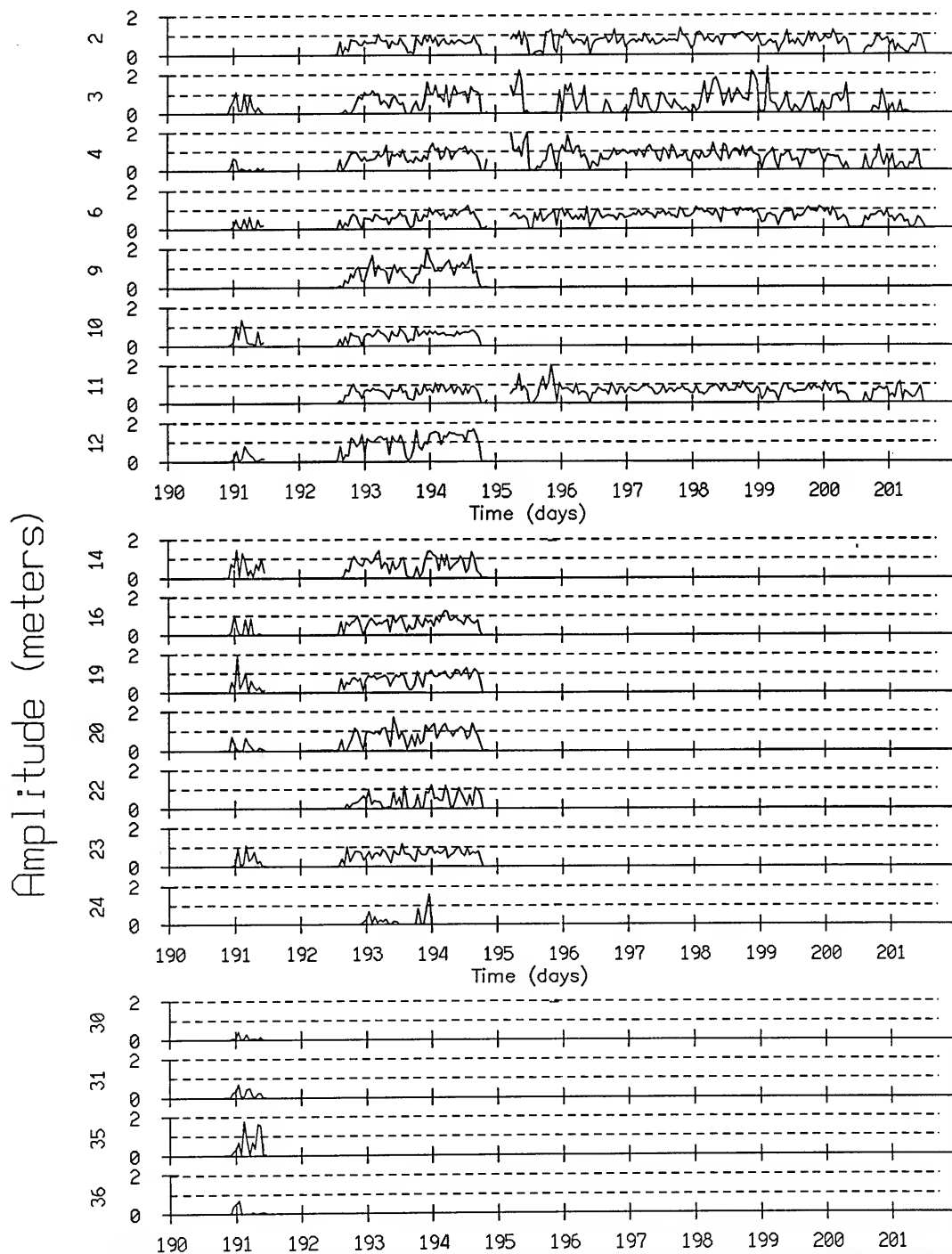


Figure 7B

Standard Deviation of (highpassed) 10000 Hz Slant Ranges
Each sample represents a 1 hr. average, $f_s = 2$ min.

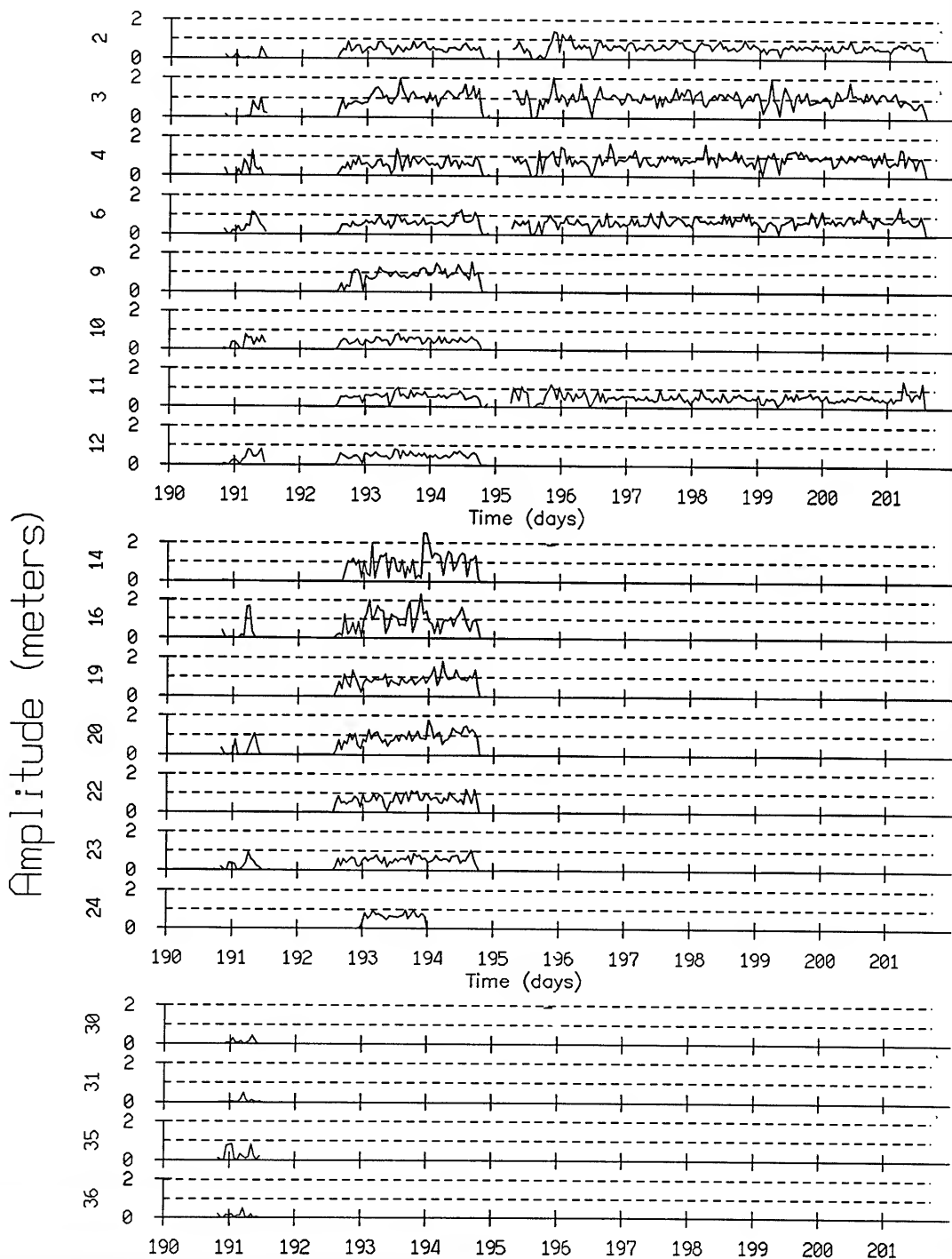


Figure 7C

Standard Deviation of (highpassed) 10500 Hz Slant Ranges
Each sample represents a 1 hr. average, $f_s = 2$ min.

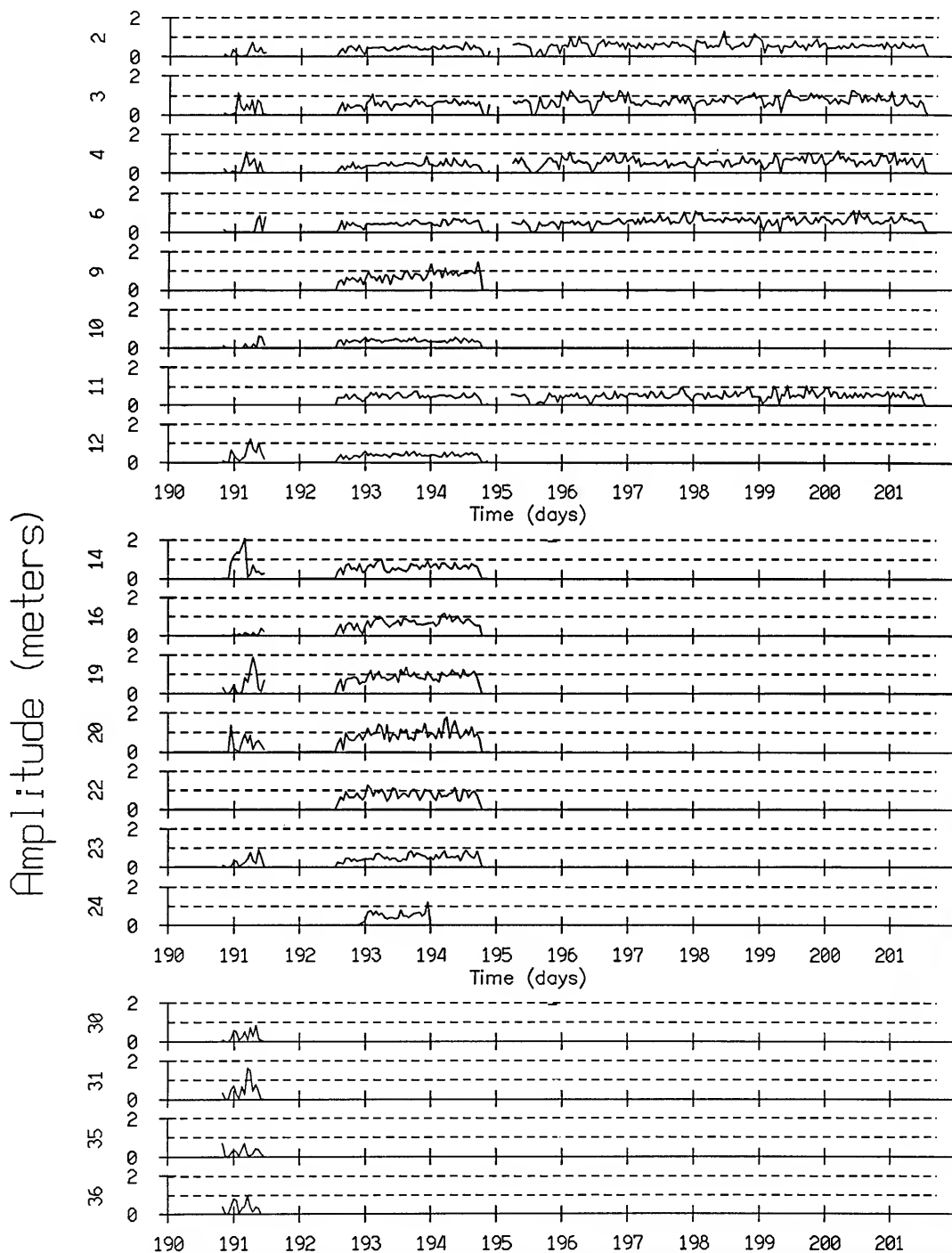


Figure 7D

Standard Deviation of (highpassed) 13000 Hz Slant Ranges
Each sample represents a 1 hr. average, $f_s = 2$ min.

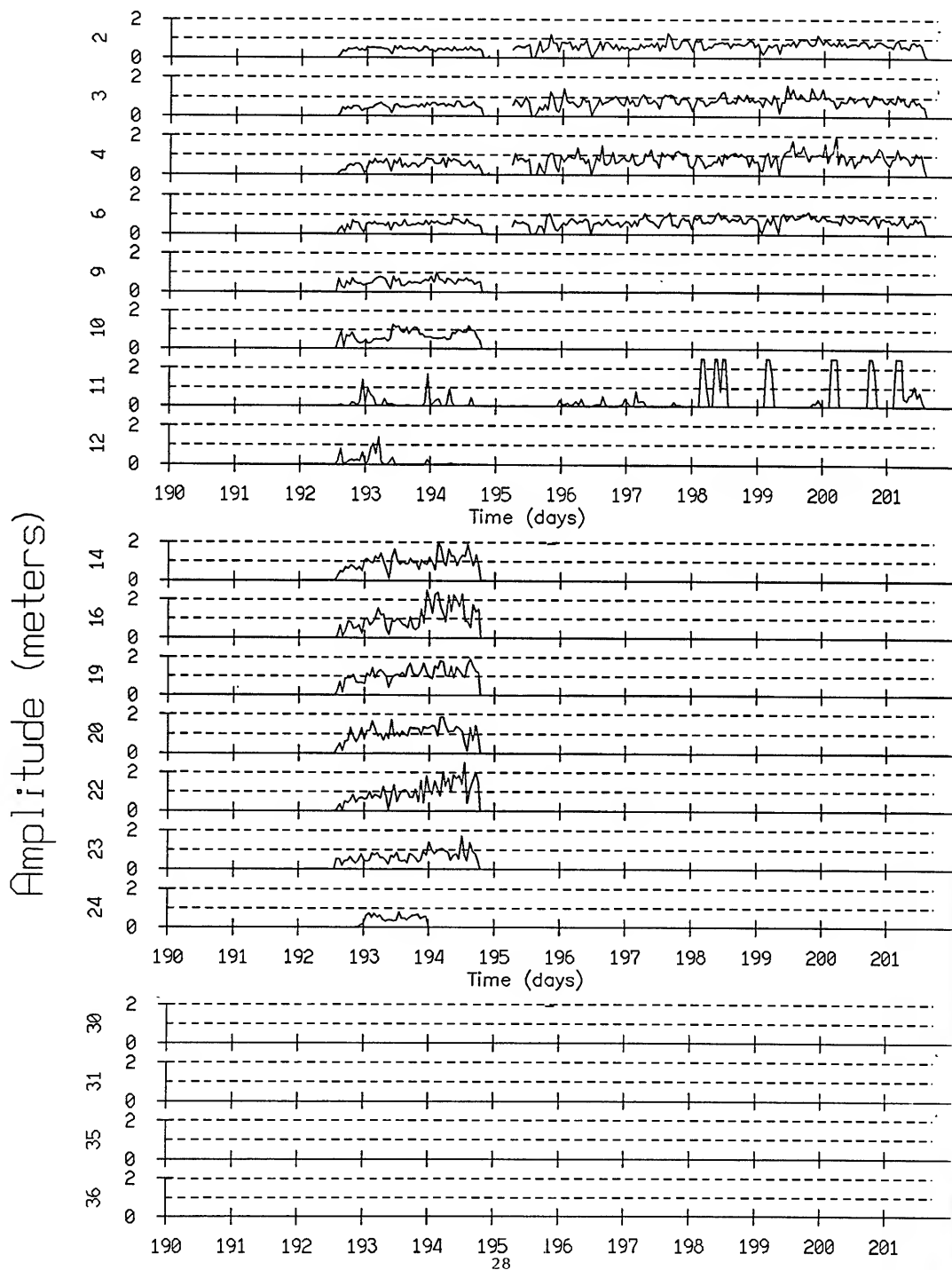


Figure 7E

Standard Deviation of (highpassed) 13500 Hz Slant Ranges
Each sample represents a 1 hr. average, $f_s = 2$ min.

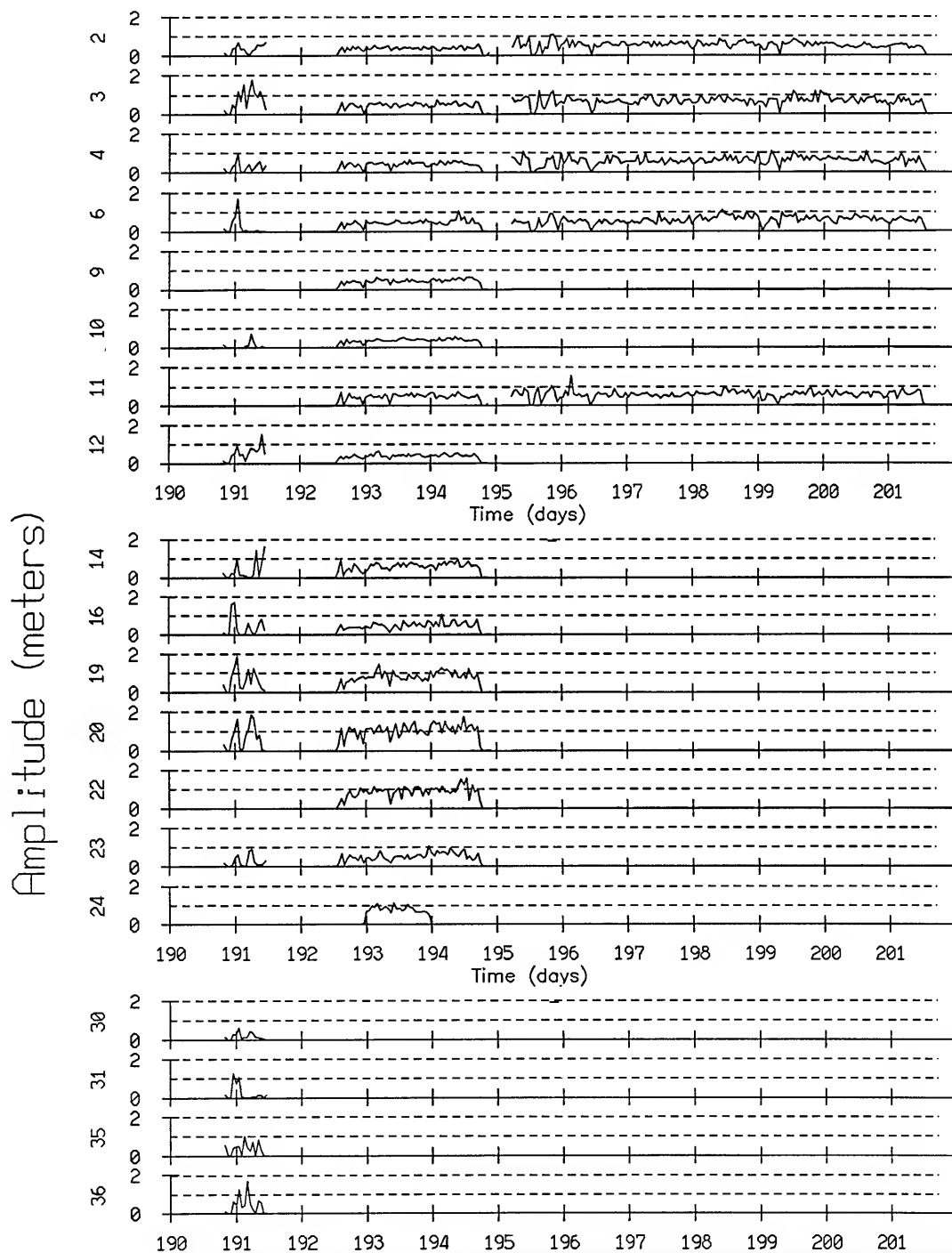
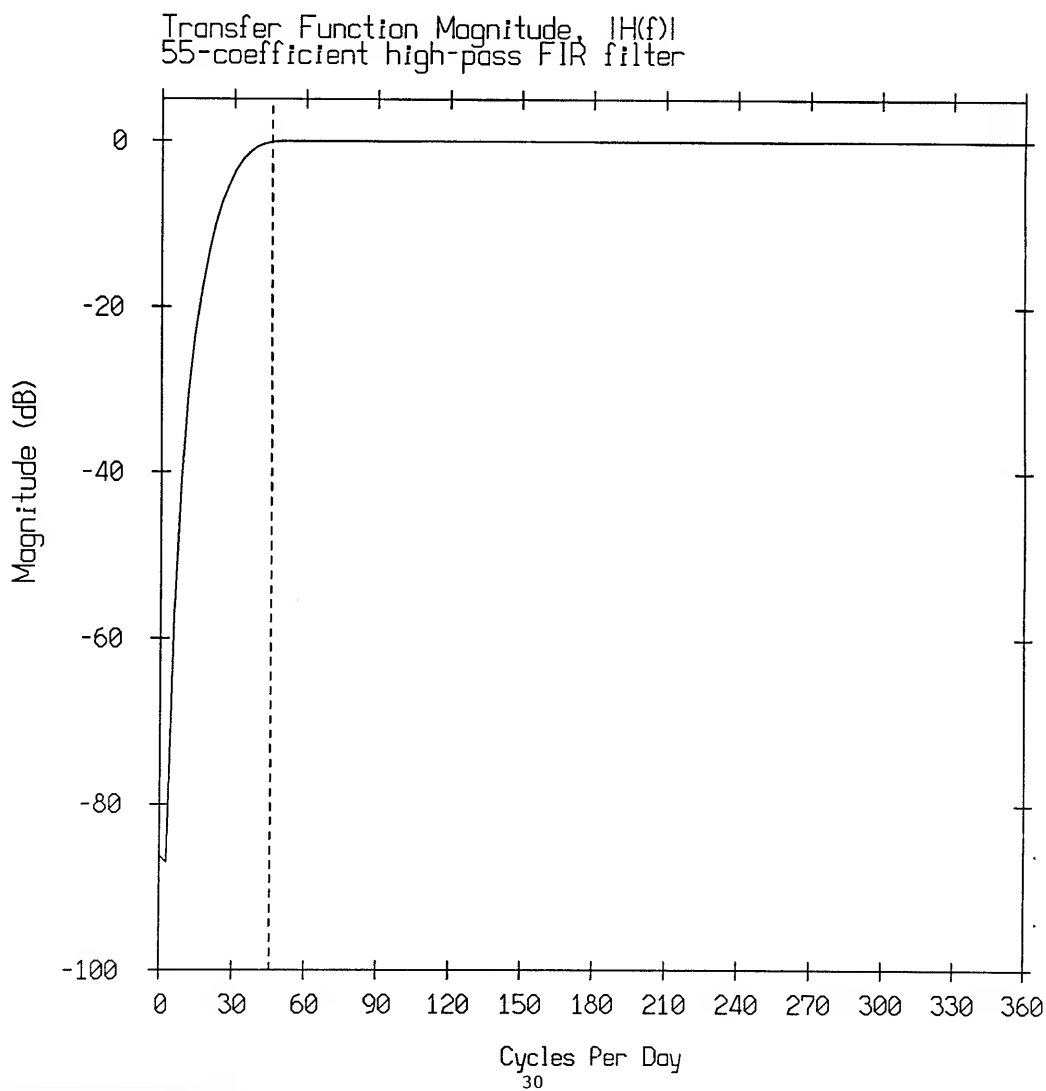


Figure 8



Figures 9 A-I, Table 1

These figures show how the the array elements move when each transponder is perturbed by ten meters in X, Y, or Z. Elements 1, 2 and 3 are the top, middle and bottom elements of Leg A (umbilical) leg, elements 4, 5, and 6 the top, middle and bottom elements of leg B, and 7, 8, and 9 the top, middle and bottom elements of leg C. The actual transponder and element positions used are:

	X	Y	Z
Transponder# 2	-6080.6	-48.0	5158.4
Transponder# 3	-3287.2	-5580.0	5229.3
Transponder# 4	2363.7	-4313.6	5181.7
Transponder# 6	3002.5	5212.0	5110.5
Transponder# 7	-96.8	77.5	5156.5
Element# 1	519.4	-1009.0	158.9
Element# 2	1143.4	-961.1	941.7
Element# 3	1769.7	-894.7	1791.8
Element# 4	455.6	-1056.3	157.7
Element# 5	222.7	-1644.2	939.6
Element# 6	-4.0	-2213.8	1795.4
Element# 7	445.5	-976.7	160.0
Element# 8	75.7	-479.3	962.9
Element# 9	-281.0	28.3	1812.1

The corresponding tables list the values of the offsets (in meters) that are used in the plots.

How to interpret the tables / figures:

Looking at the first table:

.....
table.X
.....

Transp. 2	10	0	0	:	Leg A, top	#1	6.1	-1.9	-0.7	6.4
Transp. 3	0	0	0	:	Leg A, middle	#2	6.2	-1.7	0.0	6.5
Transp. 4	0	0	0	:	Leg A, bottom	#3	6.3	-1.4	1.0	6.5
Transp. 6	0	0	0	:	Leg B, top	#4	6.0	-2.0	-0.8	6.4
Transp. 7	0	0	0	:	Leg B, bottom	#5	5.5	-1.8	-0.9	5.9
					Leg B, middle	#6	5.0	-1.7	-1.2	5.4
					Leg C, top	#7	6.0	-2.0	-0.8	6.4
					Leg C, middle	#8	5.9	-1.9	-1.4	6.4
					Leg C, bottom	#9	5.9	-1.8	-2.2	6.6

This suggests that an error of +10 meters in the X position of transponder #2 will perturb the top element of leg A by +6.1 meters in X, +1.9 meters in Y, and -.7 meters in Z. These changes suggest element #1 will have a (Euclidean) magnitude of 6.4 meters which is printed in the fourth column.

Corresponding plots show how each leg is affected by a given transponder perturbed by adding and subtracting 10 meters to each coordinate. There are three sets of these plots; Leg A is represented with the numbers 1, 2 and 3 inside the plots; these correspond to no correction, -10 meters of correction and +10 meters of correction. Similarly Leg B is represented by the numbers 4, 5 and 6, and Leg C the numbers 7, 8 and 9. For example the first row of plots, Transponder 2 (W) (x-10,x,x+10) (with 1, 2 and 3 inside the boxes) shows how the top, middle and bottom elements of leg A are affected by 10 meters of error both subtracted and added to the X position of Transponder #2. In particular the leg A element's X positions are affected by about three times as much as their Y positions, and their Y positions about one to two times as much as their Z positions for this case.

```

:::table.X

```

[illegible]

```

:-----:
table %
:-----:

```

```

0 0 10 : -4.6 1.5 0.5 4.9
0 0 0 : -3.6 1.0 0.0 3.8
0 0 0 : -2.7 0.6 -0.4 2.8
0 0 0 : -4.6 1.5 0.6 4.9
0 0 0 : -3.7 1.2 0.6 3.9
0 0 0 : -2.7 0.9 0.7 3.0
0 0 0 : -4.6 1.5 0.6 4.9
-4.1 1.3 1.0 4.4
-3.4 1.0 1.3 3.8

0 0 0 : -1.9 -2.6 1.1 3.4
0 10 : -1.8 -2.0 0.7 2.7
0 0 0 : -1.5 -1.4 0.3 2.1
0 0 0 : -1.9 -2.7 1.2 3.5
0 0 0 : -1.9 -2.5 1.5 3.5
-1.8 -2.2 1.9 3.4
-1.8 -2.7 1.1 3.4
-1.4 -2.3 1.0 2.9
-0.9 -1.8 0.7 2.2

0 0 0 : 4.6 4.1 3.1 6.9
0 0 0 : 4.2 -3.7 3.7 6.7
0 10 : 3.6 -3.2 4.3 6.4
0 0 0 : 4.6 -4.1 3.0 6.8
0 0 0 : 4.1 -3.5 3.3 6.3
3.5 -2.8 3.6 5.7
4.5 -4.1 3.0 6.8
3.6 -3.4 2.1 5.4
2.6 -2.7 1.1 3.9

0 0 0 : 1.7 3.4 1.7 4.2
0 0 0 : 1.5 2.9 1.9 3.8
0 10 : 1.3 2.3 2.0 3.4
0 0 0 : 1.7 3.4 1.7 4.1
0 0 0 : 1.3 2.6 1.1 3.1
0 0 0 : 0.9 1.8 0.6 2.1
1.7 3.4 1.7 4.2
1.7 3.6
1.2 2.2 1.6 3.0

0 0 0 : 0.2 1.9 3.6 4.0
0 0 0 : -1.8 3.8 4.2
0 0 0 : -0.7 1.6 3.8 4.2
0 10 : 0.2 1.9 3.5 4.0
0 0 0 : 0.2 2.2 3.3 4.0
0.2 1.8 3.6 4.0
0.3 1.6 4.3 4.6
0.5 1.2 5.3 5.4

0 0 -10 : 4.6 -1.5 -0.5 4.9
0 0 0 : 3.6 -1.0 0.0 3.8
0 0 0 : 2.7 -0.6 0.4 2.8
0 0 0 : 4.6 -1.5 -0.6 4.9
0 0 0 : 3.7 -1.2 -0.5 3.9
0 0 0 : 2.7 -0.9 -0.7 3.0
0 0 0 : 4.6 -1.5 -0.6 4.9
4.0 -1.3 -0.9 4.3
3.4 -1.0 -1.3 3.8

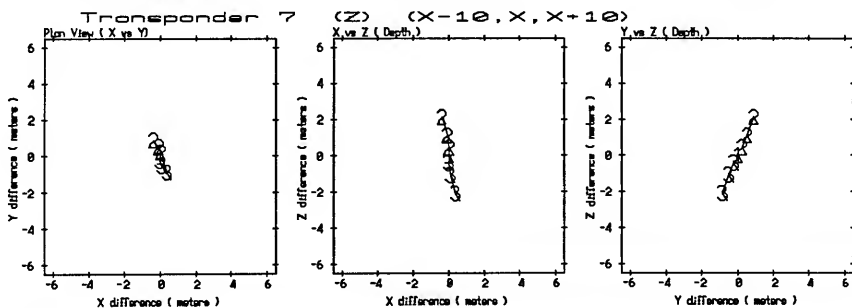
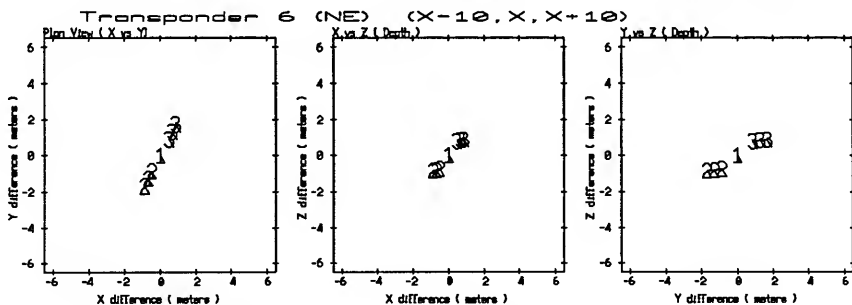
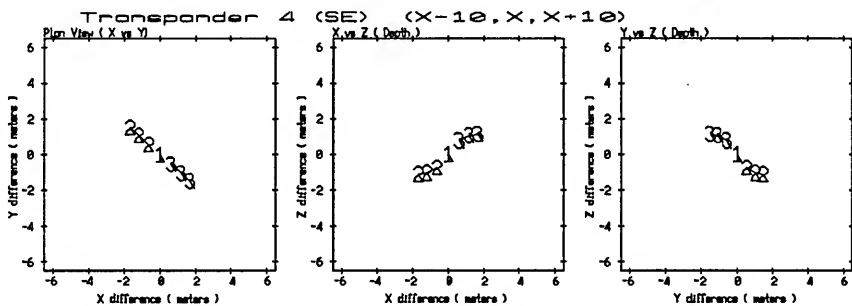
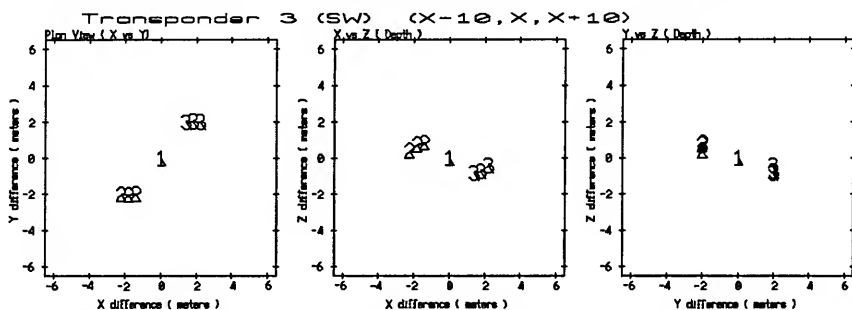
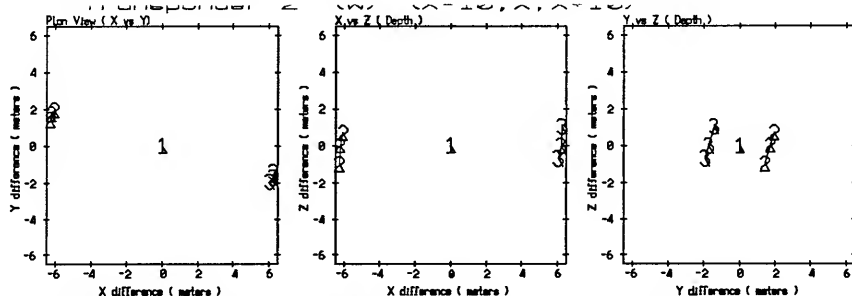
0 0 0 : 1.9 2.6 -1.1 3.4
0 -10 : 1.8 2.0 -0.7 2.7
0 0 0 : 1.5 1.4 -0.3 2.1
0 0 0 : 1.9 2.7 -1.2 3.5
0 0 0 : 1.9 2.5 -1.5 3.5
1.9 2.2 -1.9 3.4
1.8 2.7 -1.1 3.4
1.4 2.3 -1.0 2.8
0.9 1.8 -0.7 2.2

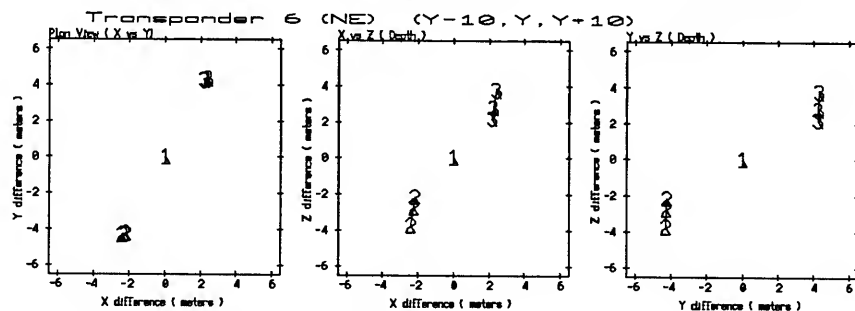
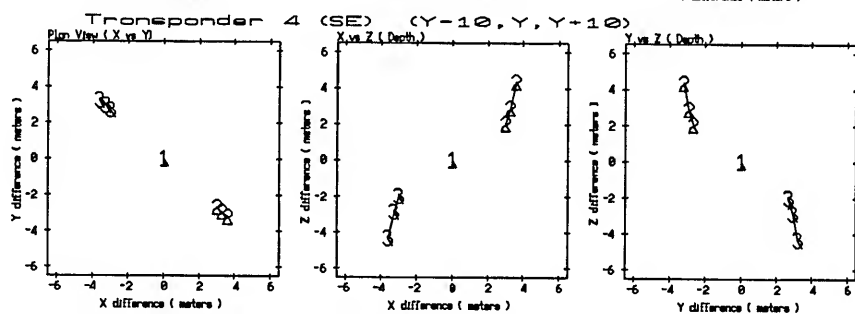
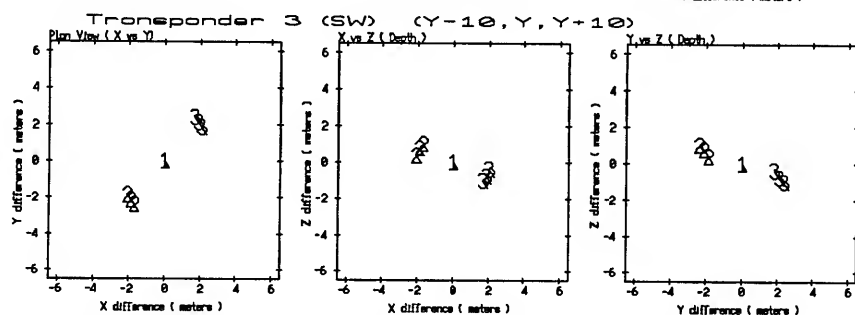
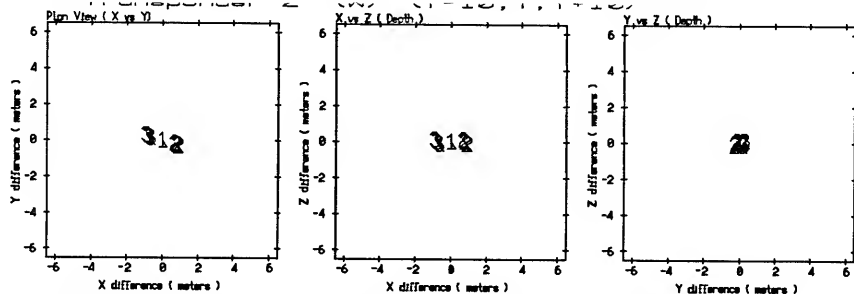
0 0 0 : -4.6 4.1 -3.1 6.9
0 0 0 : -4.2 3.7 -3.6 6.7
0 -10 : -3.6 3.2 -4.3 6.4
0 0 0 : -4.6 4.1 -3.0 6.8
0 0 0 : -4.1 3.5 -3.3 6.3
-3.5 2.8 -3.6 5.7
-4.5 4.1 -3.0 6.8
-3.6 3.4 -2.1 5.4
-2.6 2.7 -1.1 3.9

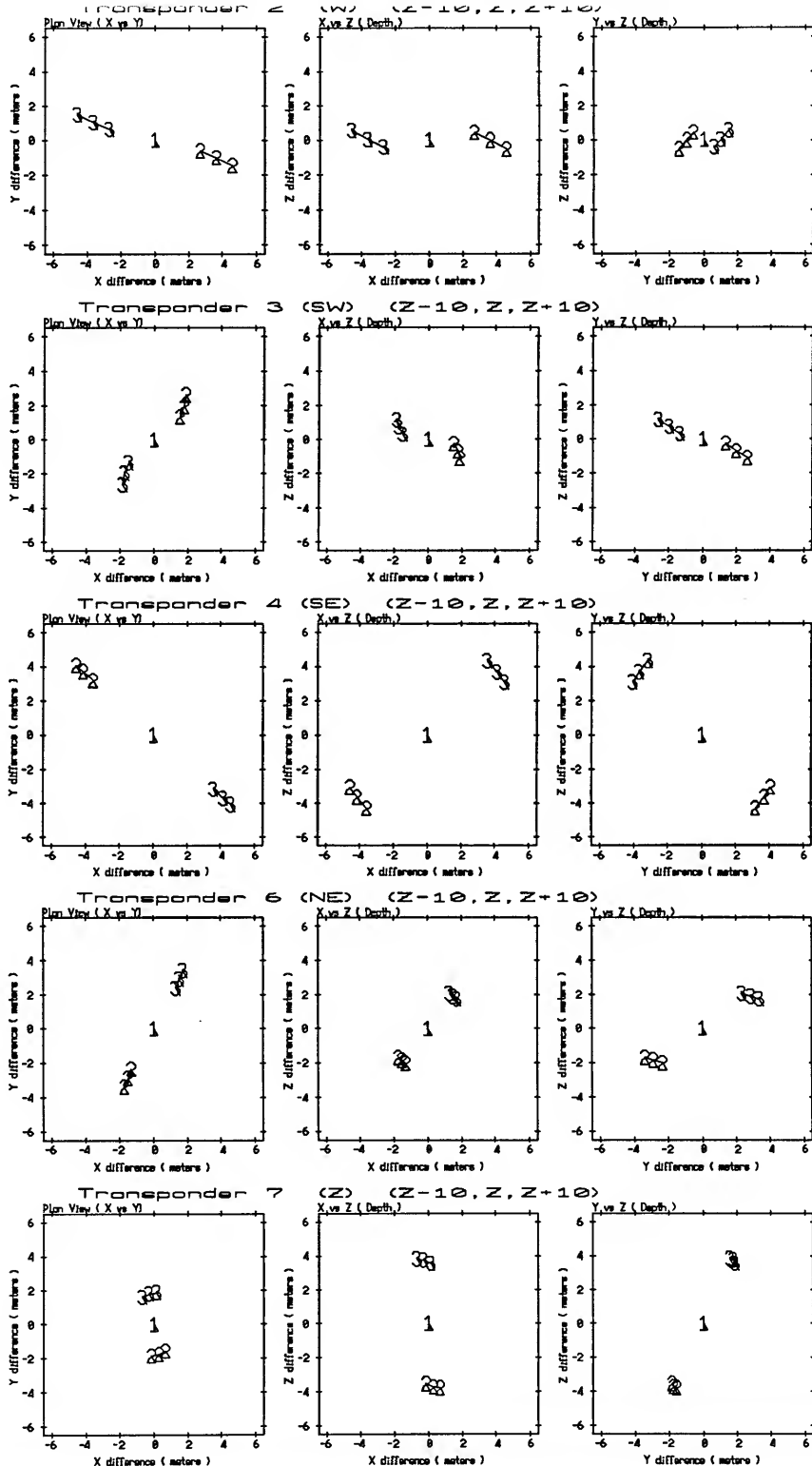
0 0 0 : -1.7 -3.4 -1.7 4.2
0 0 0 : -1.5 -2.9 -1.8 3.8
0 0 0 : -1.3 -2.3 -2.0 3.4
0 -10 : -1.7 -3.4 -1.7 4.1
0 0 0 : -1.3 -2.6 -1.1 3.1
0 0 0 : -0.9 -1.8 -0.6 2.1
-1.7 -3.4 -1.7 4.2
-1.5 -2.8 -1.7 3.6
-1.2 -2.2 -1.6 3.0

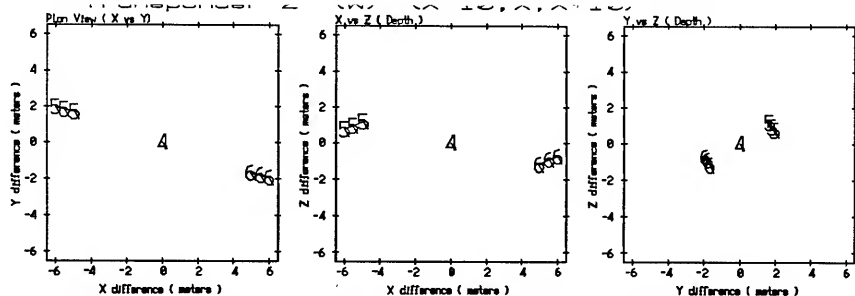
0 0 0 : -0.1 -1.9 -3.5 4.0
0 0 0 : 0.3 -3.7 4.2
0 0 0 : 0.7 -3.8 4.2
0 0 0 : -0.2 -1.9 -3.5 4.1
0 -10 : -0.2 -2.2 -3.3 4.1
0 0 0 : -0.2 -2.3 -3.3 4.0
-0.2 -1.9 -3.6 4.0
-0.3 -1.6 4.3 4.6
-0.5 -1.2 -5.3 5.4

```

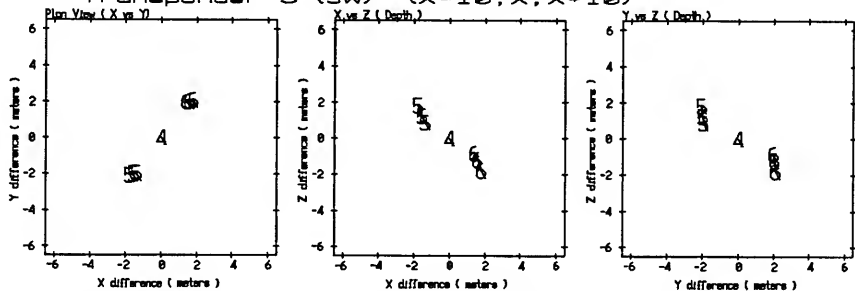




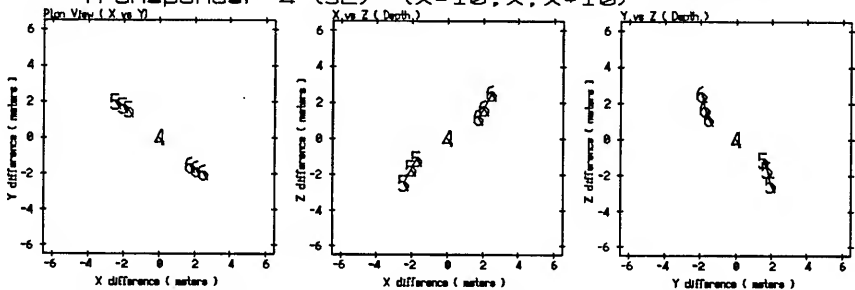




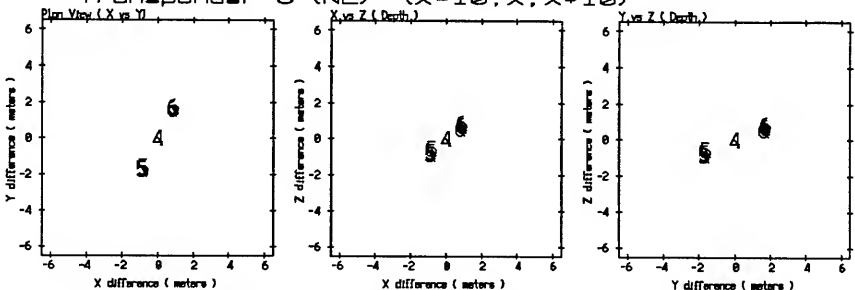
Transponder 3 (SW) (X-10, X, X+10)



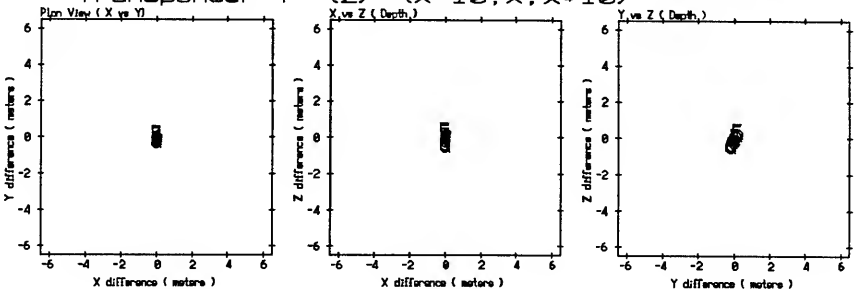
Transponder 4 (SE) (X-10, X, X+10)

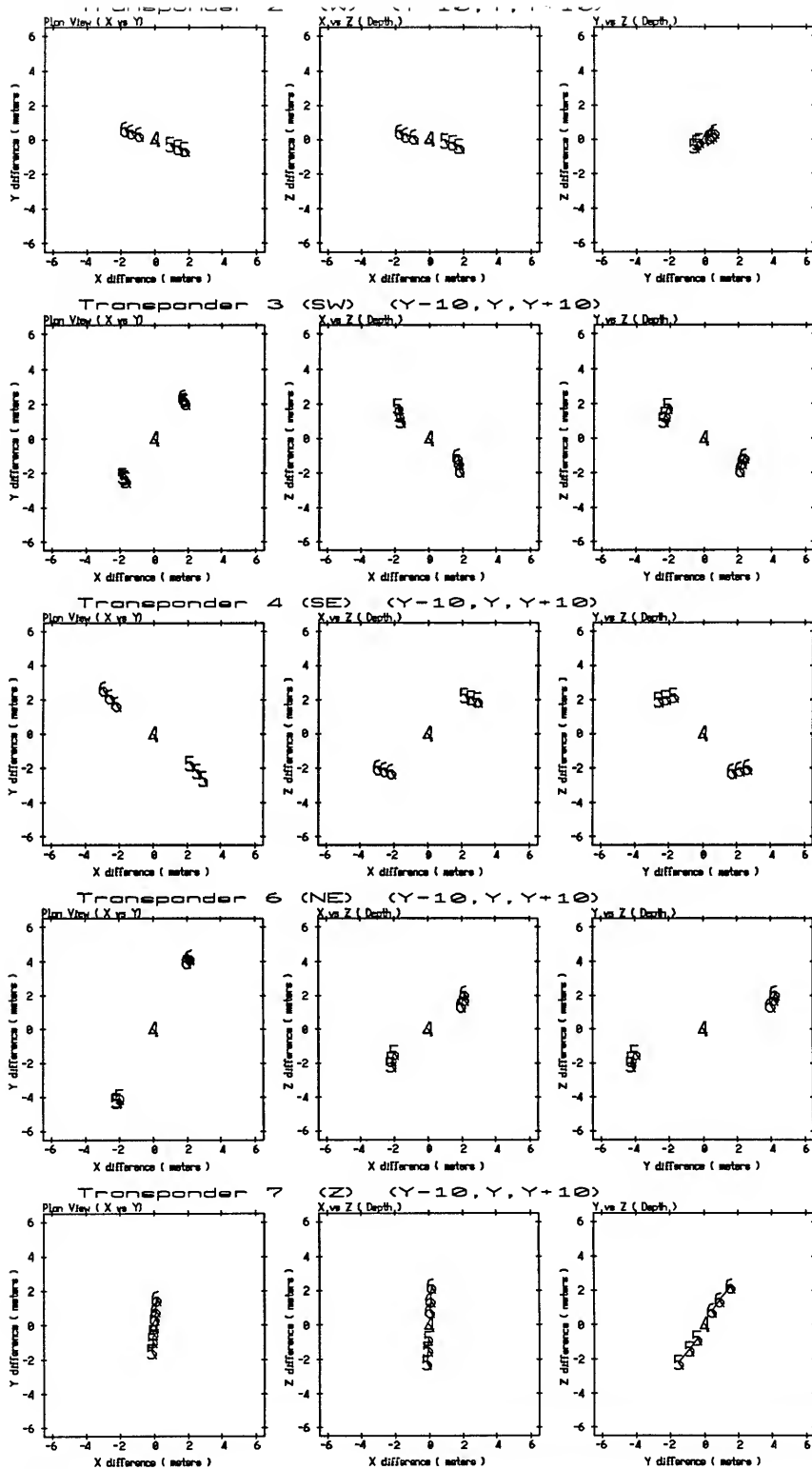


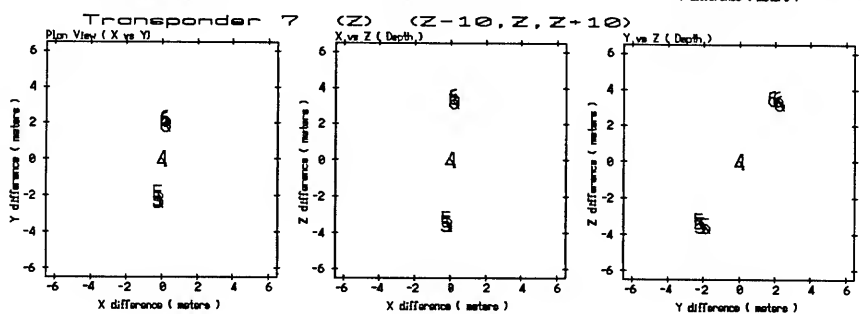
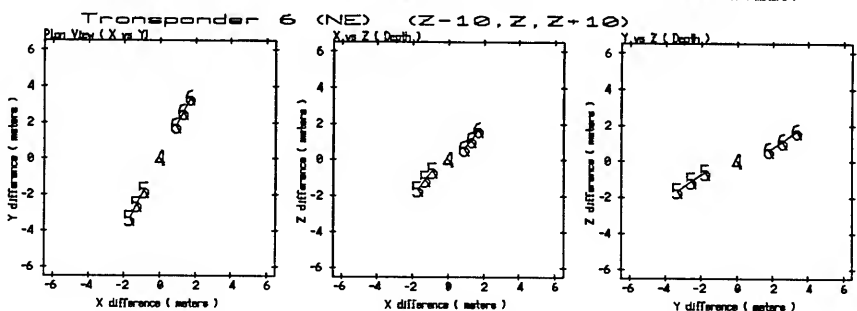
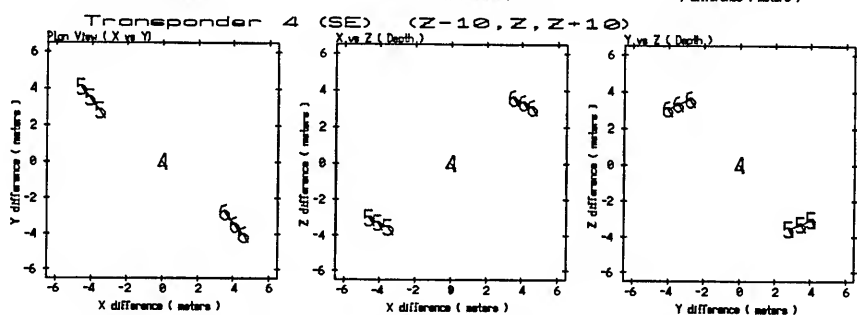
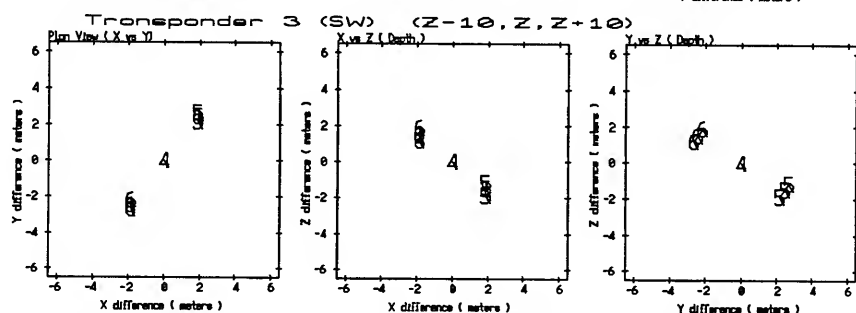
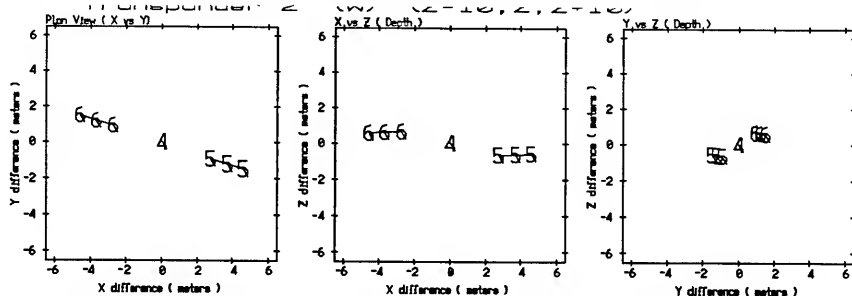
Transponder 6 (NE) (X-10, X, X+10)

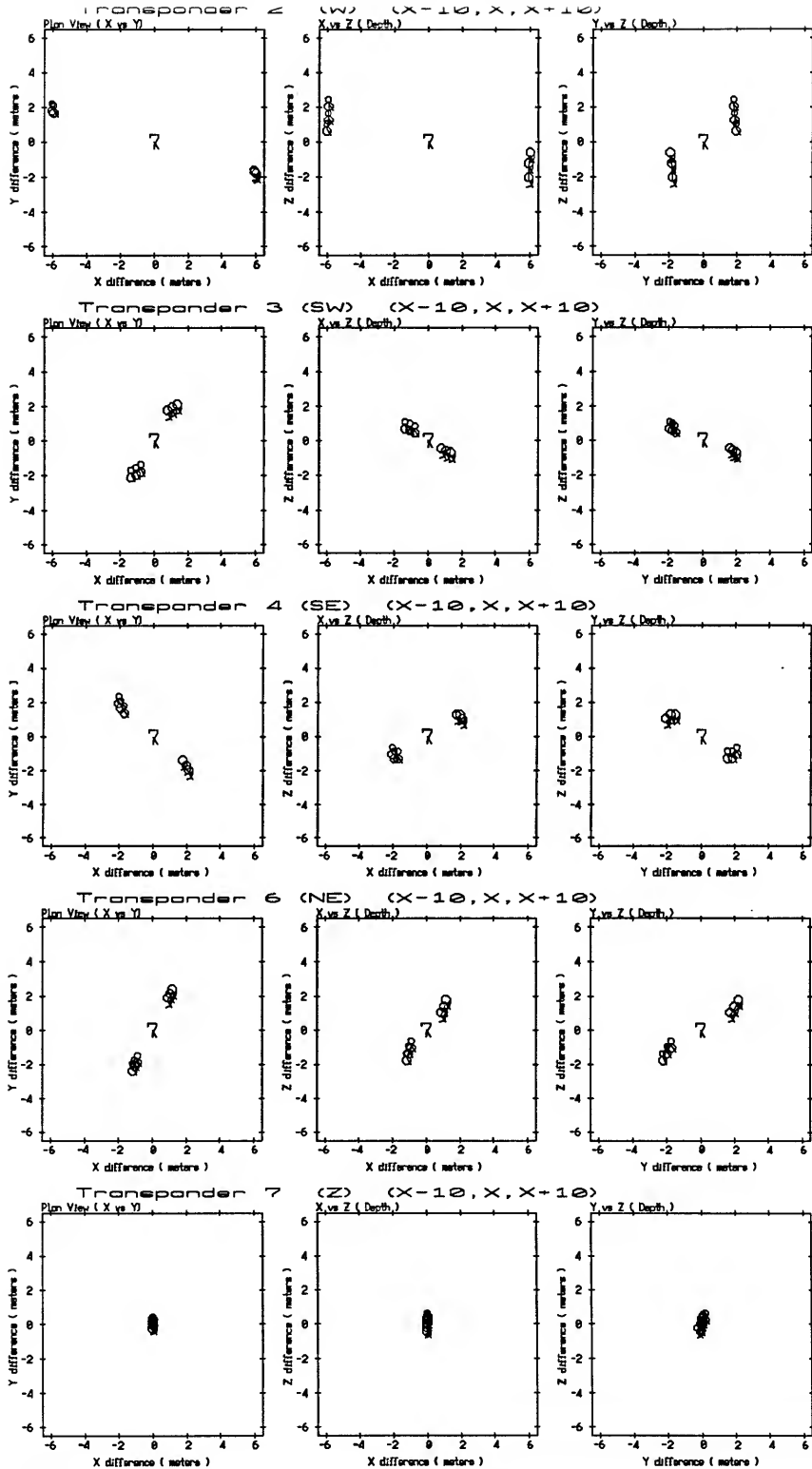


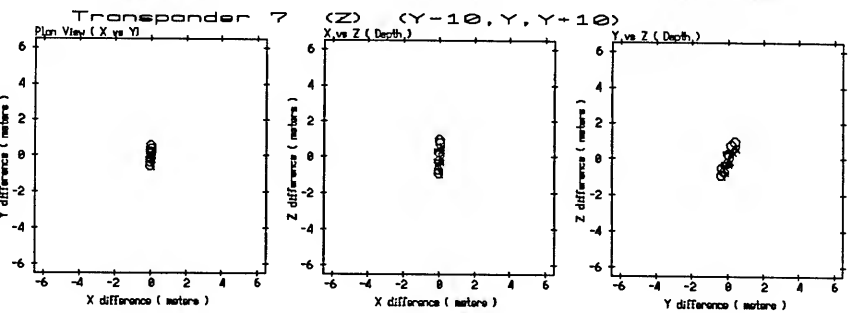
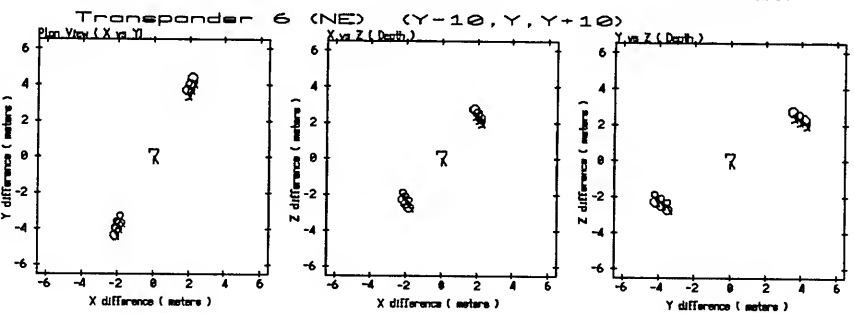
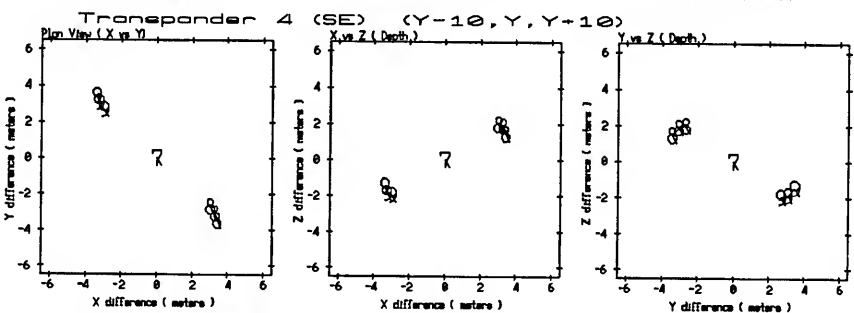
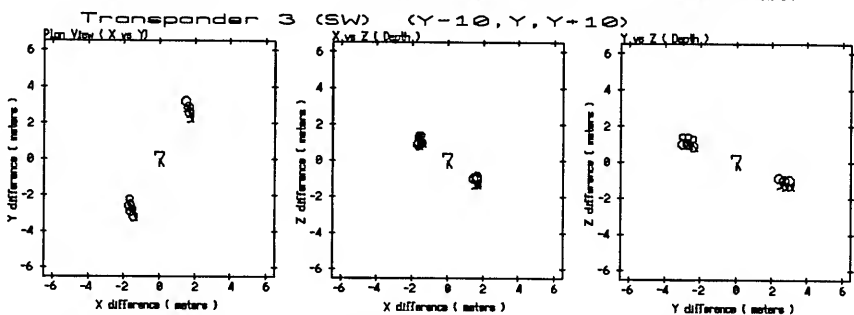
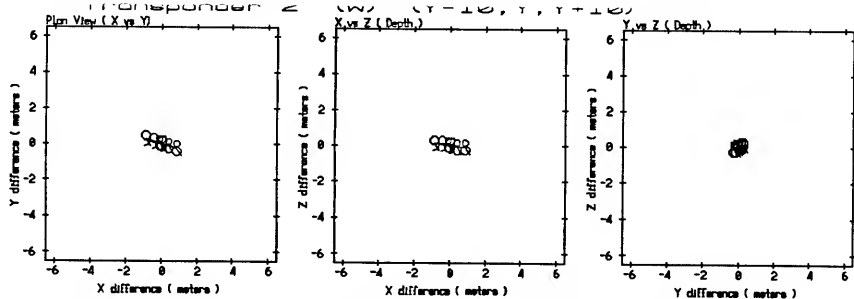
Transponder 7 (Z) (X-10, X, X+10)

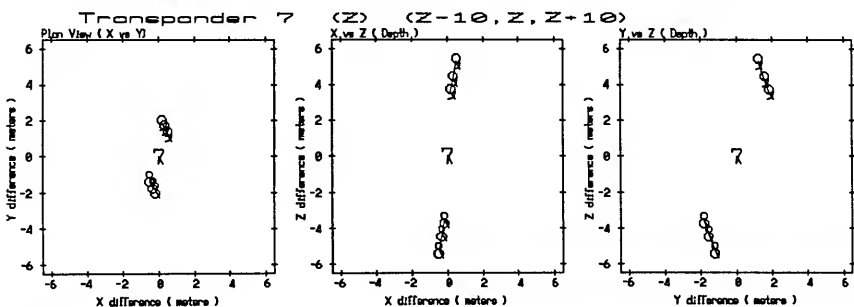
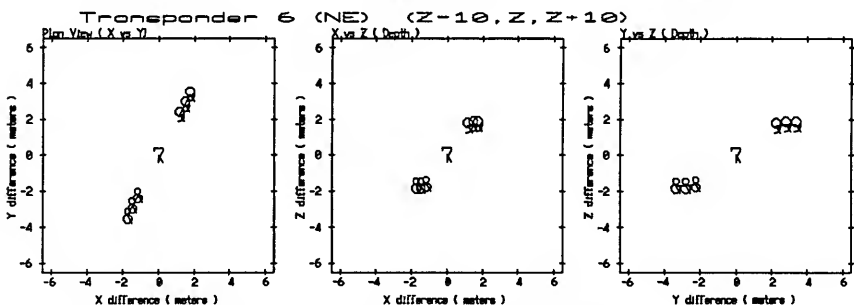
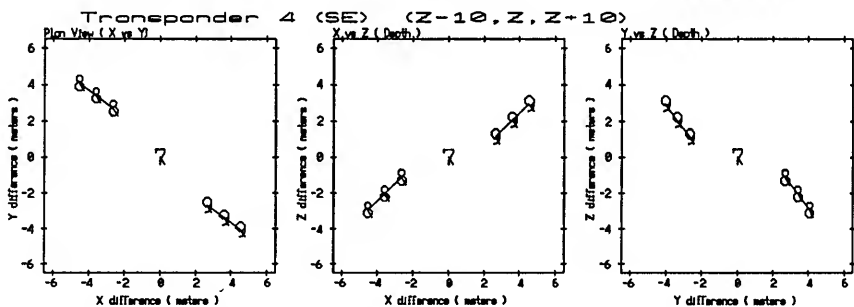
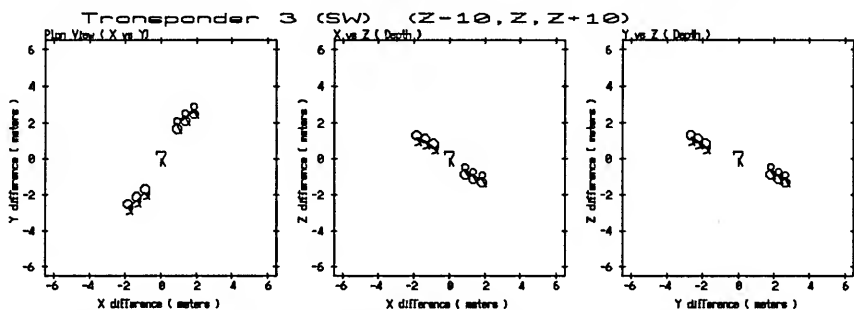
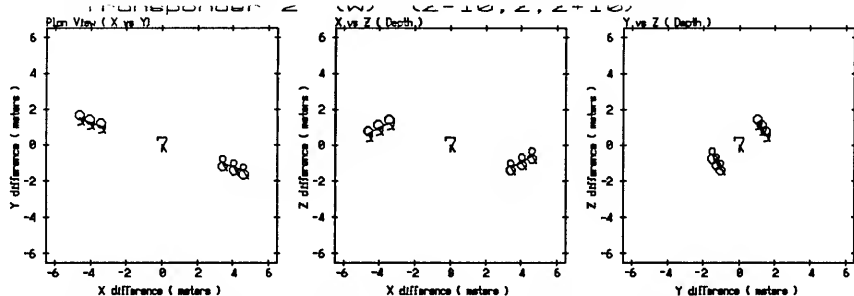












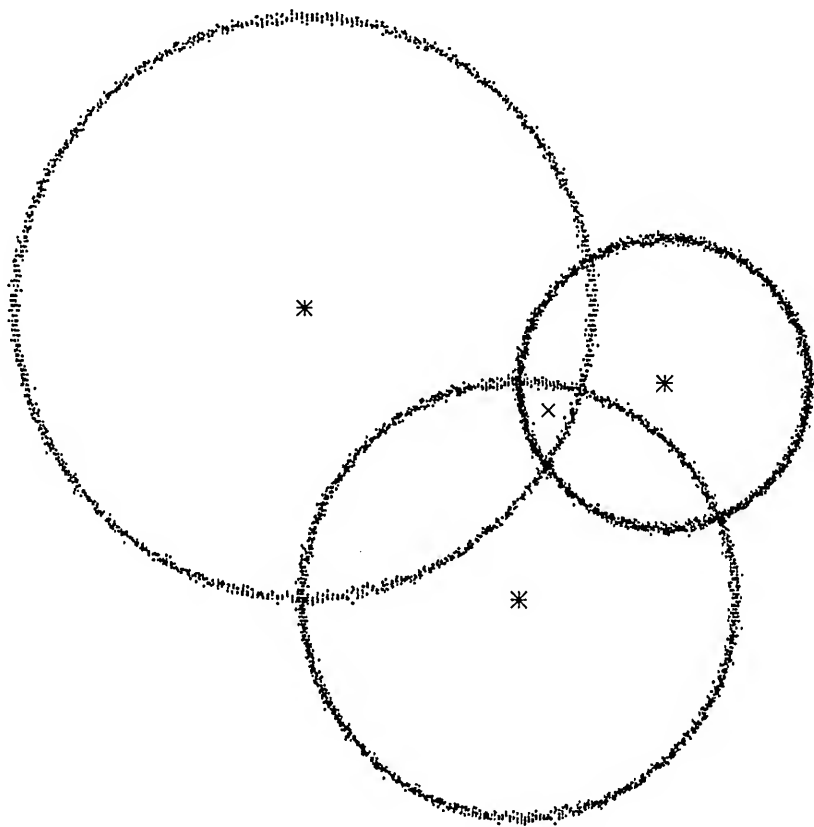


Figure 10 Slant range error decomposition

This is a two dimensional example of error decomposition into bias and random components. In this case the slant ranges are all too long (positive bias) which leads to the overlapping circles. In this two dimensional case the additive bias errors cancel if the transponders (*) are symmetric. The width in the circles represents the random component and were in fact generated by adding Gaussian noise to the radii of the circles. The navigated solution (position with the minimum mean square error) is denoted by the x.

Appendix A. MDA-I Navigation Bias Error

After ray trace corrections have been incorporated, the greatest source of bias error in MDA-I navigation is sound speed error. This error is from the (Del Grosso) sound speed equation being in error or from errors in the measurements of depth, temperature or salinity which go into the calculation of sound speed.

Seabird claims the following CTD measurement accuracies: temperature to 0.01 degrees C, salinity to 0.01 psu, and pressure to 0.5% full scale range or 10 dBar (~ 10 meters). It has been suggested that in practice one probably gets accuracies in temperature and salinity from one half to a full order of magnitude worse than this. The following table shows this worst case at five different water depths:

Sound Speed Variability (Del Grosso)				
Depth,m (Z)	Temperature	Salinity	Sound Speed	delta
20.00	27.01	36.57	1541.0	-
20.00	27.11	36.57	1541.2	0.2
20.00	27.01	36.67	1541.1	0.1
30.00	27.01	36.57	1541.2	0.2
200.00	19.65	36.65	1525.6	-
200.00	19.75	36.65	1525.9	0.3
200.00	19.65	36.75	1525.8	0.2
210.00	19.65	36.65	1525.8	0.2
700.00	10.78	35.41	1504.6	-
700.00	10.88	35.41	1504.9	0.4
700.00	10.78	35.51	1504.7	0.3
710.00	10.78	35.41	1504.8	0.2
2000.00	3.61	34.99	1498.0	-
2000.00	3.71	34.99	1498.4	0.4
2000.00	3.61	35.09	1498.2	0.2
2010.00	3.61	34.99	1498.2	0.2
5245.00	2.23	34.87	1548.8	-
5245.00	2.33	34.87	1549.2	0.4
5245.00	2.23	34.97	1548.9	0.1
5255.00	2.23	34.87	1549.0	0.2

Taking these we get 2 sound speed profiles (the second by adding or subtracting the error to the original sound speed estimates).

Then computing a typical harmonic mean sound speed from the ship to a transponder we see that there is ~ 0.8 m/s difference.

The 9 element positions used were the following; these were estimated by using average element positions for the 3 leg deployment:

Element Positions

X	Y	Z
519.4	-1009.1	158.9
1143.5	-961.1	941.7
1769.7	-894.7	1791.8
455.6	-1056.4	157.7
222.7	-1644.2	939.6
-4.0	-2213.8	1795.4
445.5	-976.7	160.06
75.7	-479.3	962.9
-281.0	28.3	1812.1

Adding a one meter/second bias moved the transponders about seven meters (primarily in a radial direction) as follows:

Original Transponder Positions

X	Y	Z
-3975.3	7352.2	5164.9
-6069.5	-49.9	5157.8
-3278.9	-5578.4	5228.2
2367.8	-4313.5	5180.5
5902.0	-44.1	5192.9

Transponder Positions via adding bias

X	Y	Z
-3978.2	7357.7	5168.4
-6073.4	-50.0	5163.3
-3280.4	-5583.2	5232.7
2370.9	-4317.3	5184.9
5907.8	-44.9	5196.5

Transponder Position Differences (X,Y,Z, total distance):

X	Y	Z	total distance
-2.90	5.48	3.51	7.13
-3.96	-0.06	5.54	6.81
-1.56	-4.82	4.52	6.79
3.07	-3.88	4.41	6.63
5.82	-0.81	3.60	6.89

Then these different transponder positions were compared to see how much their slant ranges differed. The slant range errors are differentially biased as follows:

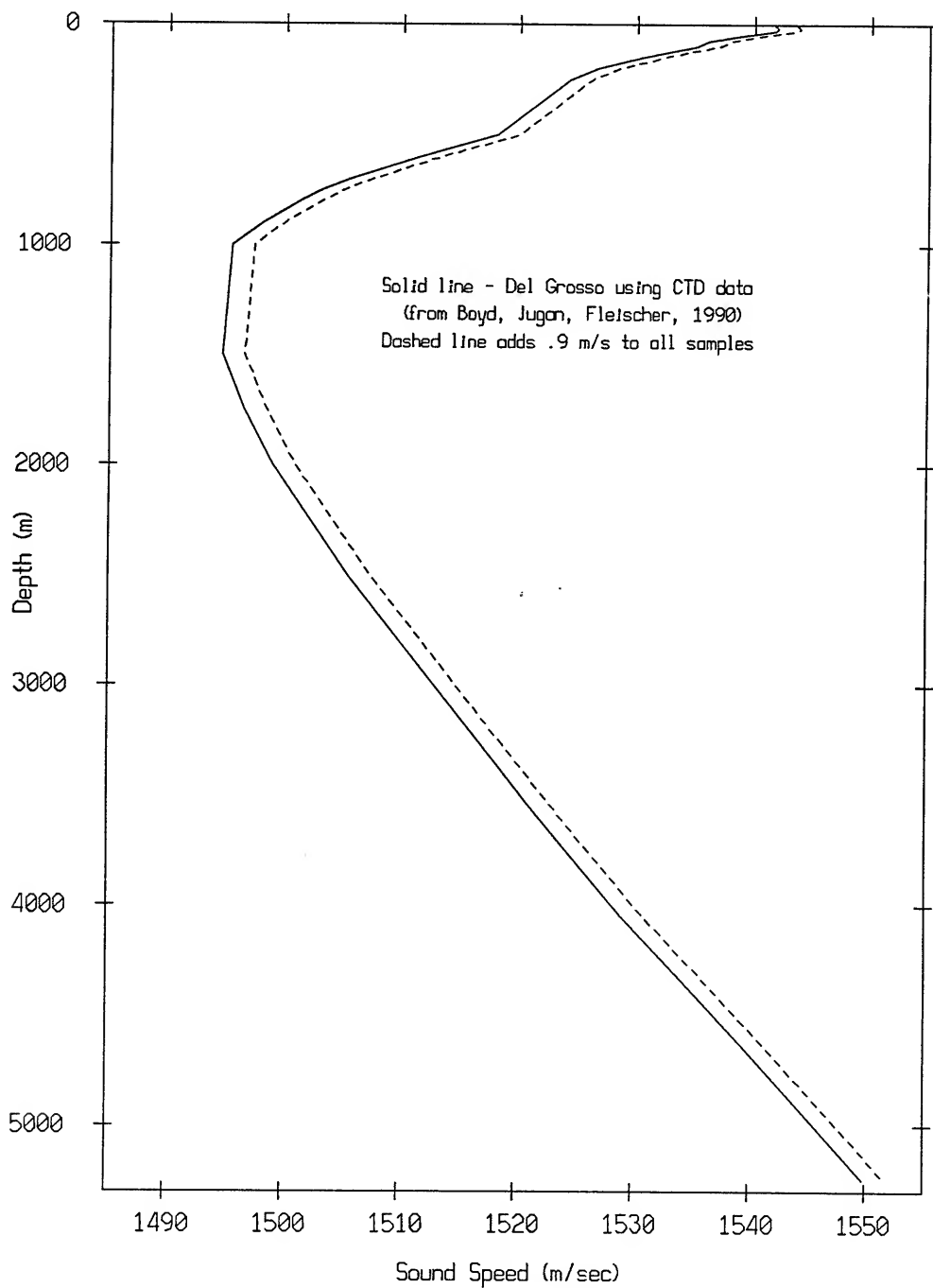
Elements	Transponders					max. dif.
	#2	#3	#4	#5	#6	
Leg 1, top	7.12	6.45	6.51	6.46	6.54	0.67
Leg1, middle	7.07	6.17	6.31	6.40	6.55	0.91
Leg1, bottom	6.95	5.79	5.98	6.20	6.57	1.16
Leg2, top	7.12	6.45	6.52	6.47	6.54	0.67
Leg2, middle	7.07	6.22	6.45	6.54	6.47	0.85
Leg2, bottom	6.96	5.85	6.34	6.55	6.27	1.11
Leg3, top	7.12	6.46	6.53	6.48	6.56	0.66
Leg3, middle	7.11	6.38	6.59	6.60	6.76	0.73
Leg3, bottom	7.07	6.20	6.53	6.53	6.84	0.87

(slant ranges in the above table are in meters)

Looking across each of the 9 elements, we see that there is a maximum differential (bias) distance of < 1.2m for Leg 1, bottom element. As we have seen a slant range bias of this magnitude will show up as a bias error of about half of this at the array, hence this worst case scenario should contribute less than 1m of (consistently) biased AEL position error.

The plots in appendix D show a similar radial expansion in the transponder positions when applying ray trace corrections.

'91 MDA-I Sound Speed Profiles
Comparison of Sound Speed Profiles

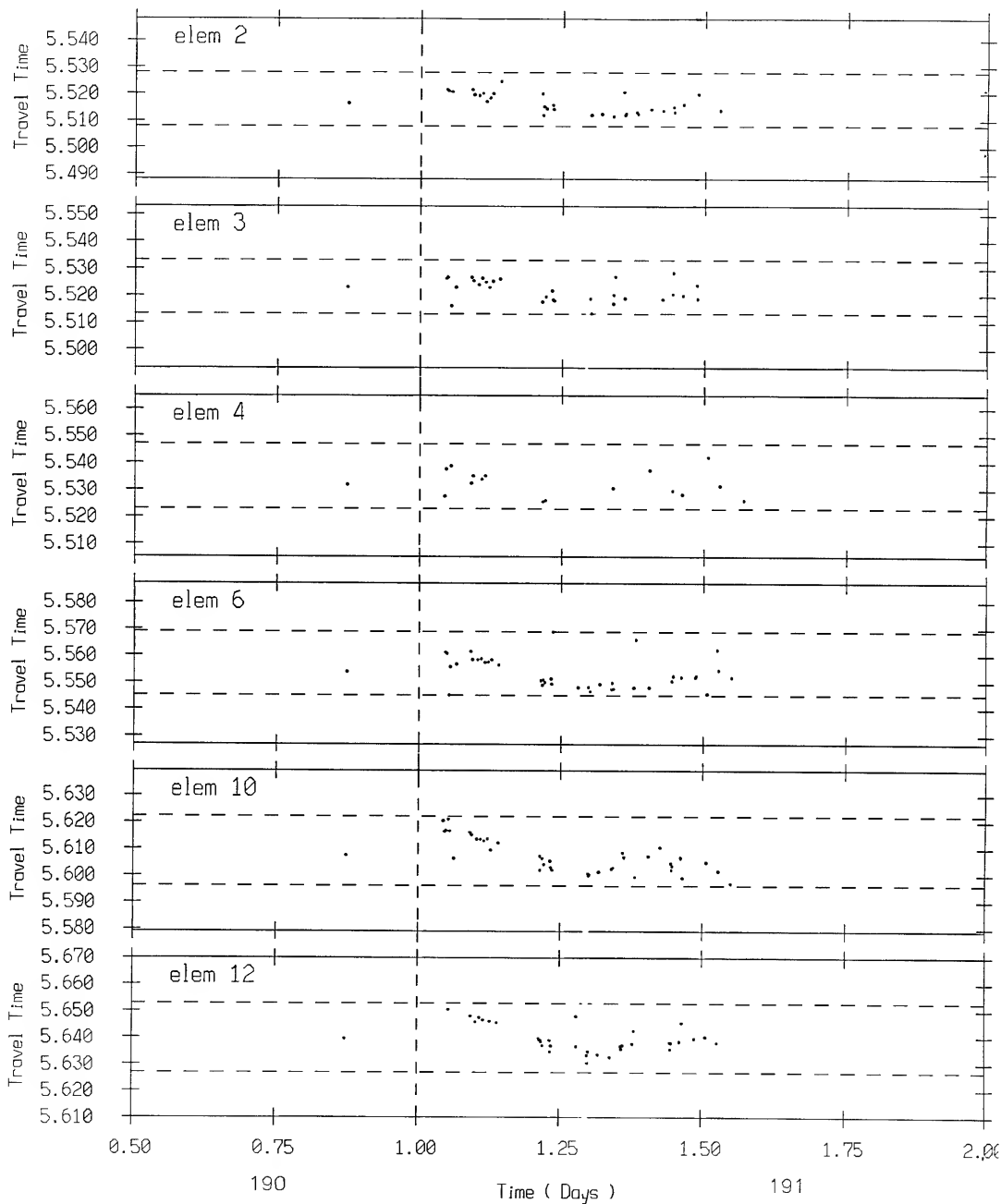


Appendix B. Raw Slant Range Plots

The following are plots of the slant ranges from the five transponders to the navigable elements for three, two and one leg deployments. These are a good indicator of raw slant range data quality as a function of time.

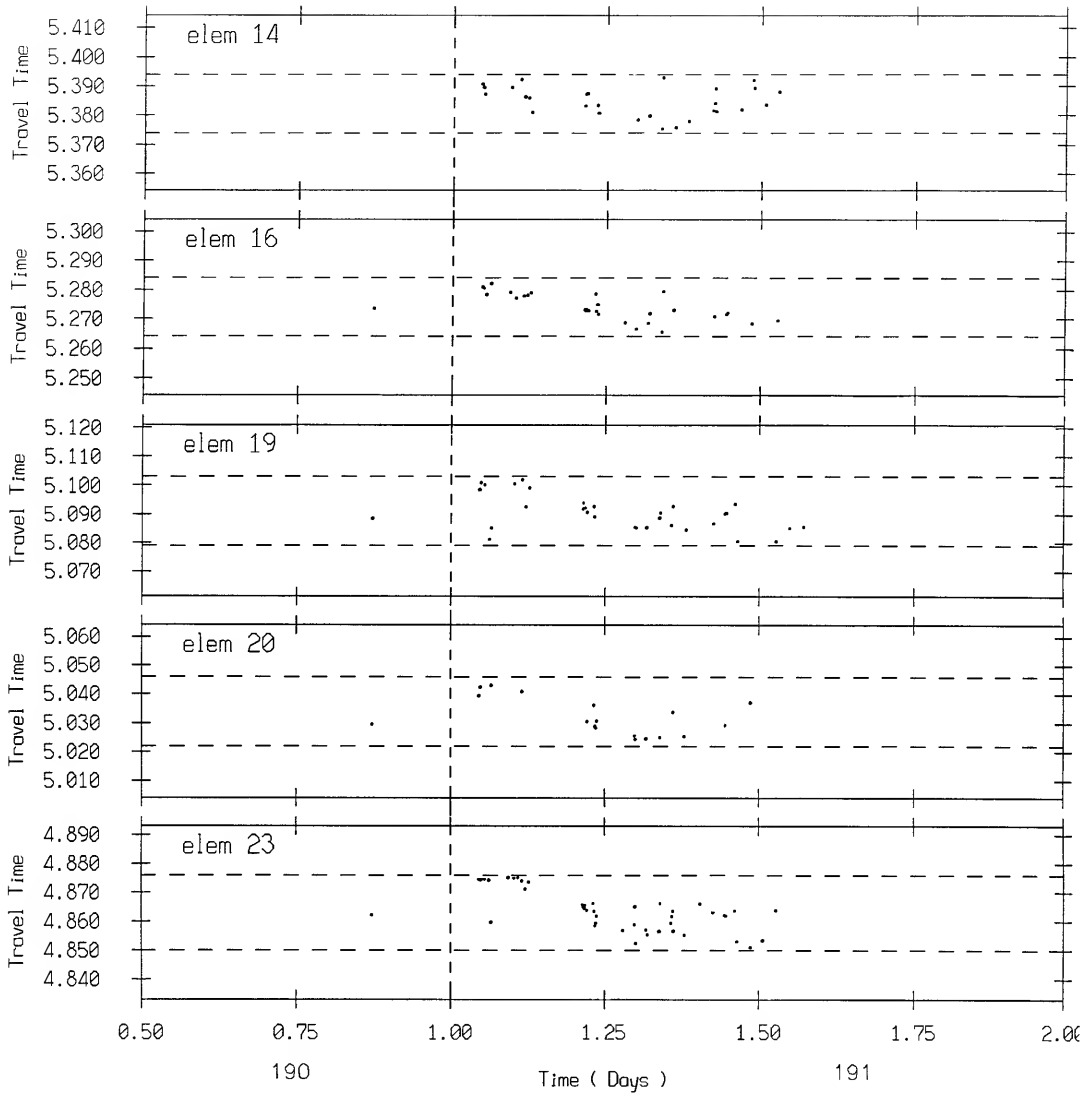
Freq: 9500

190 15:30 -> 191 14:30



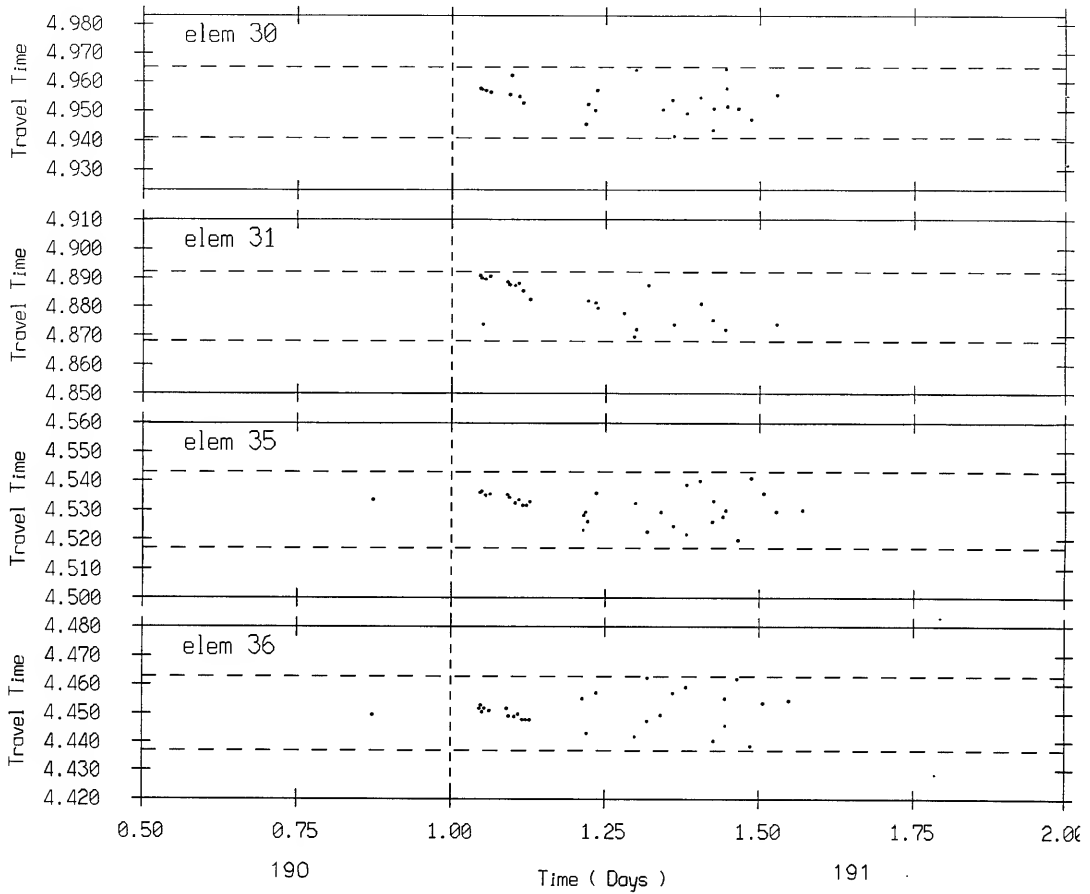
Freq: 9500

190 15:30 -> 191 14:30



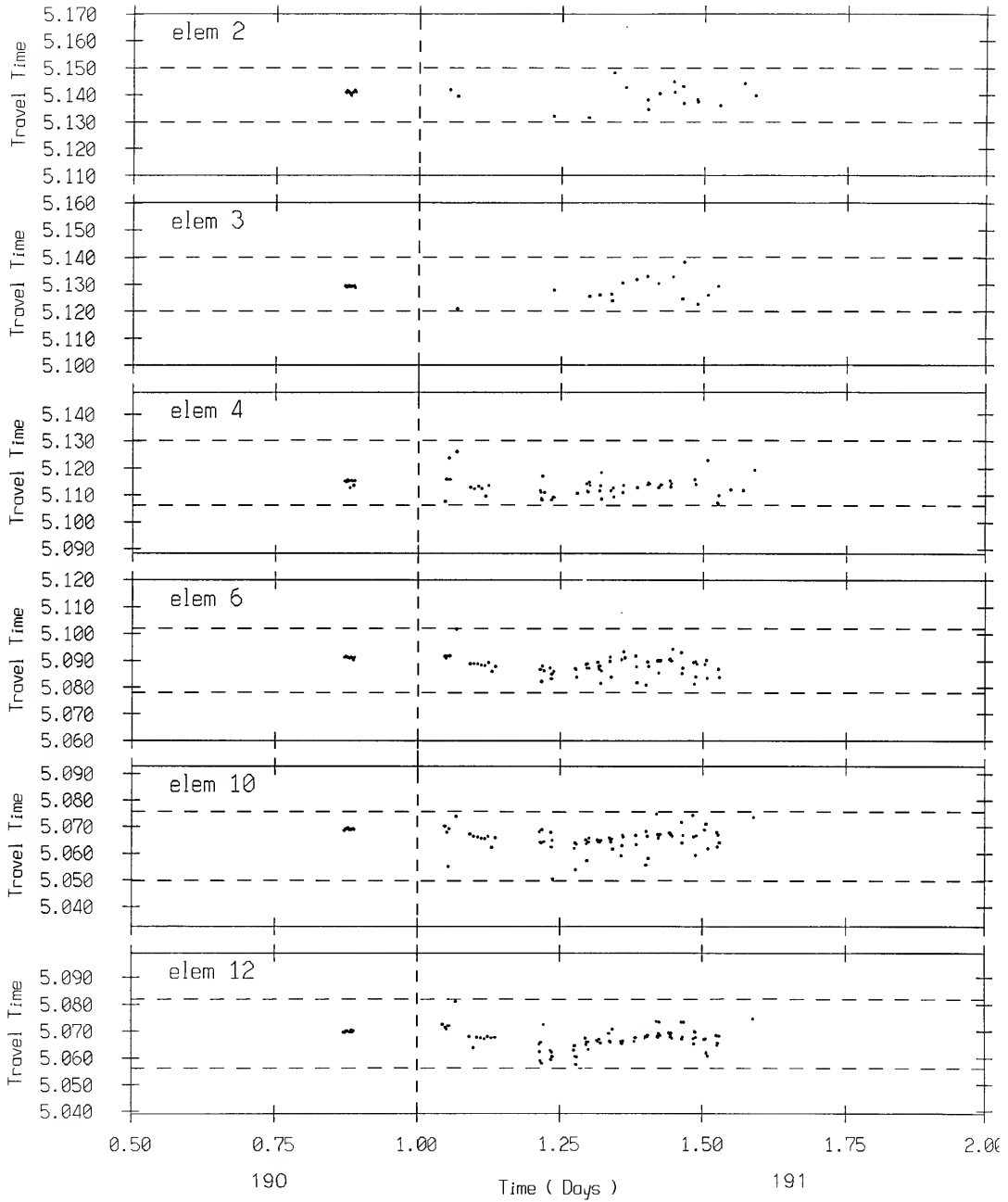
Freq: 9500

190 15:30 -> 191 14:30



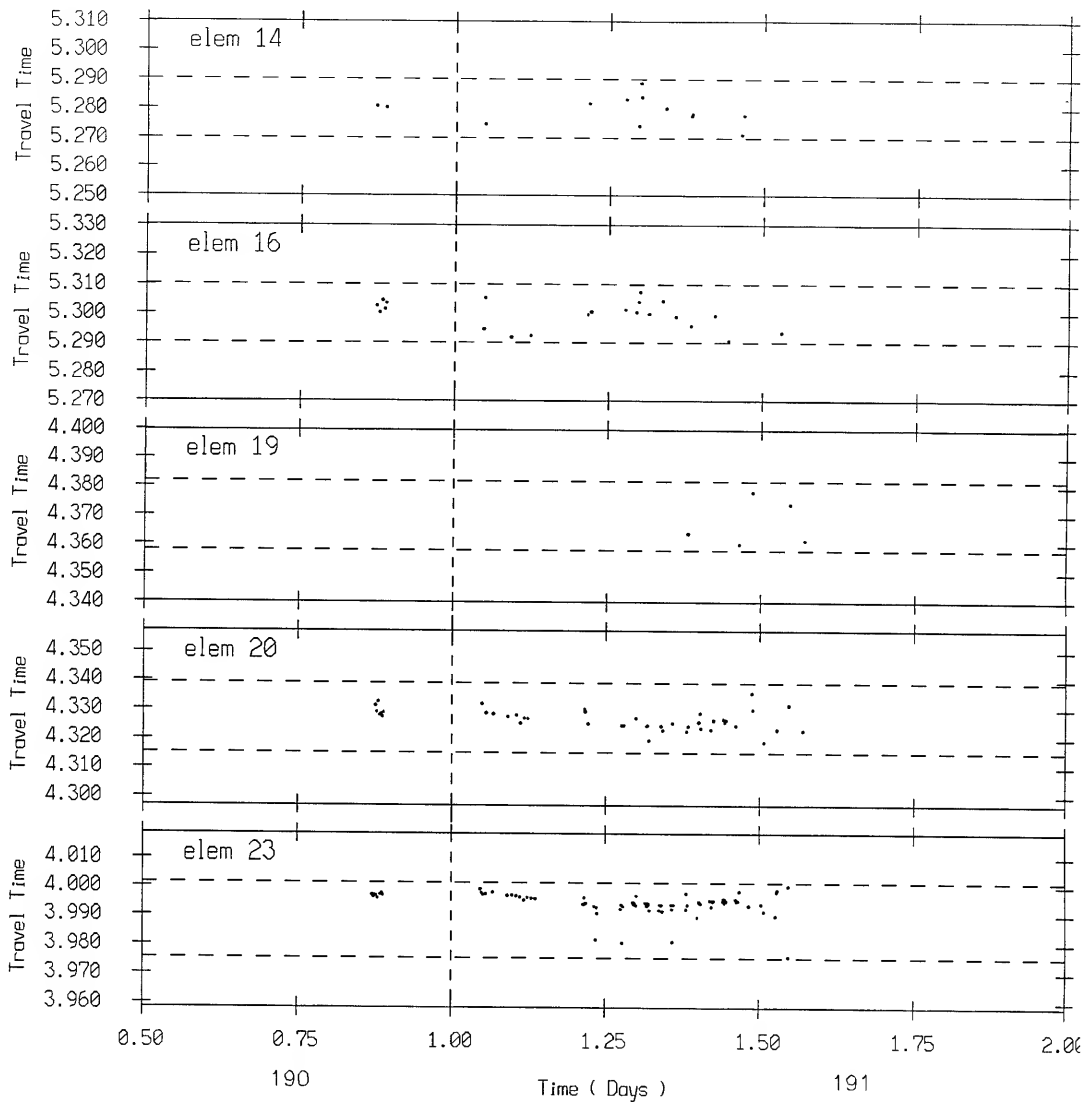
Freq: 10000

190 15:30 -> 191 14:30



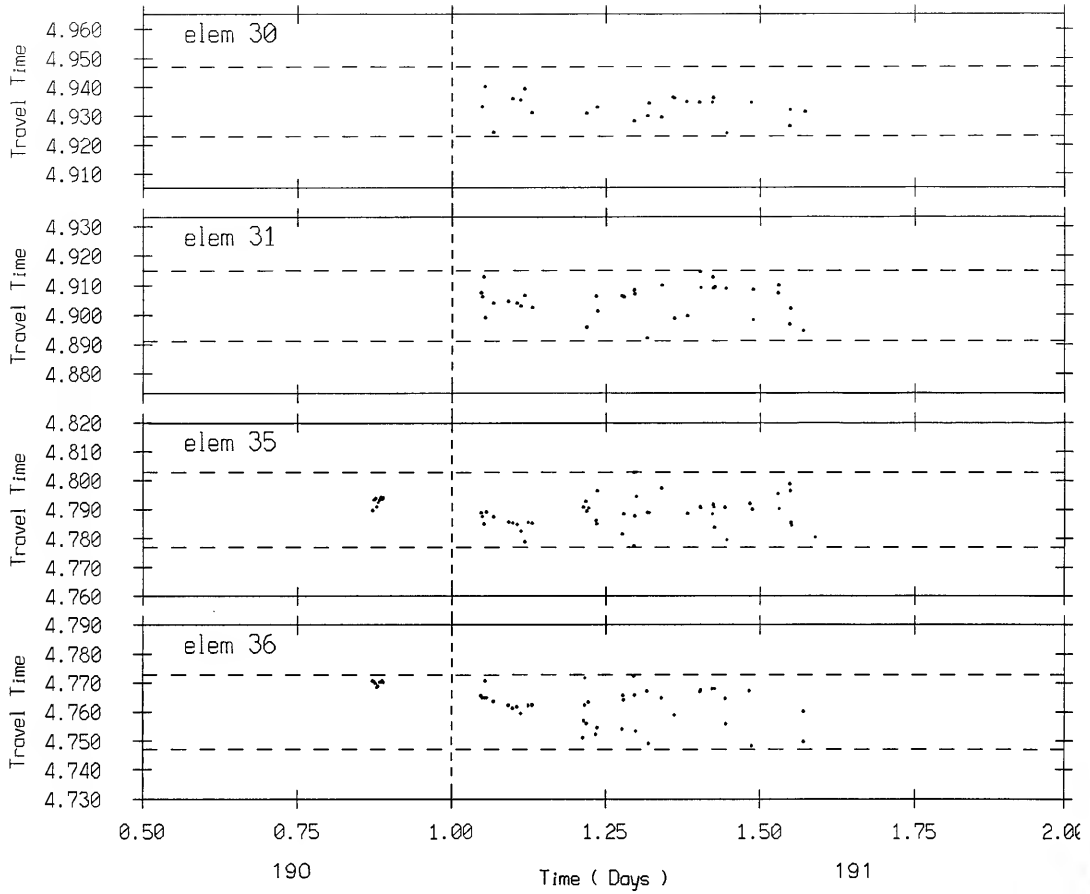
Freq: 10000

190 15:30 -> 191 14:30



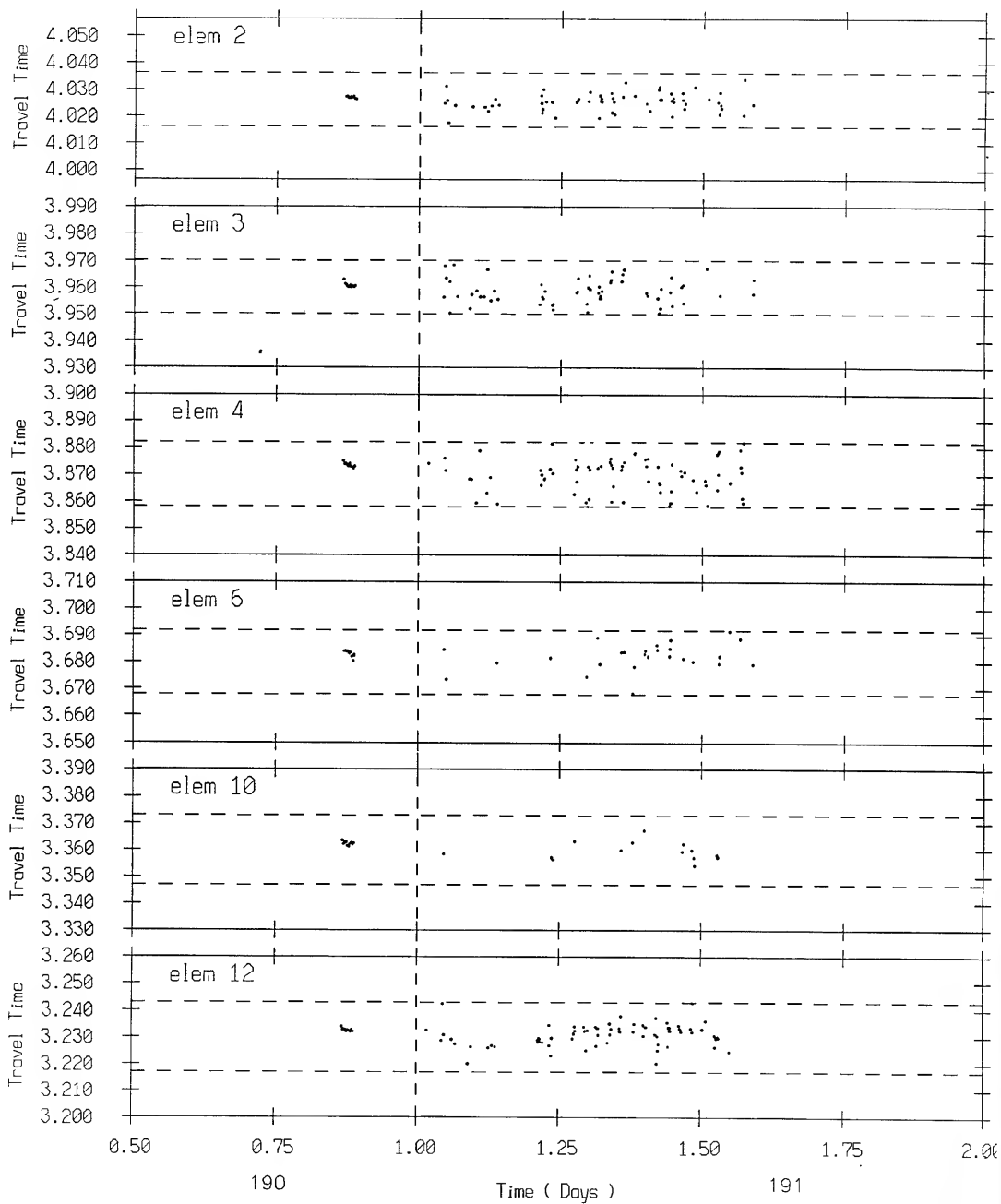
Freq: 10000

190 15:30 -> 191 14:30



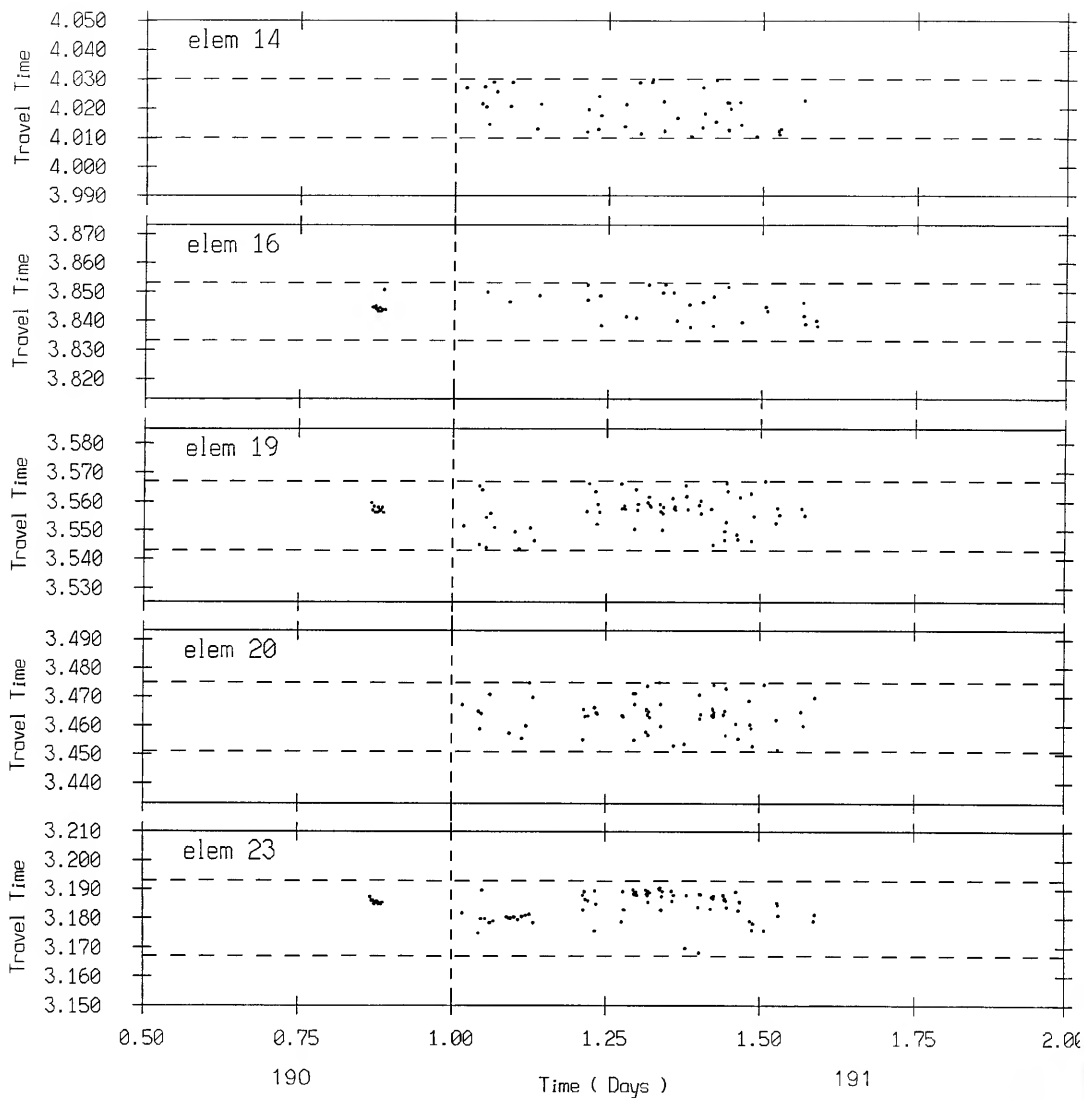
Freq: 10500

190 15:30 -> 191 14:30



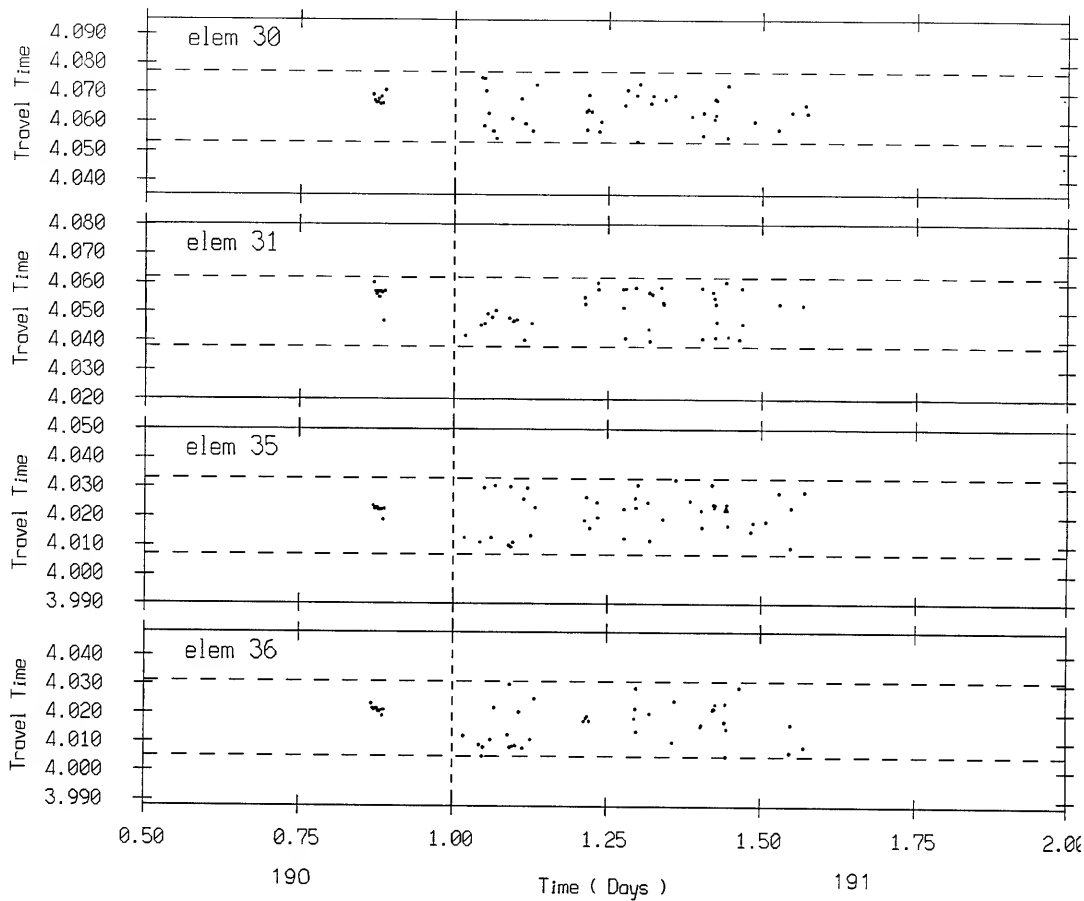
Freq: 10500

190 15:30 -> 191 14:30



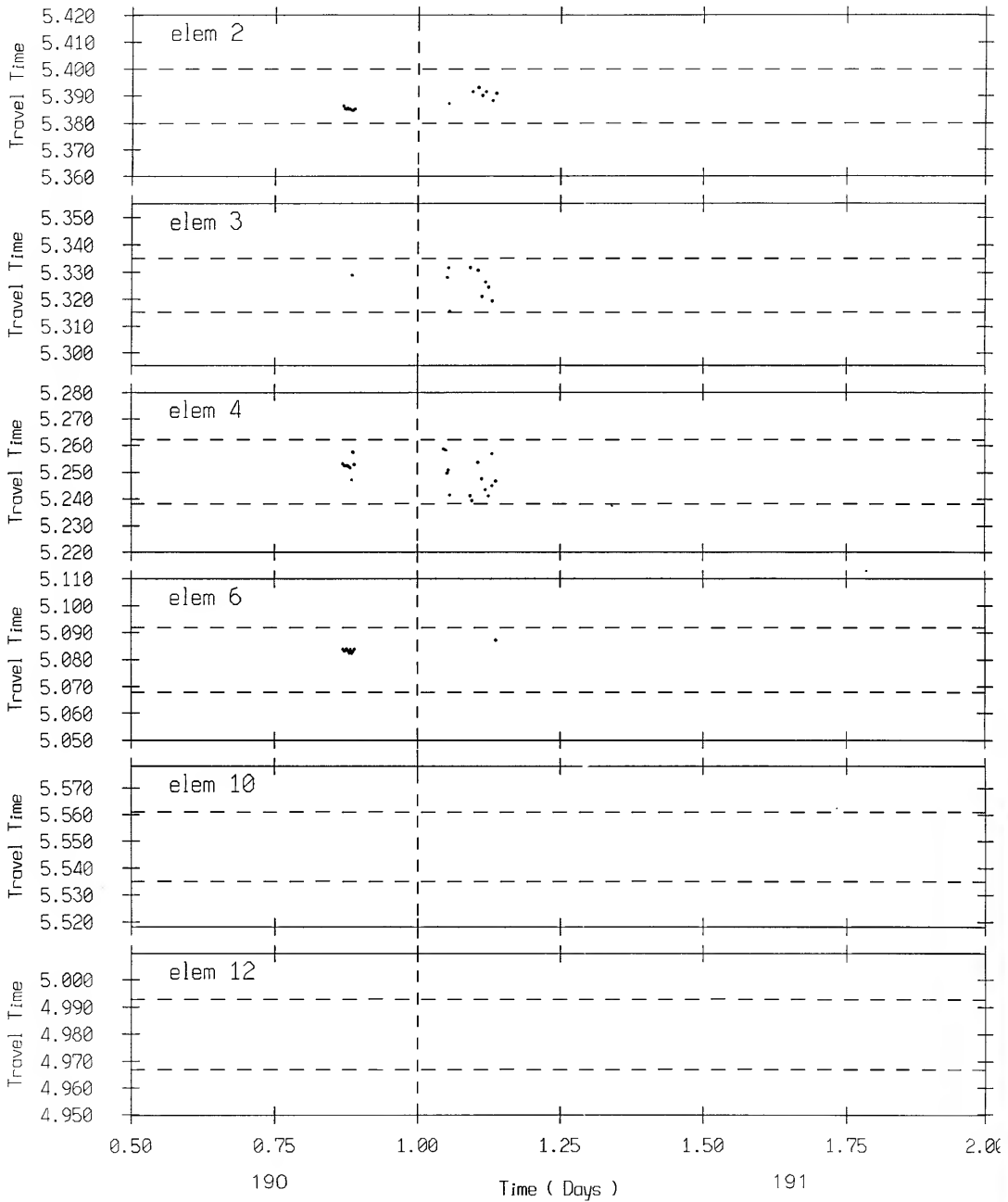
Freq: 10500

190 15:30 -> 191 14:30



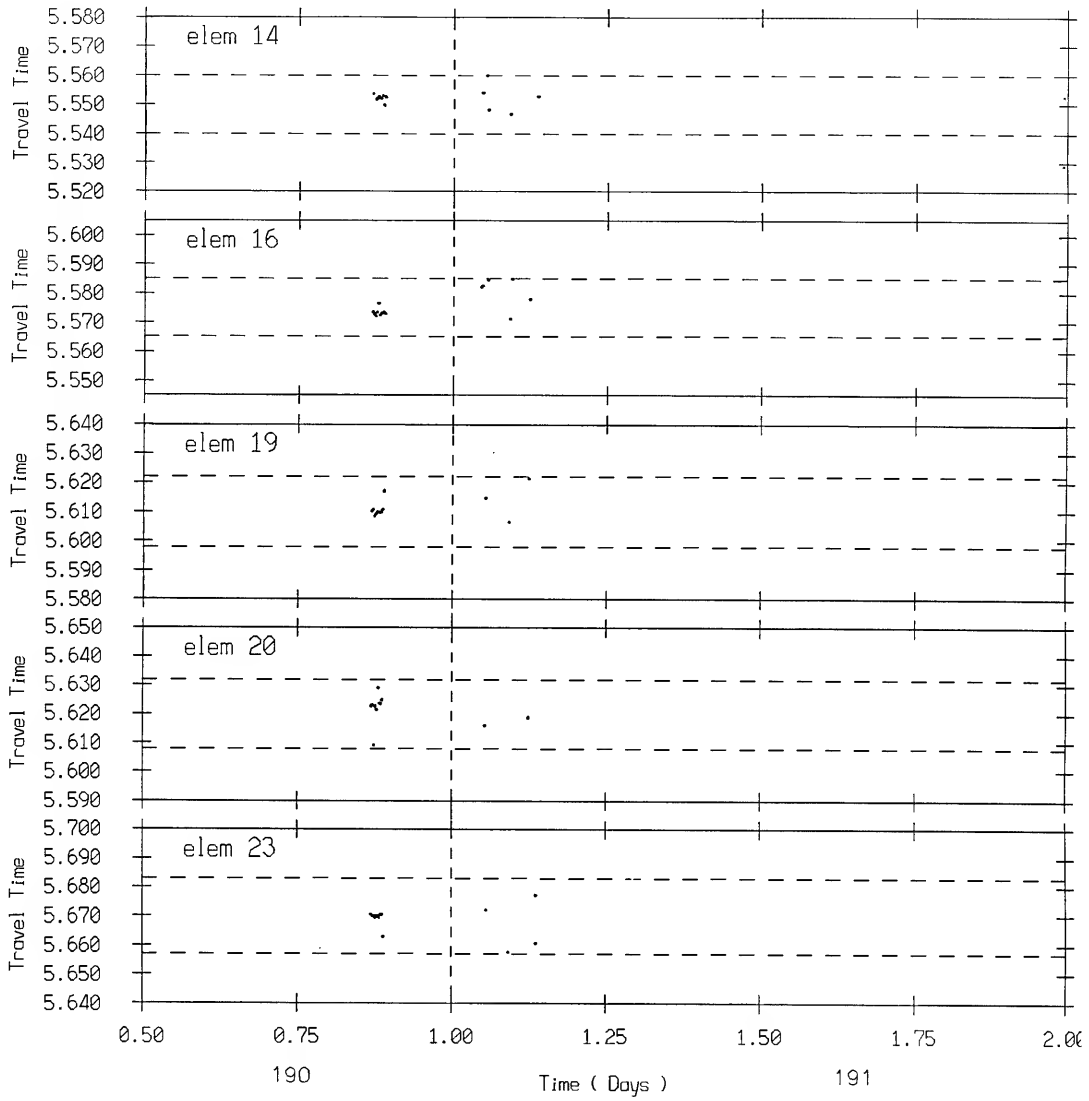
Freq: 13000

190 15:30 -> 191 14:30



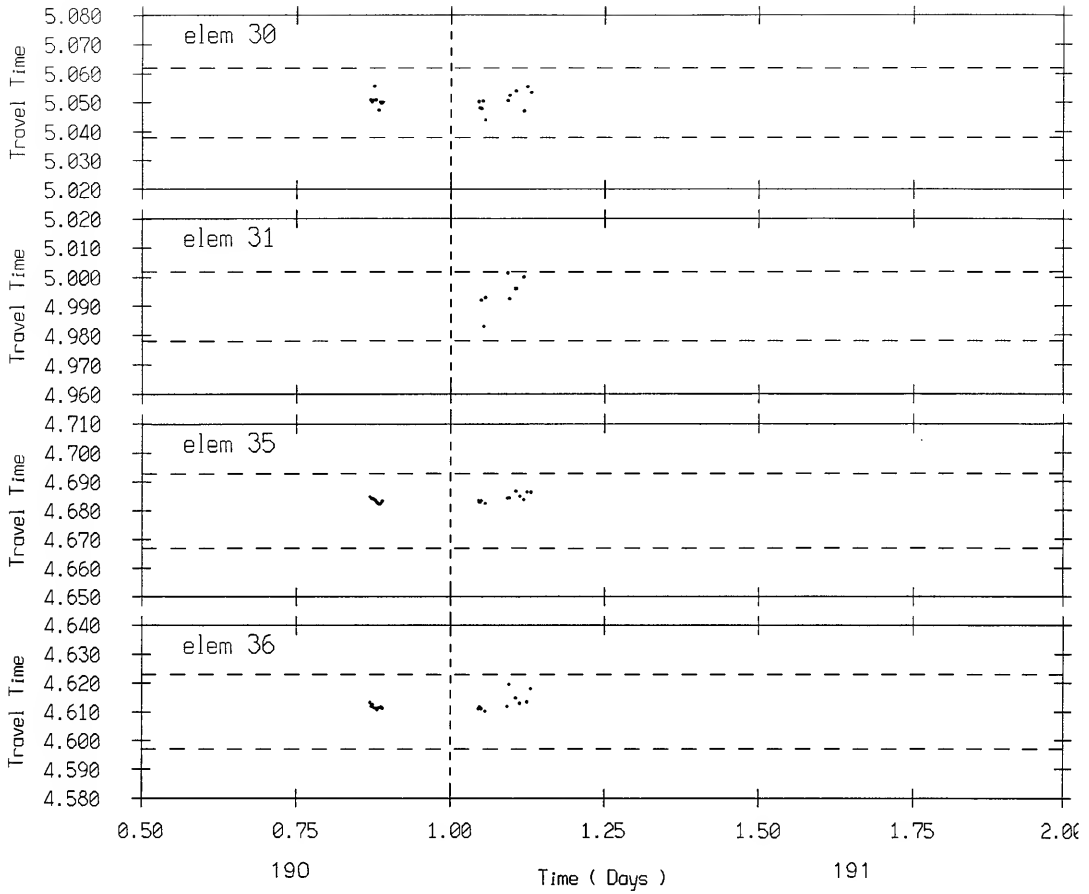
Freq: 13000

190 15:30 -> 191 14:30



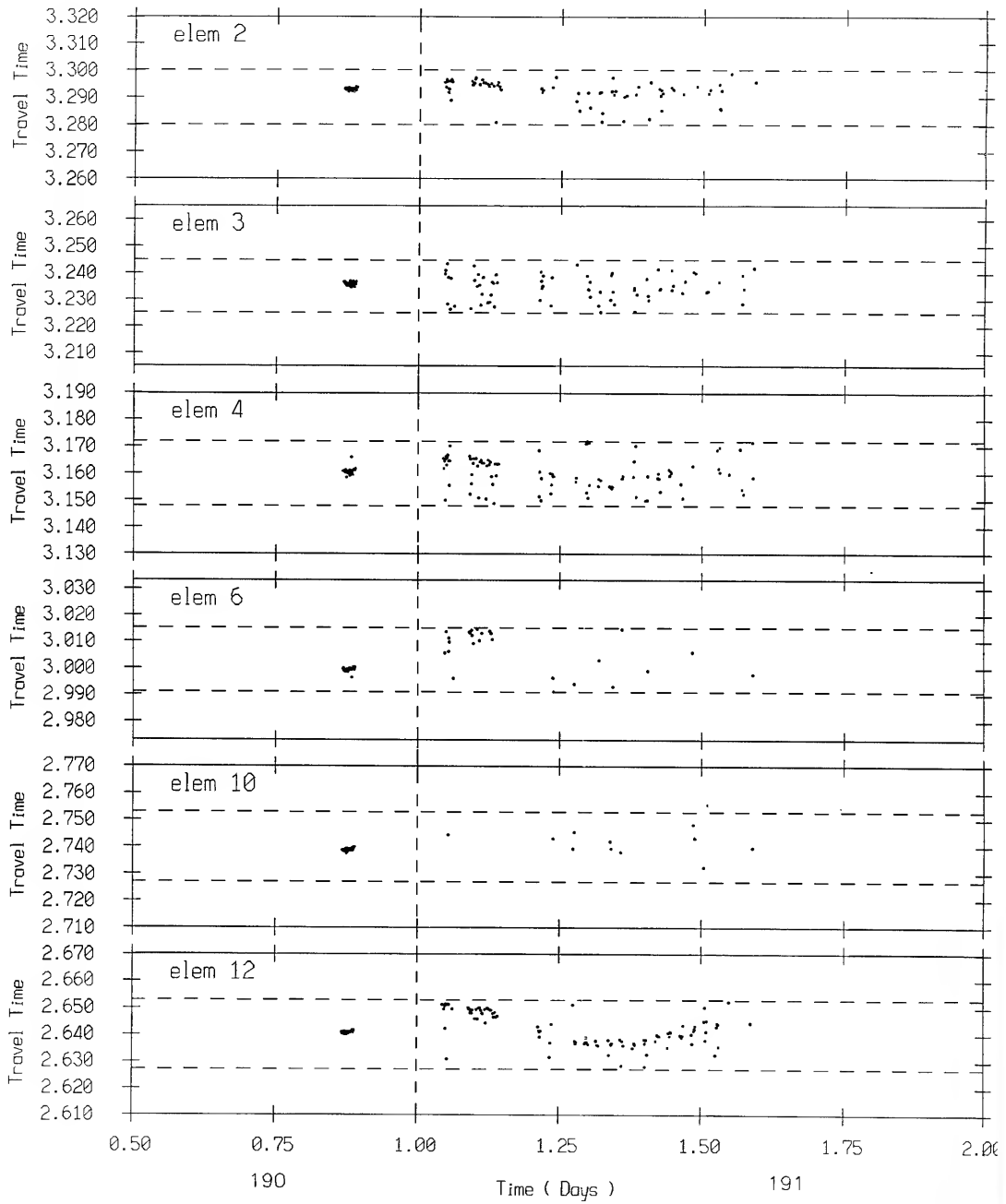
Freq: 13000

190 15:30 -> 191 14:30



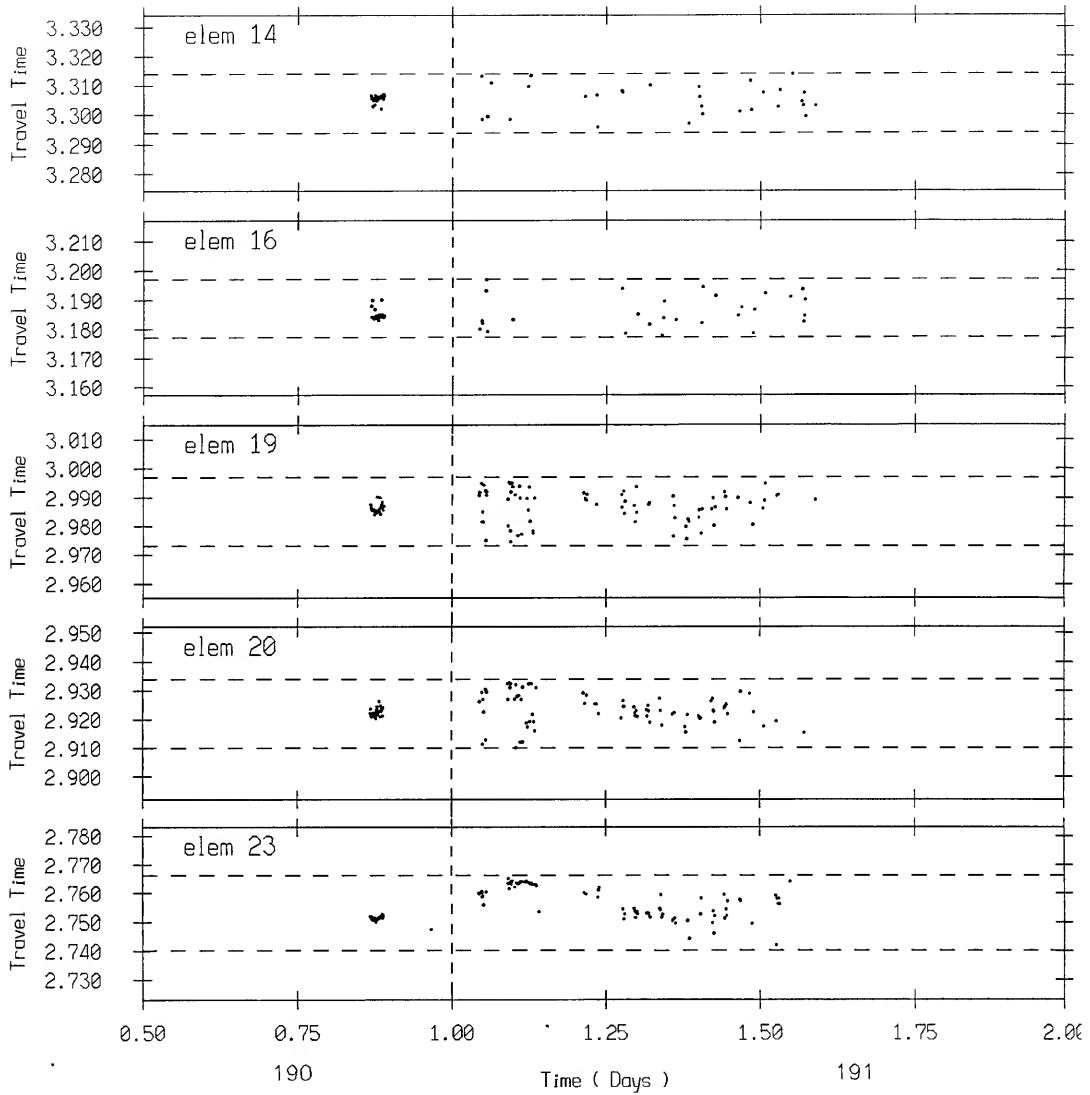
Freq: 13500

190 15:30 -> 191 14:30



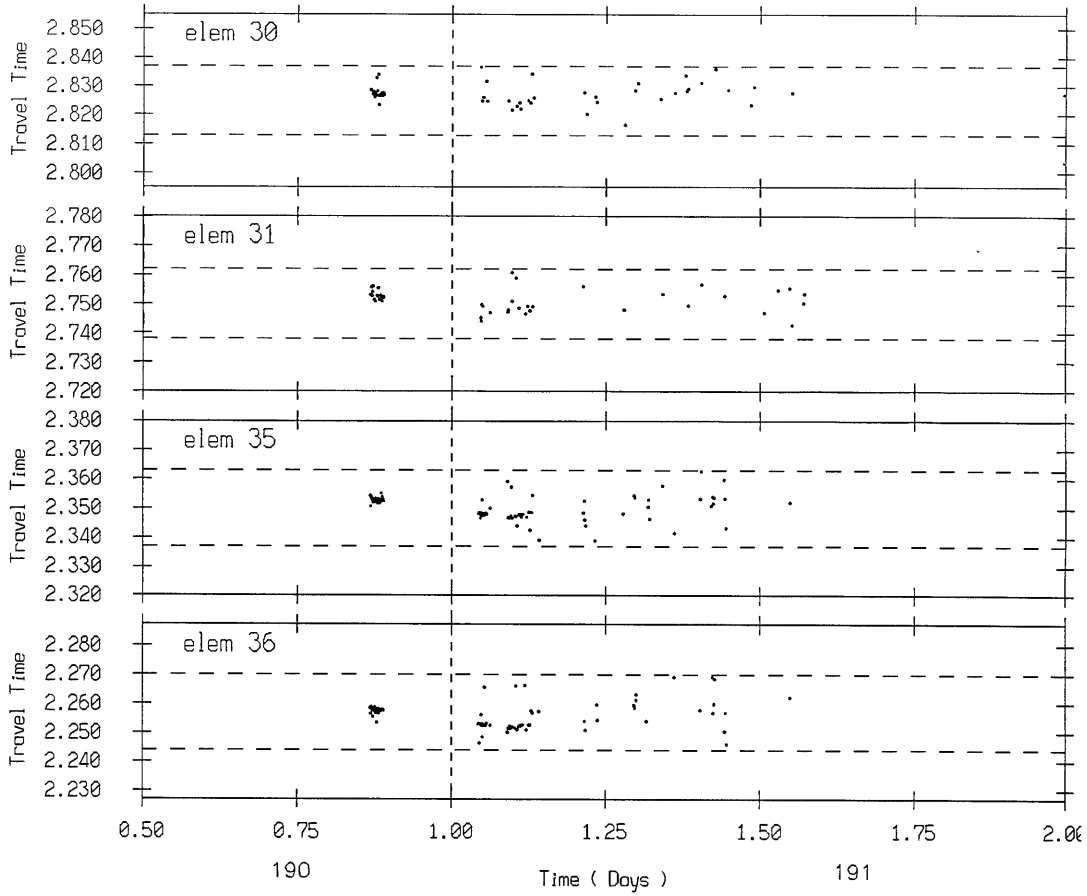
Freq: 13500

190 15:30 -> 191 14:30



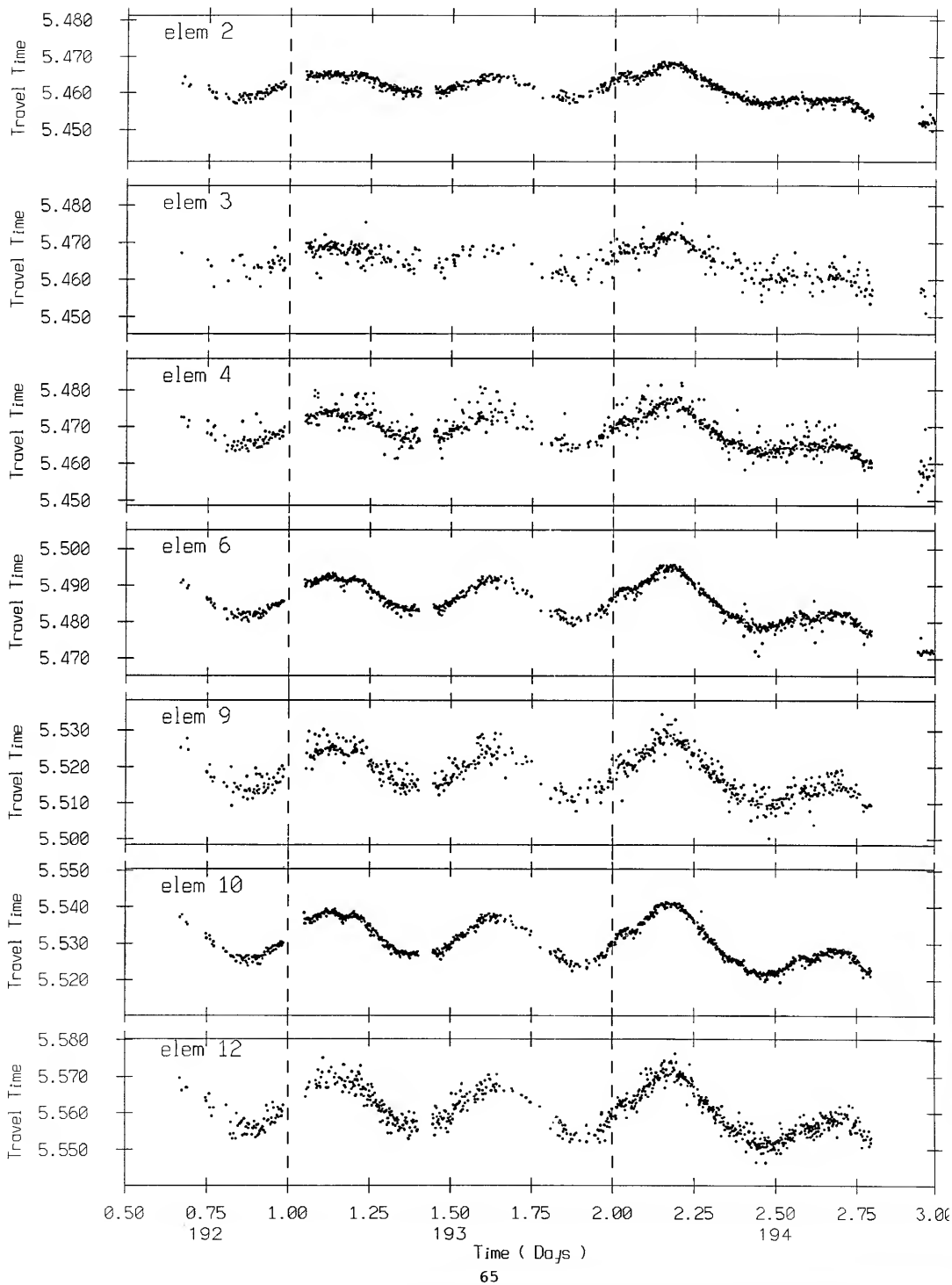
Freq: 13500

190 15:30 -> 191 14:30



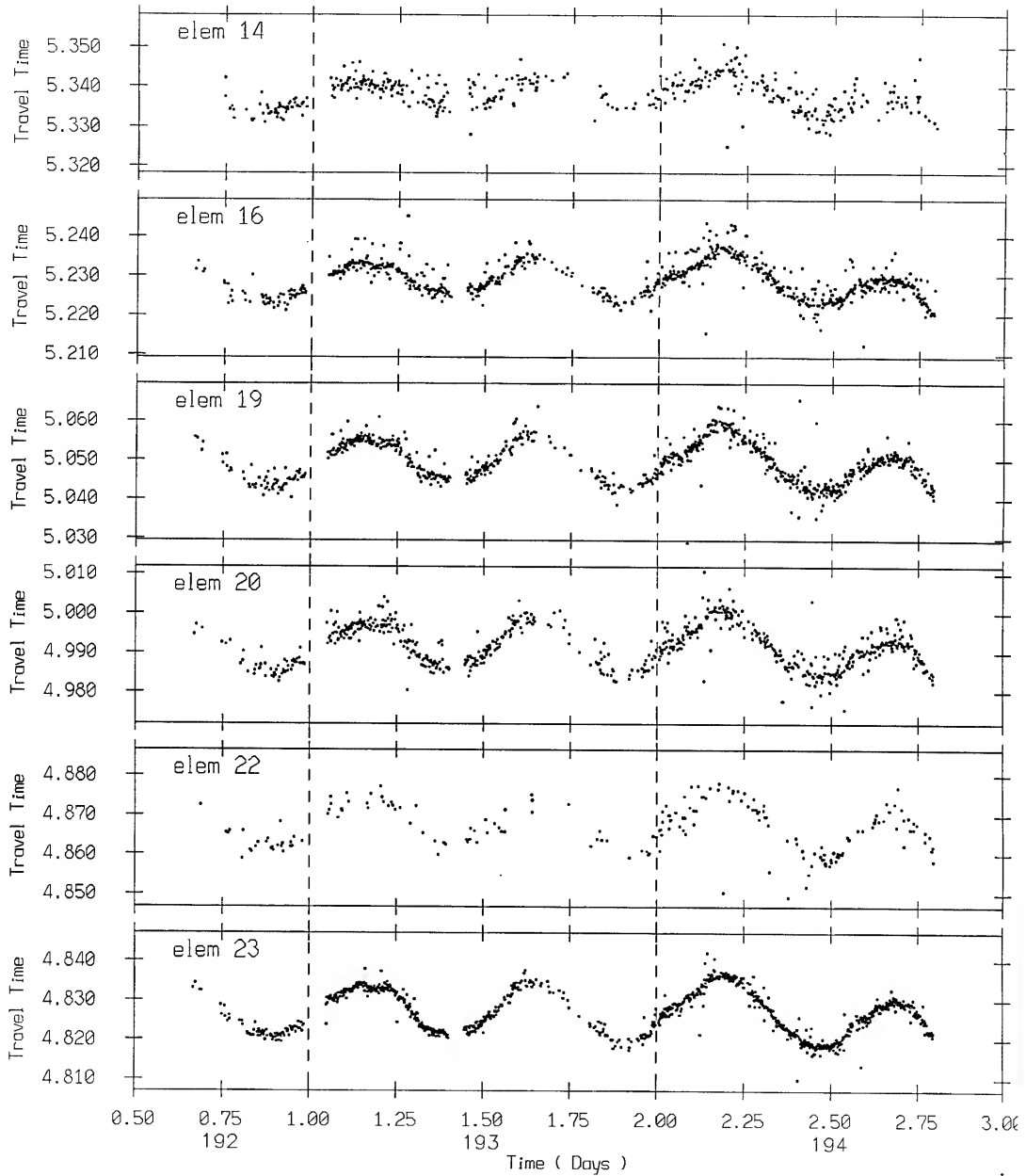
Freq: 9500

192 15:10 -> 194 24:00



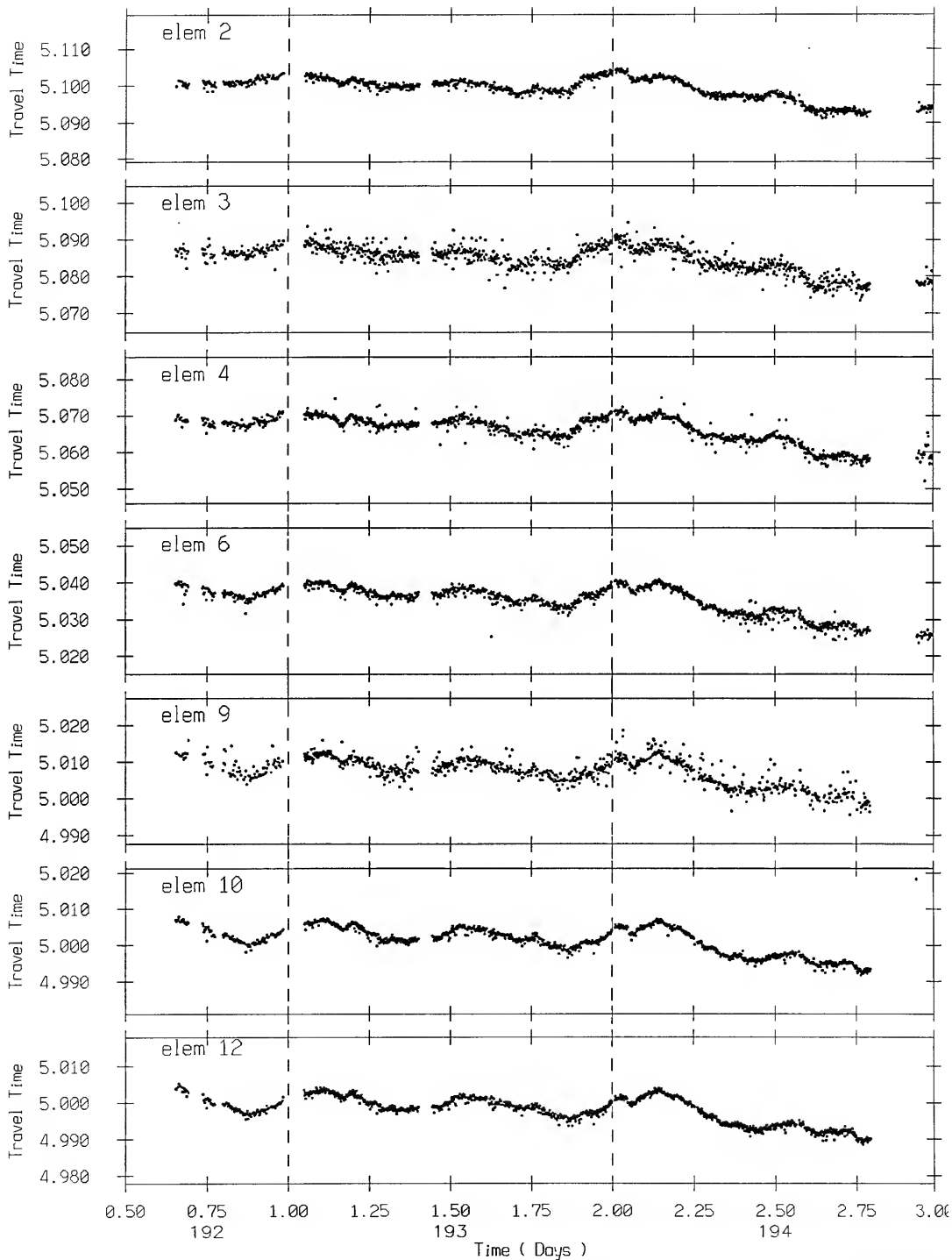
Freq: 9500

192 15:10 -> 194 24:00



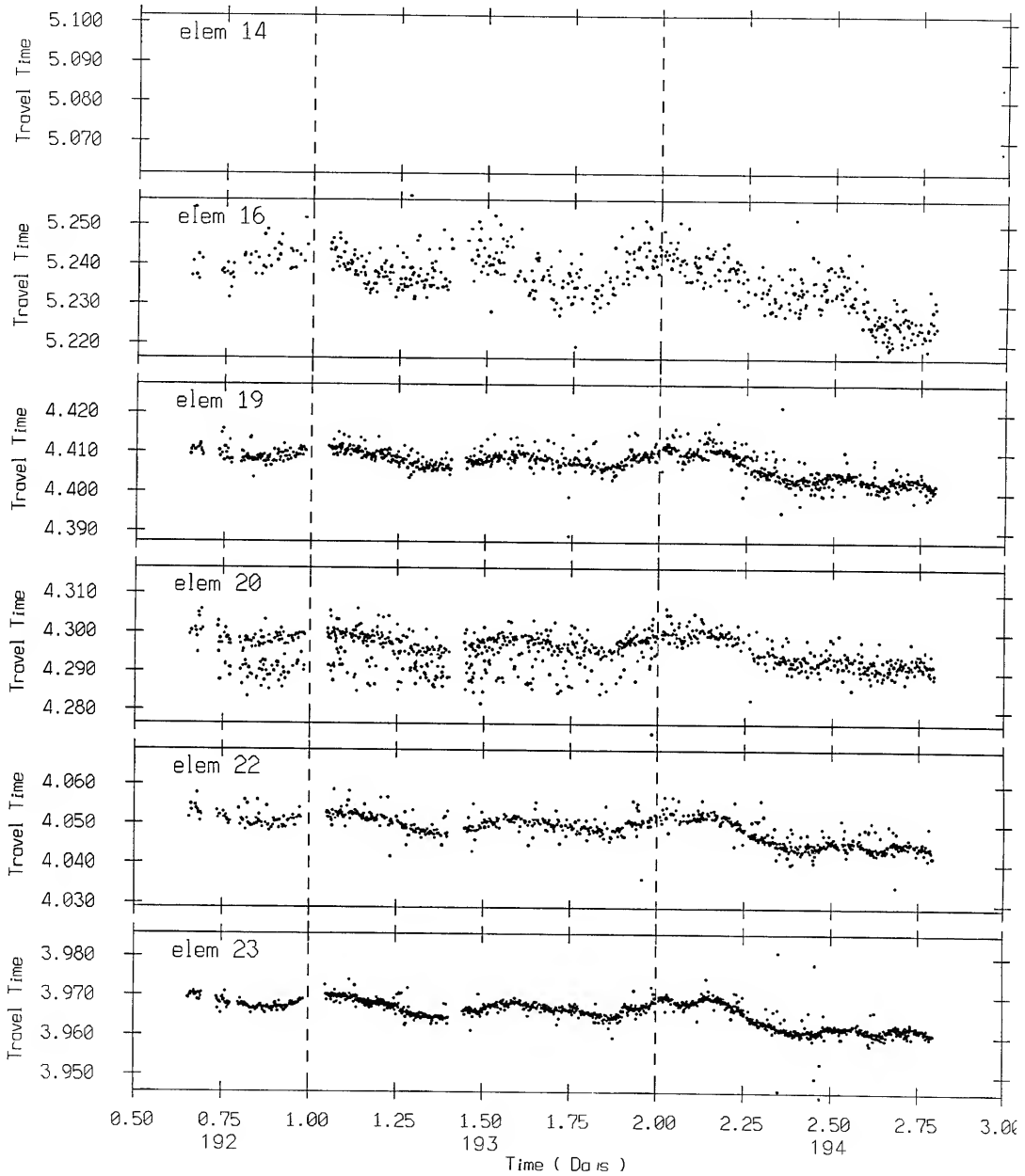
Freq: 10000

192 15:10 -> 194 24:00



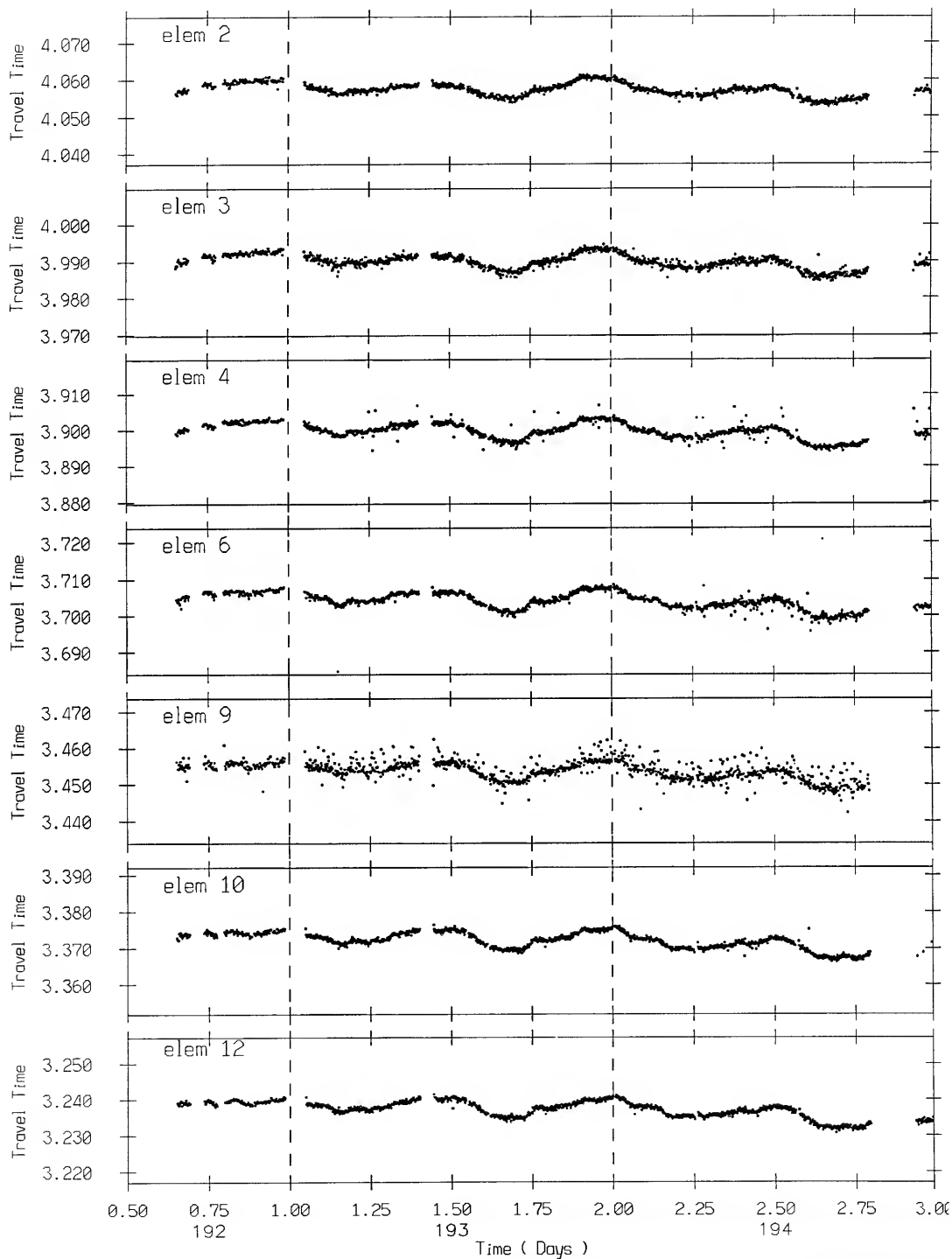
Freq: 10000

192 15:10 -> 194 24:00



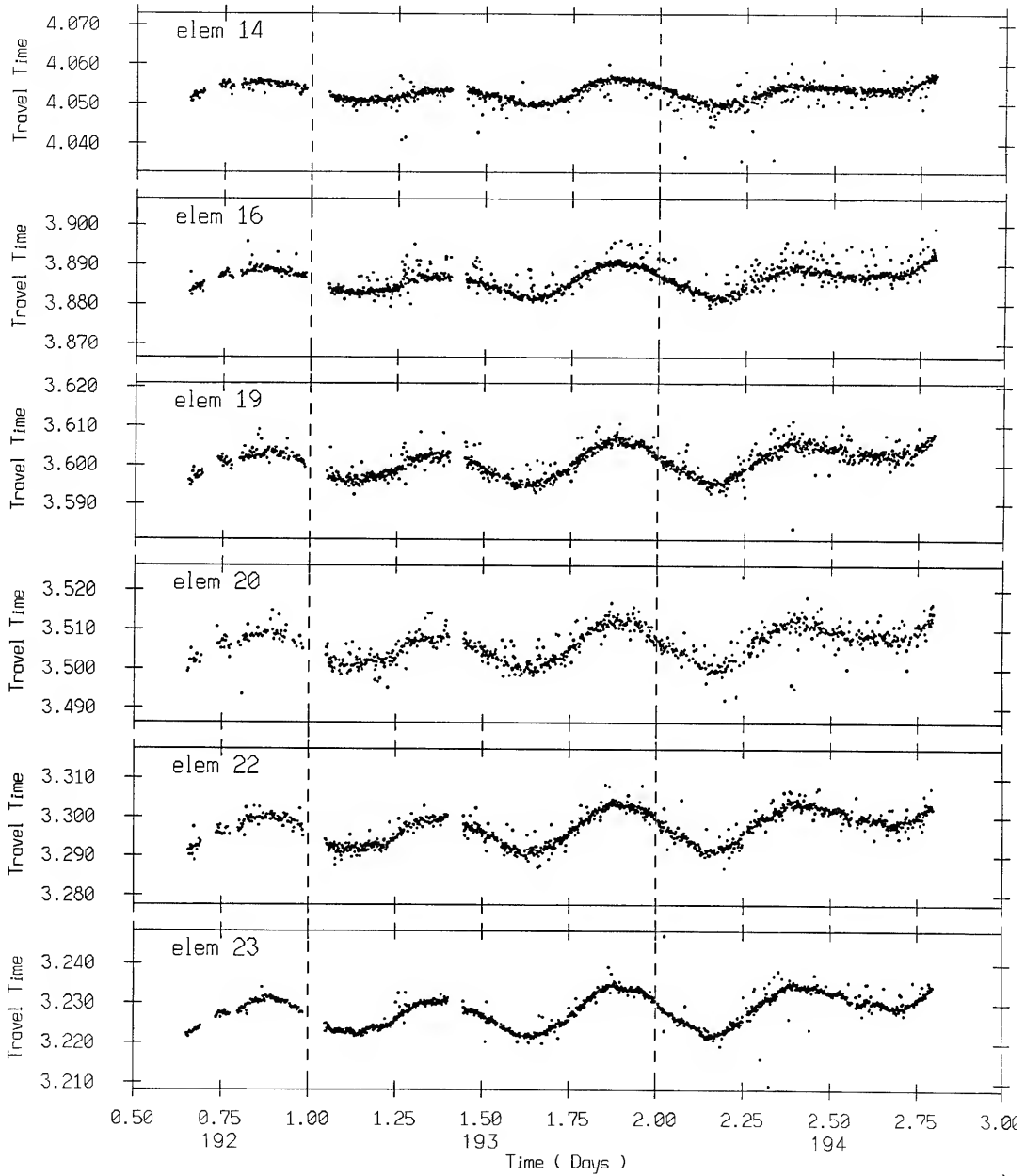
Freq: 10500

192 15:10 -> 194 24:00



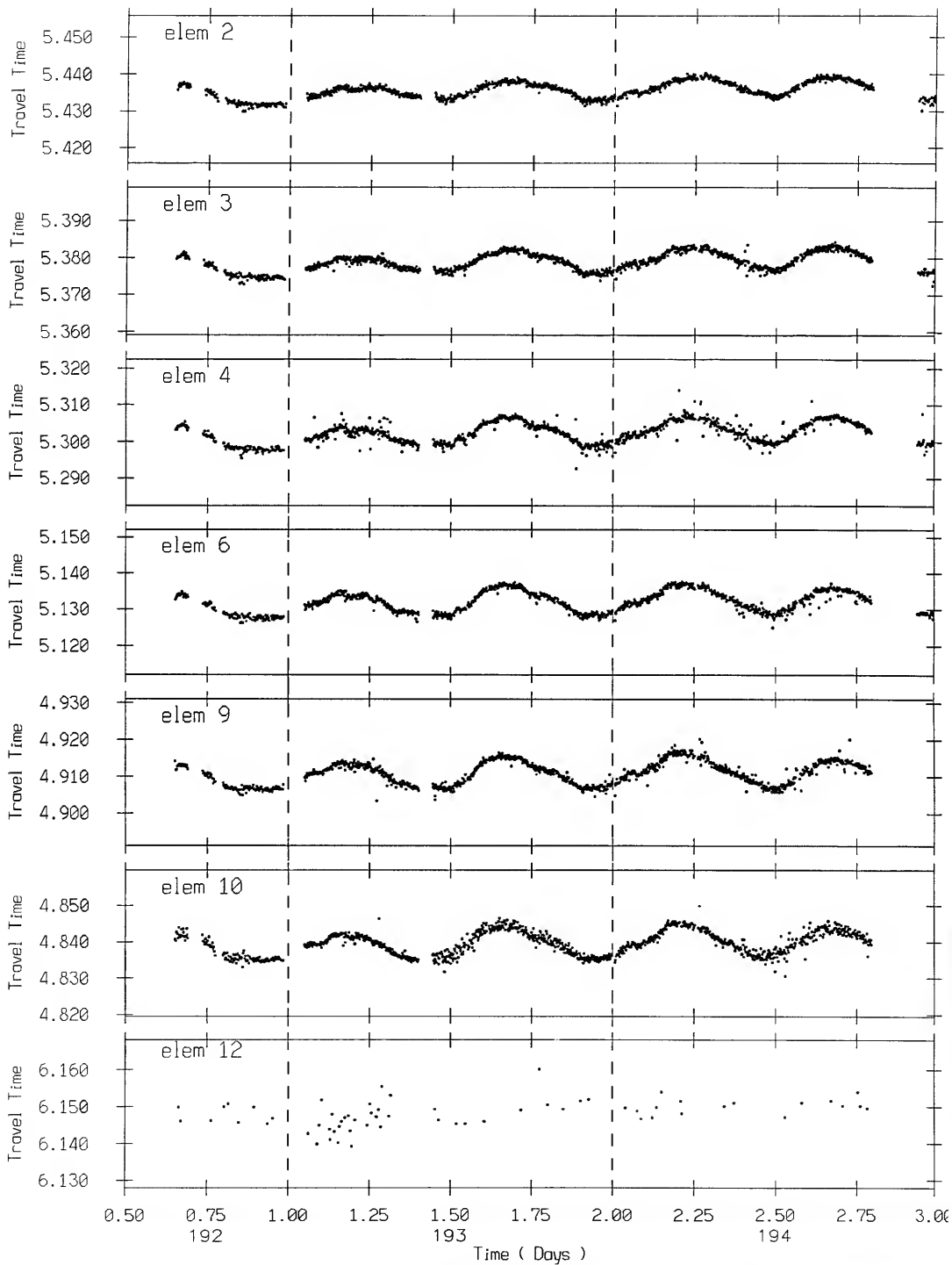
Freq: 10500

192 15:10 -> 194 24:00



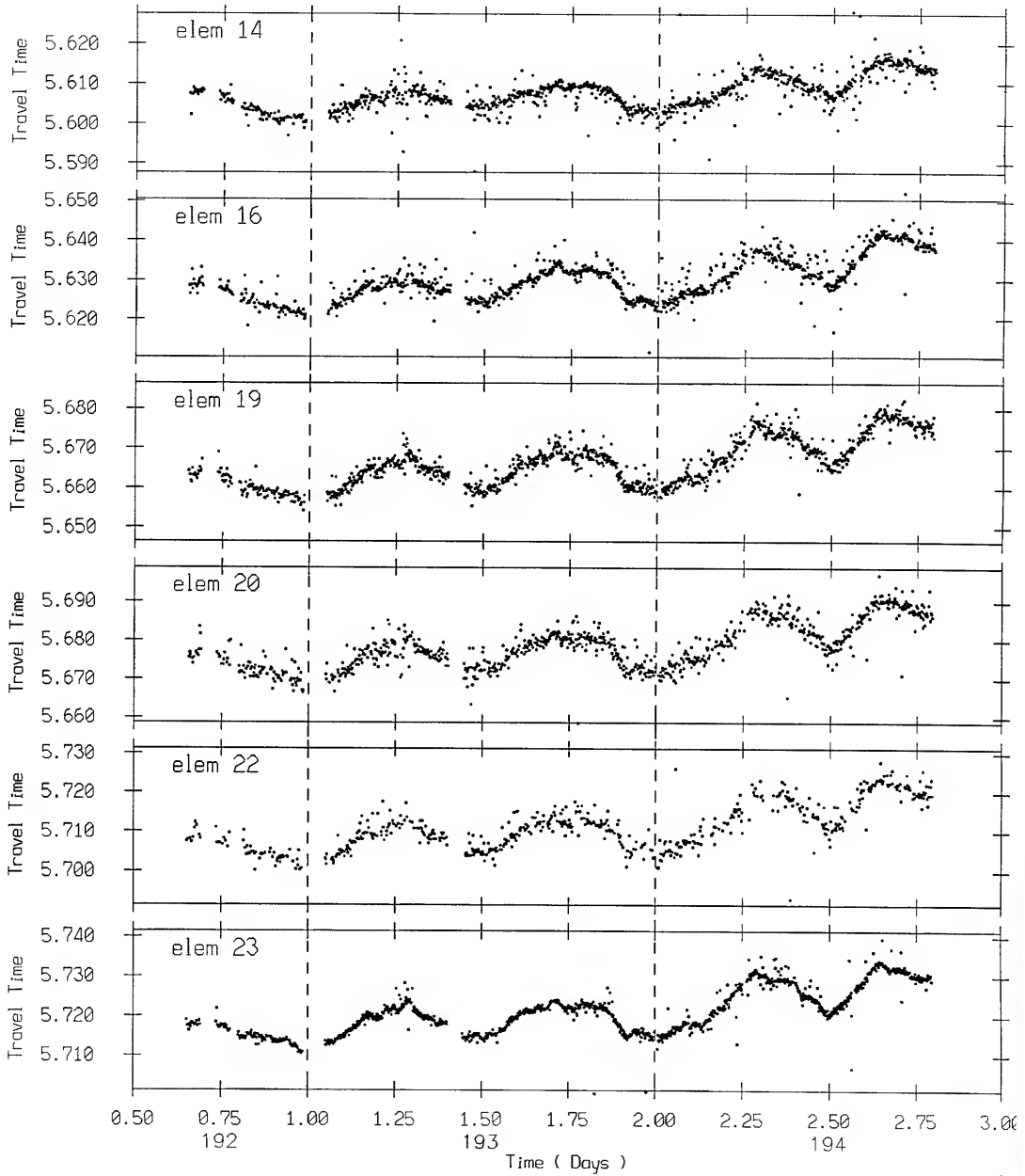
Freq: 13000

192 15:10 -> 194 24:00



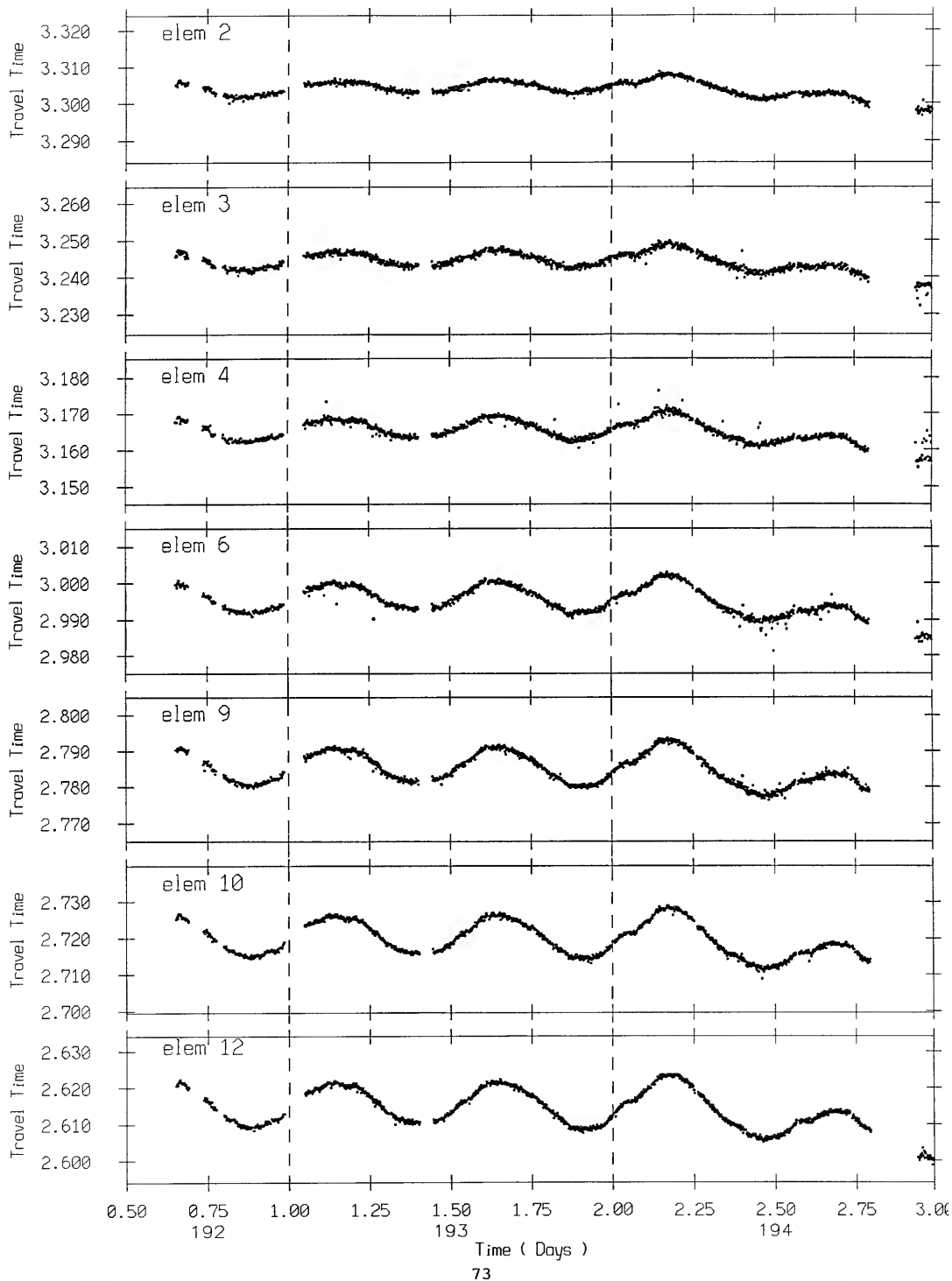
Freq: 13000

192 15:10 -> 194 24:00



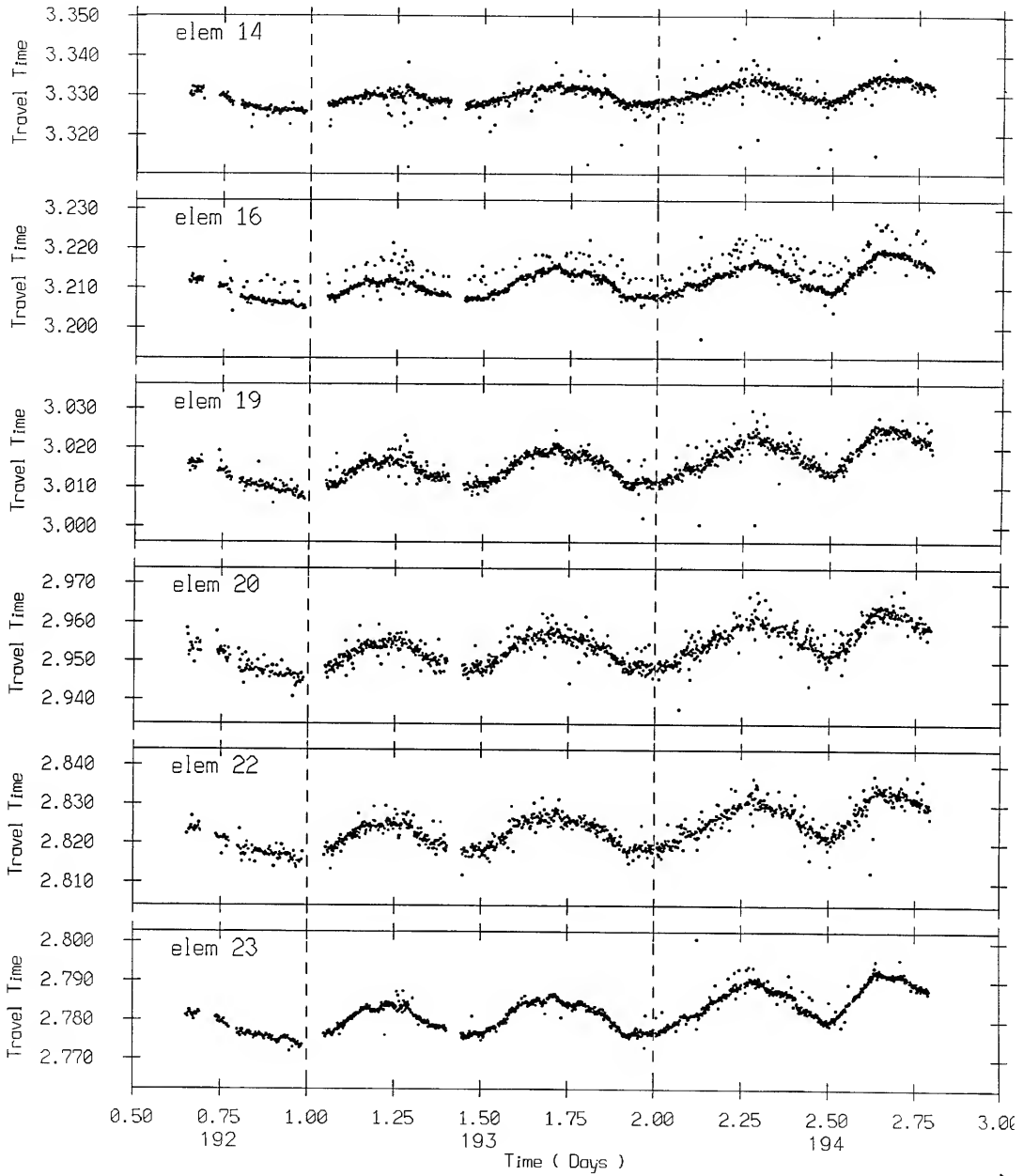
Freq: 13500

192 15:10 -> 194 24:00



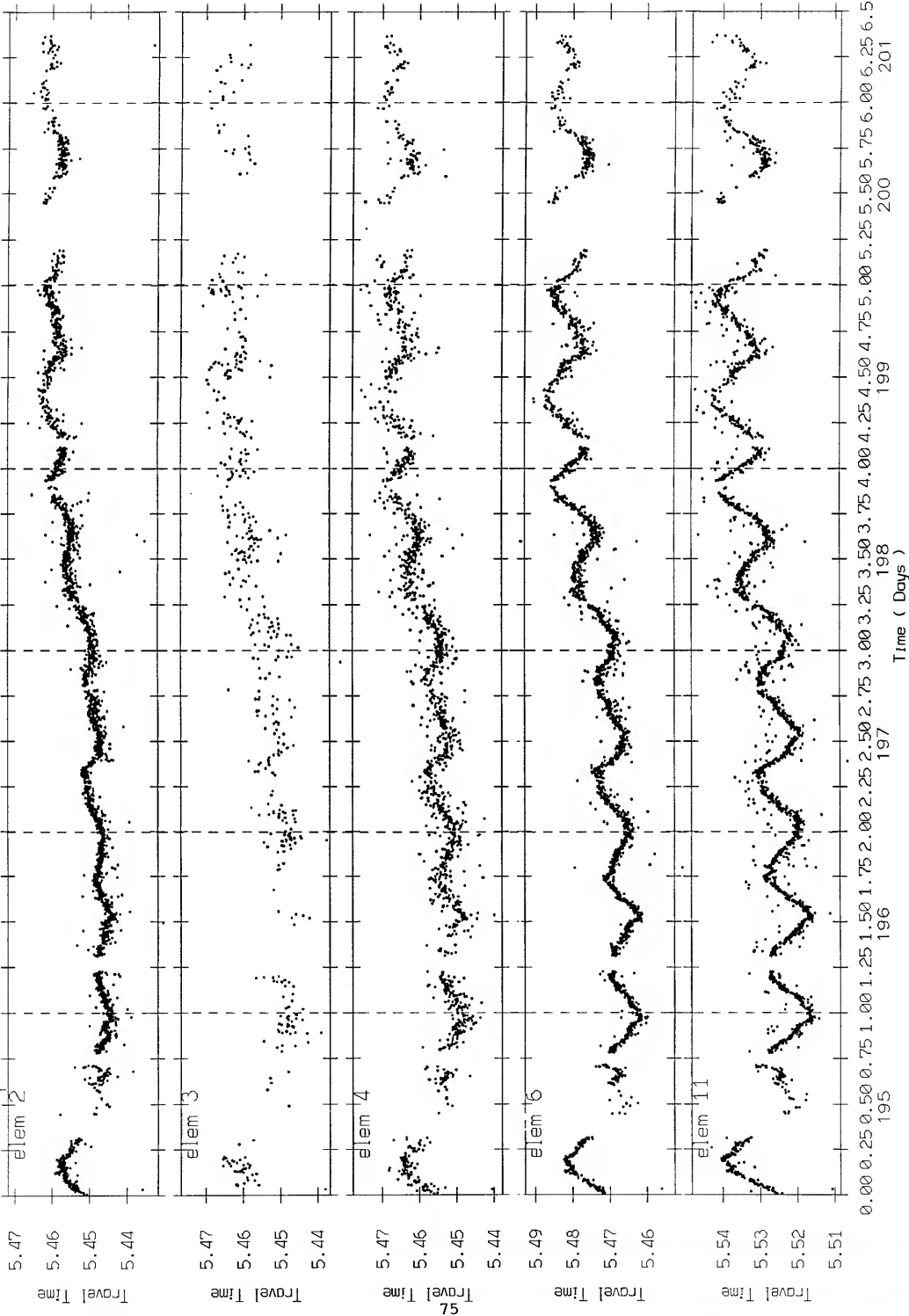
Freq: 13500

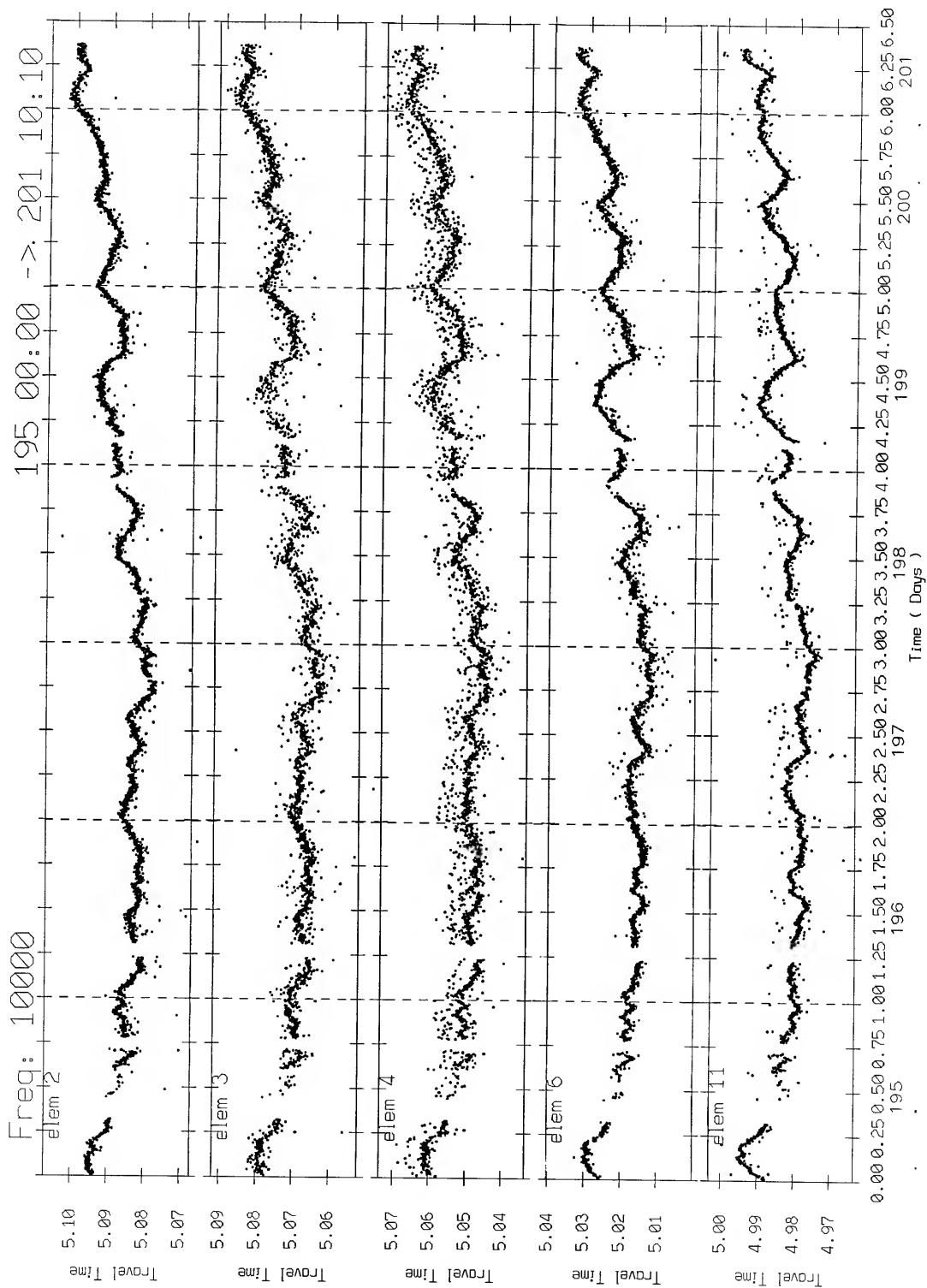
192 15:10 -> 194 24:00

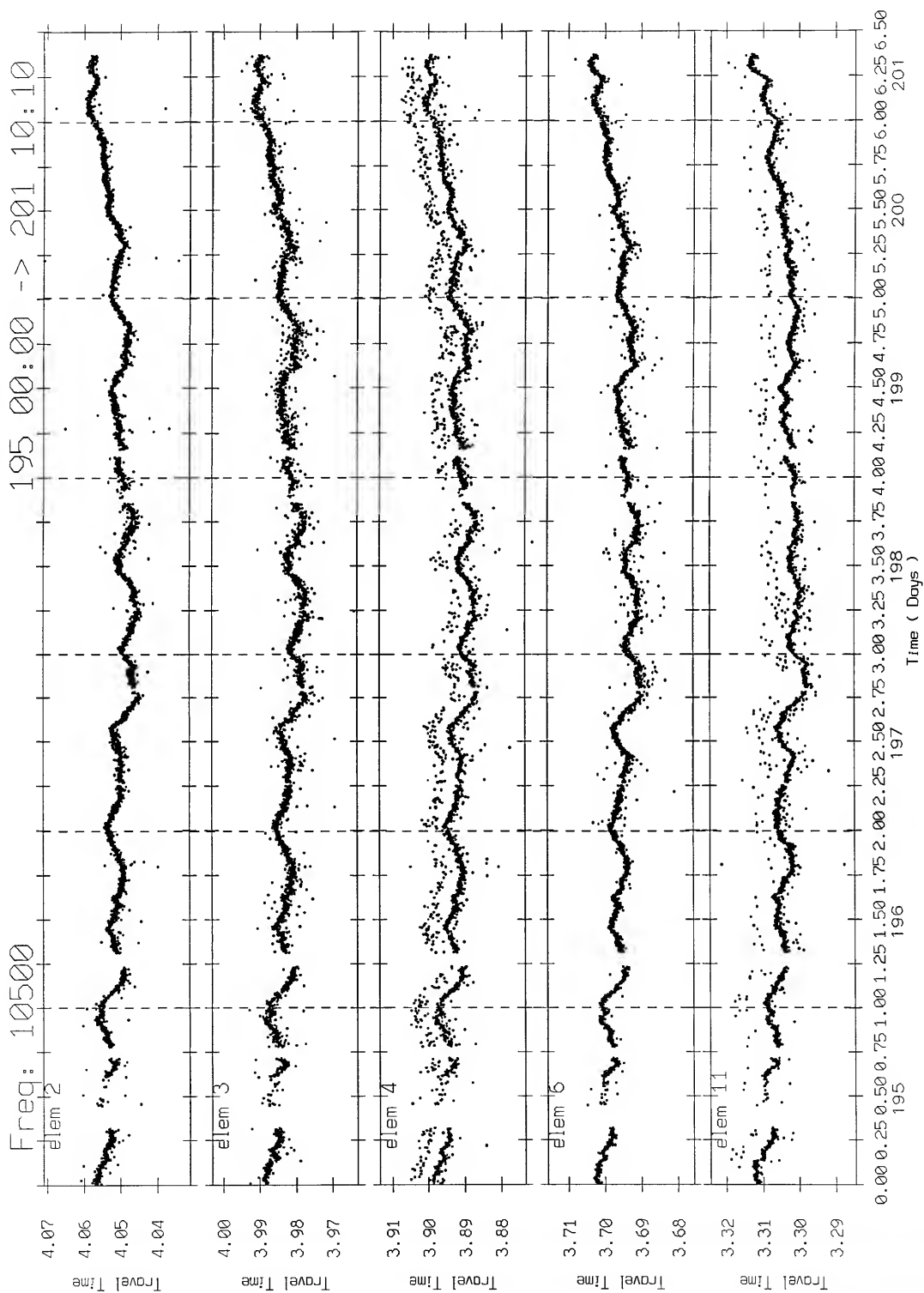


Freq: 9500

195 00:00 -> 201 10:10

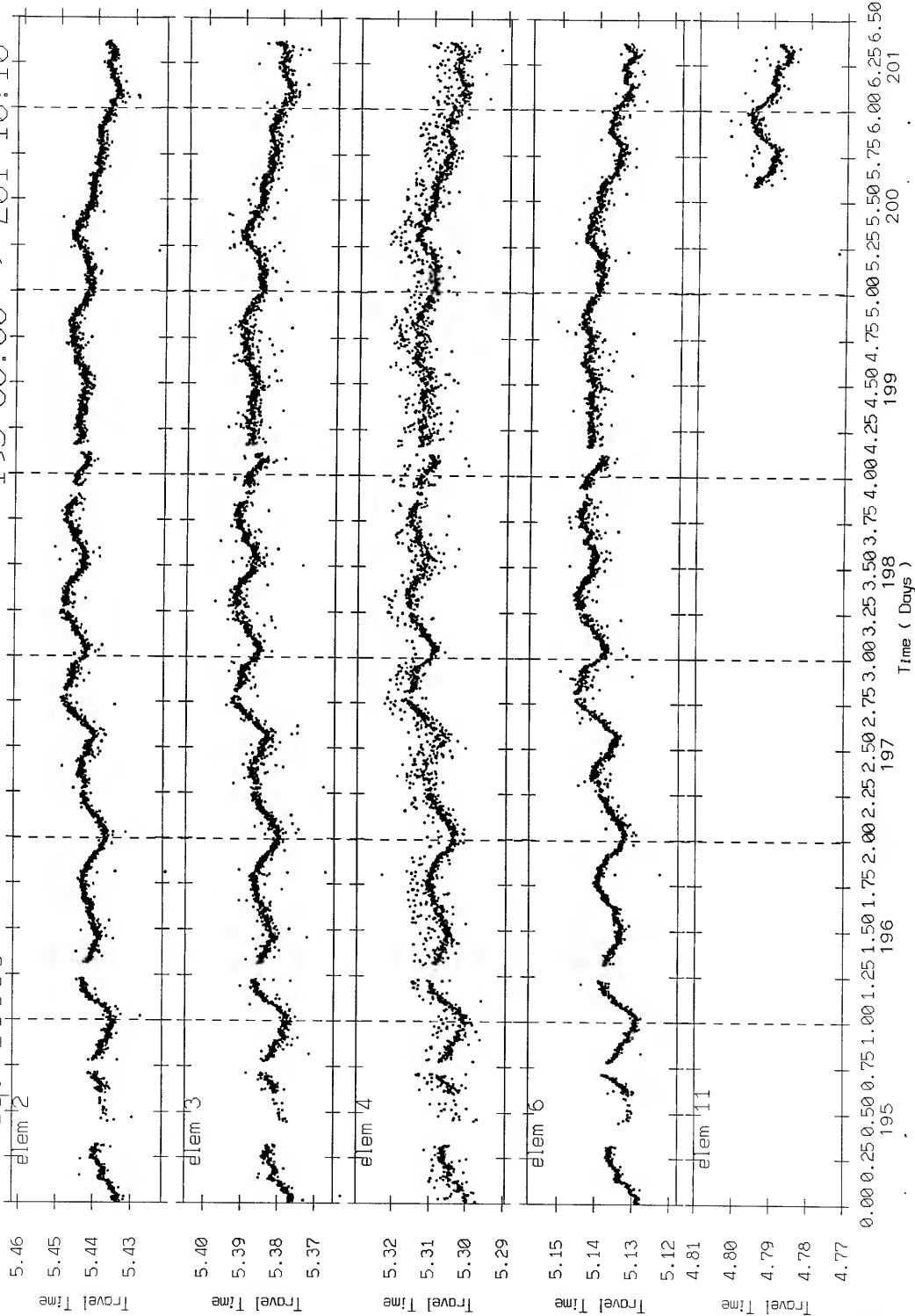


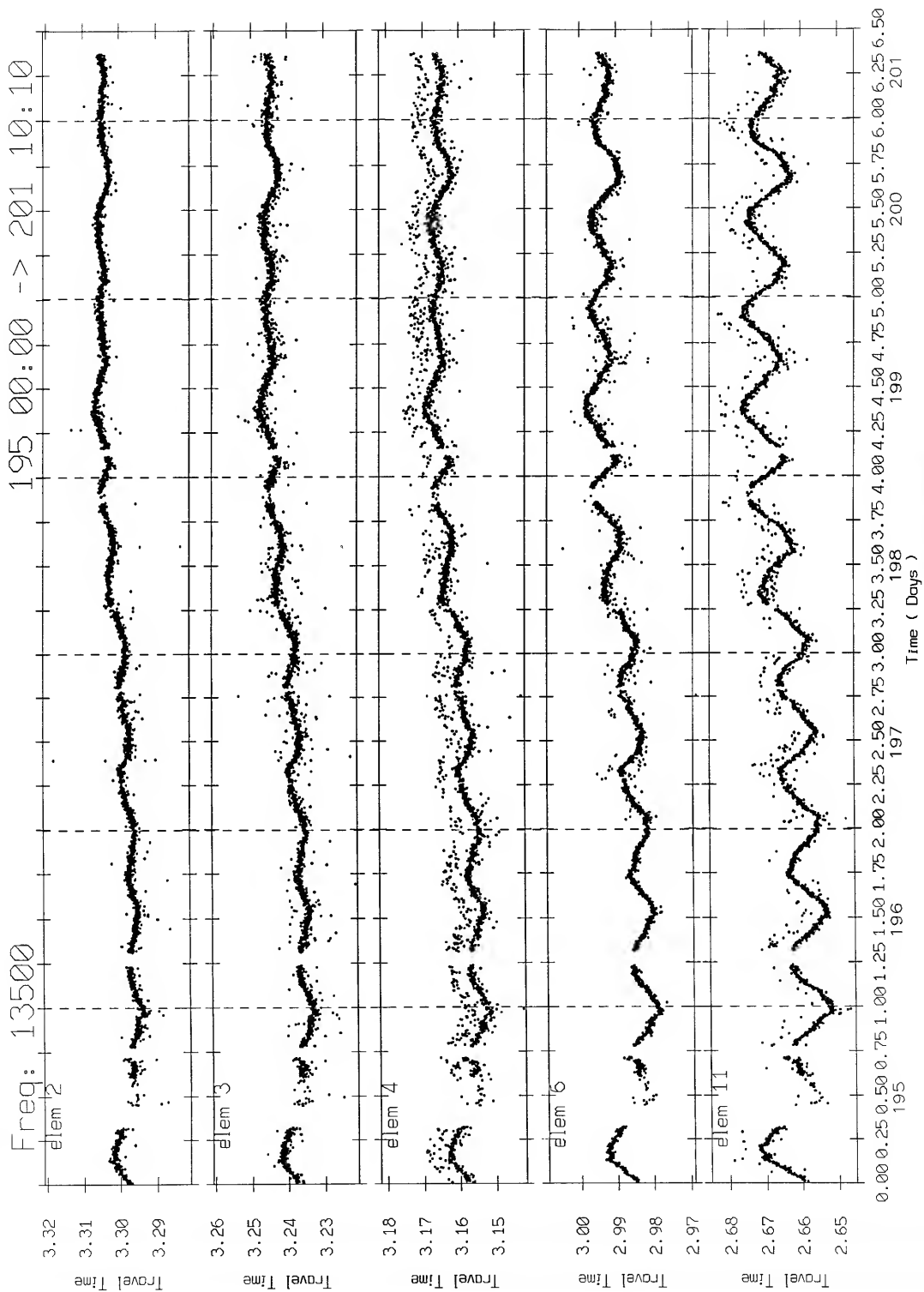




Freq: 13000

195 00:00 -> 201 10:10





Appendix C. Bias Correction Plots

The plots demonstrate how an appropriate bias number was derived for correcting slant ranges so as to reduce the array navigation bias error. A justification for this procedure is described in Figure 4.

Two techniques were used and their results averaged. Each line connecting dots on the plots represents an array element.

The first technique was to simply subtract a bias (from zero to sixteen meters) and compute the RMS error. The winner possesses the lowest RMSE.

The second technique was to subtract the travel time of the direct arrival from the surface reflected arrival, for both the actual data and a GSM simulation. This was done with a similar grid of bias numbers as in the first technique. Then these two results (for each bias number) were compared and the bias chosen that minimizes the difference.

day 195 7 8 7 8 7

7 7 8 10 7

7 7 7 9 7

-1 -1 8 -1 -1

avg = 7.60000 nsamples= 15

day 196 11 9 11 11 9

10 11 10 11 10

-1 -1 8 11 9

-1 11 11 11

avg = 10.18750 nsamples= 16

day 197 10 9 8 9 8

10 10 10 11 9

-1 10 9 11 9

-1 11 10 -1 11

avg = 9.64706 nsamples= 17

day 198 11 11 10 11 10

11 11 11 11 11

-1 -1 11 11 11

-1 11 11 -1 11

avg = 10.8750 nsamples= 16

day 199 9 7 9 8 8

10 9 10 11 9

-1 10 9 11 9

-1 11 10 -1 -1

avg = 9.31250 nsamples= 16

day 200 -1 11 10 11 10

-1 11 11 11 11

-1 -1 11 11 10

-1 -1 11 -1 11

avg = 10.7692 nsamples= 13

day 201 -1 11 11 11 7

-1 11 7 11 7

-1 -1 -1 11 7

-1 7 7 -1 7

avg = 8.66667 nsamples= 12

totavg = 9.60000

day 195 5 5 5 5 9

RMSE 0.5 1.4 0.8 0.6 0.4

RMSE(10) 1.1 1.5 1.2 1.3 0.4

avg= 6.20

day 196 4 5 4 4 9

RMSE 0.5 0.9 0.6 0.6 0.3

RMSE(10) 1.2 1.3 1.3 1.4 0.3

avg= 5.20

day 197 4 5 4 4 9

RMSE 0.5 0.9 0.6 0.6 0.3

RMSE(10) 1.3 1.4 1.3 1.5 0.3

avg= 5.20

day 198 4 5 4 4 8

RMSE 0.5 1.1 0.5 0.6 0.3

RMSE(10) 1.3 1.4 1.3 1.5 0.4

avg= 5.00

day 199 4 5 4 4 6

RMSE 0.5 0.7 0.7 0.5 0.3

RMSE(10) 1.2 1.1 1.4 1.4 0.4

avg= 4.60

day 200 4 7 4 4 4

RMSE 0.4 1.5 0.6 0.5 0.7

RMSE(10) 1.1 1.6 1.3 1.4 0.8

avg= 4.60

day 201 5 8 4 4 5

RMSE 0.4 2.7 0.5 0.5 0.5

RMSE(10) 1.1 2.7 1.2 1.3 1.2

avg= 5.20

totavg = 5.14286

```

day 193
  11    10    10    12    9
  12     9    10    12    10
  -1    -1    10    12    10
  -1    12    11    -1    9
  -1    -1    -1    -1    -1
  -1    -1    -1    12    -1
  -1    -1    -1    -1    -1
  11    10    11    12    11
  12    -1    12    -1    12
  -1    -1    -1    -1    12
  -1    -1    -1    -1    -1
  -1    -1    -1    -1    -1
  -1    -1    -1    -1    -1
  -1    -1    -1    -1    -1

```

avg = 10.9231 nsamples= 26

```

day 194
  9     10     9     7     7
  10    10     9    12     9
  11    11     9    11     8
  -1    -1    11    -1    -1
  -1    -1    -1    -1    -1
  -1    -1    -1    12     8
  -1    -1    -1    -1    10
  -1    -1    -1    -1    -1
  12    -1    12    12    12
  12    -1    12    -1    12
  -1    -1    -1    -1    -1
  -1    -1    -1    -1    -1
  -1    -1    -1    -1    -1
  -1    -1    -1    -1    -1

```

avg = 10.26923 nsamples= 26

totavg = 10.5962

```

day 193
  5     7     5     4     5     4    14     6     6     4     4     6     3     0
avg= 5.21

```

```

  0.4  0.7  0.5  0.3  0.8  0.4  0.4  0.8  0.3  0.6  0.8  0.8  0.5  0.8
  1.2  1.0  1.3  1.3  1.5  1.7  0.5  1.2  0.9  1.5  1.6  1.4  1.8  1.2

```

```

day 194
  6     7     5     5     5     5    11    16     6     7     5     4     6     3
avg= 6.50

```

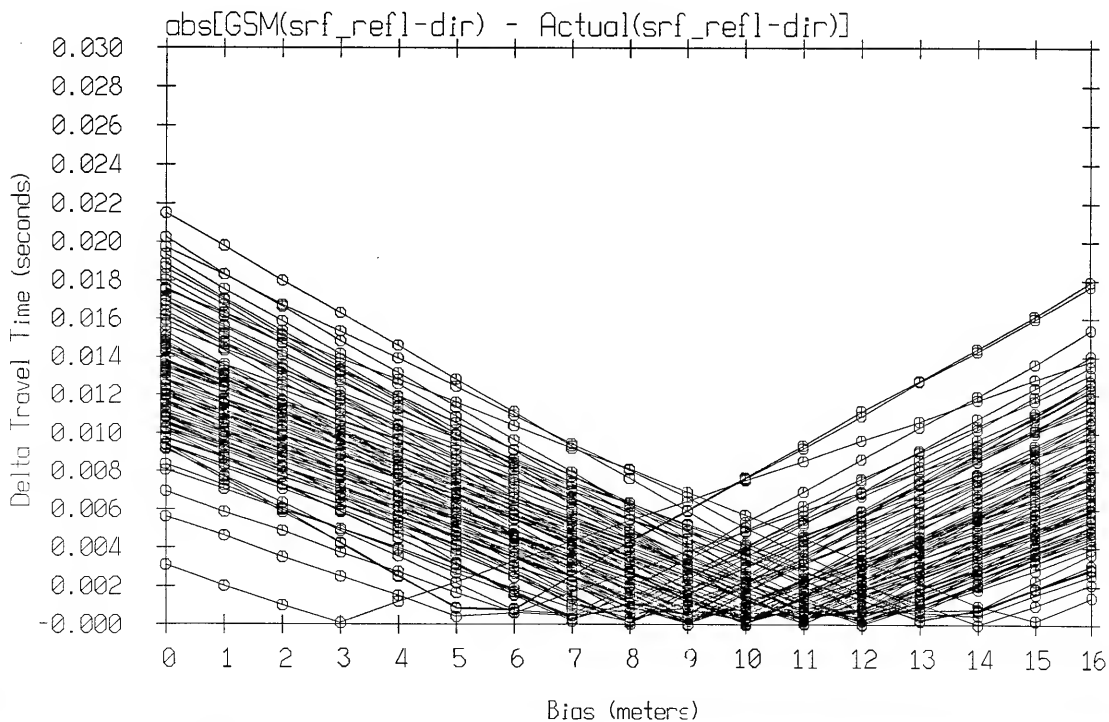
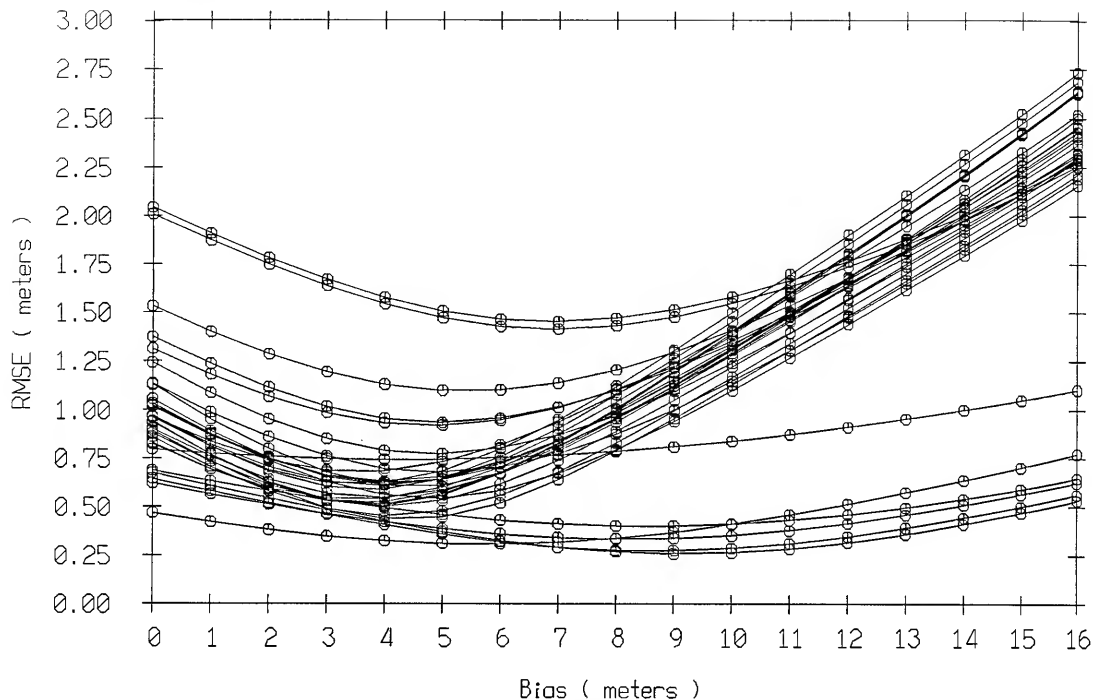
```

  0.4  0.8  0.5  0.6  1.0  0.5  0.3  0.4  0.4  0.4  0.7  0.9  0.9  0.5
  1.1  1.0  1.2  1.4  1.7  1.6  0.3  0.5  0.9  0.7  1.4  1.6  1.3  1.7

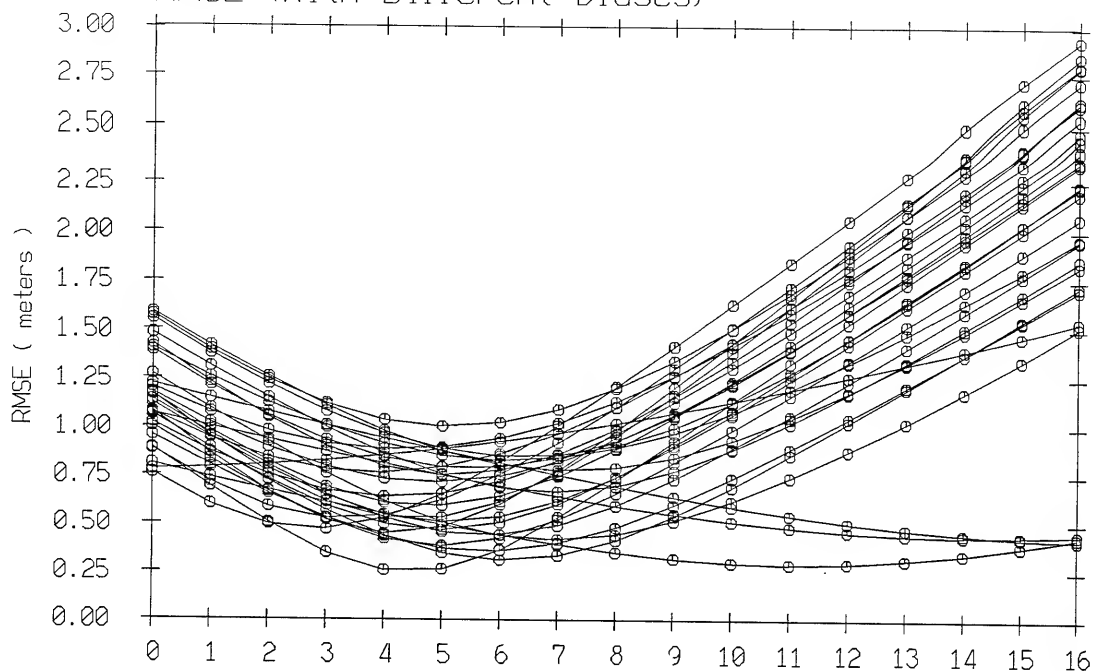
```

totavg = 5.85714

1 Leg Data Bias Correction RMSE (With Different Biases)

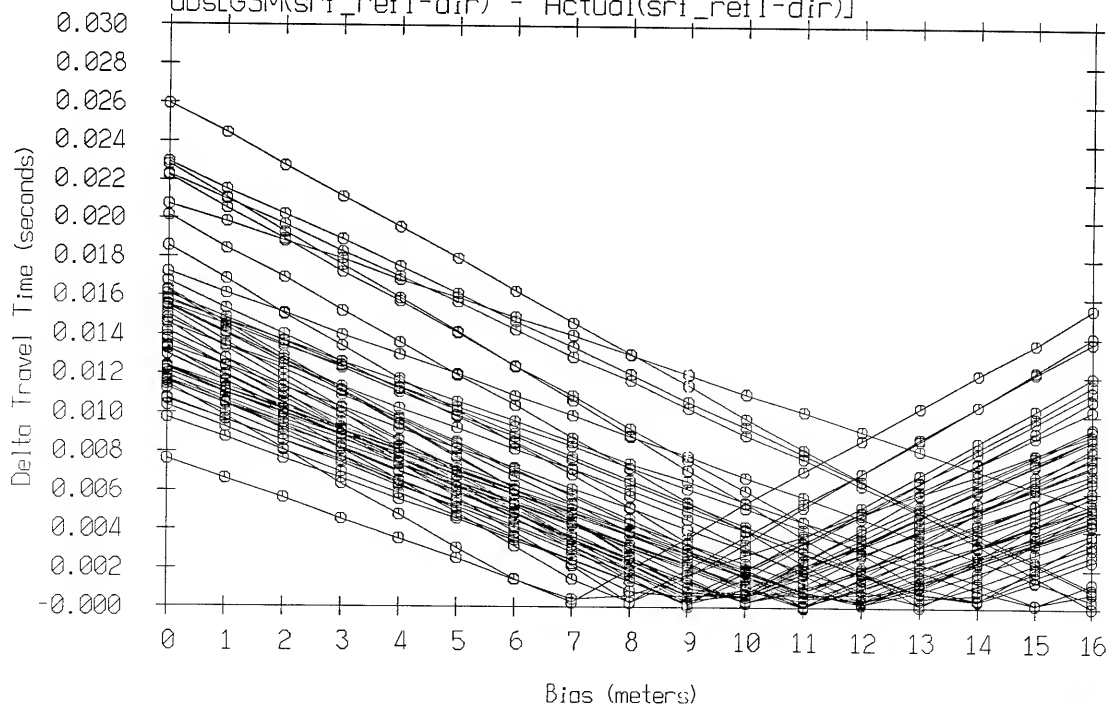


2 Leg Data Bias Correction RMSE (With Different Biases)



Bias (meters)

$\text{abs}[\text{GSM}(\text{srf_refl-dir}) - \text{Actual}(\text{srf_refl-dir})]$



Appendix D. How Ray Trace Corrections Affect Transponder Locations

The following plots demonstrate how ray trace corrections move the transponders primarily downward in a radial direction. Lines emanating from the transponders show transponder directional motion as well as the magnitude of this motion relative to the other transponders. The box in the upper right hand corner of each plot shows the overall vector sum of all the motion (in meters). Note that the X-Y changes virtually cancel each other, and that the overall motion is primarily downward due to the roughly symmetric transponder survey.

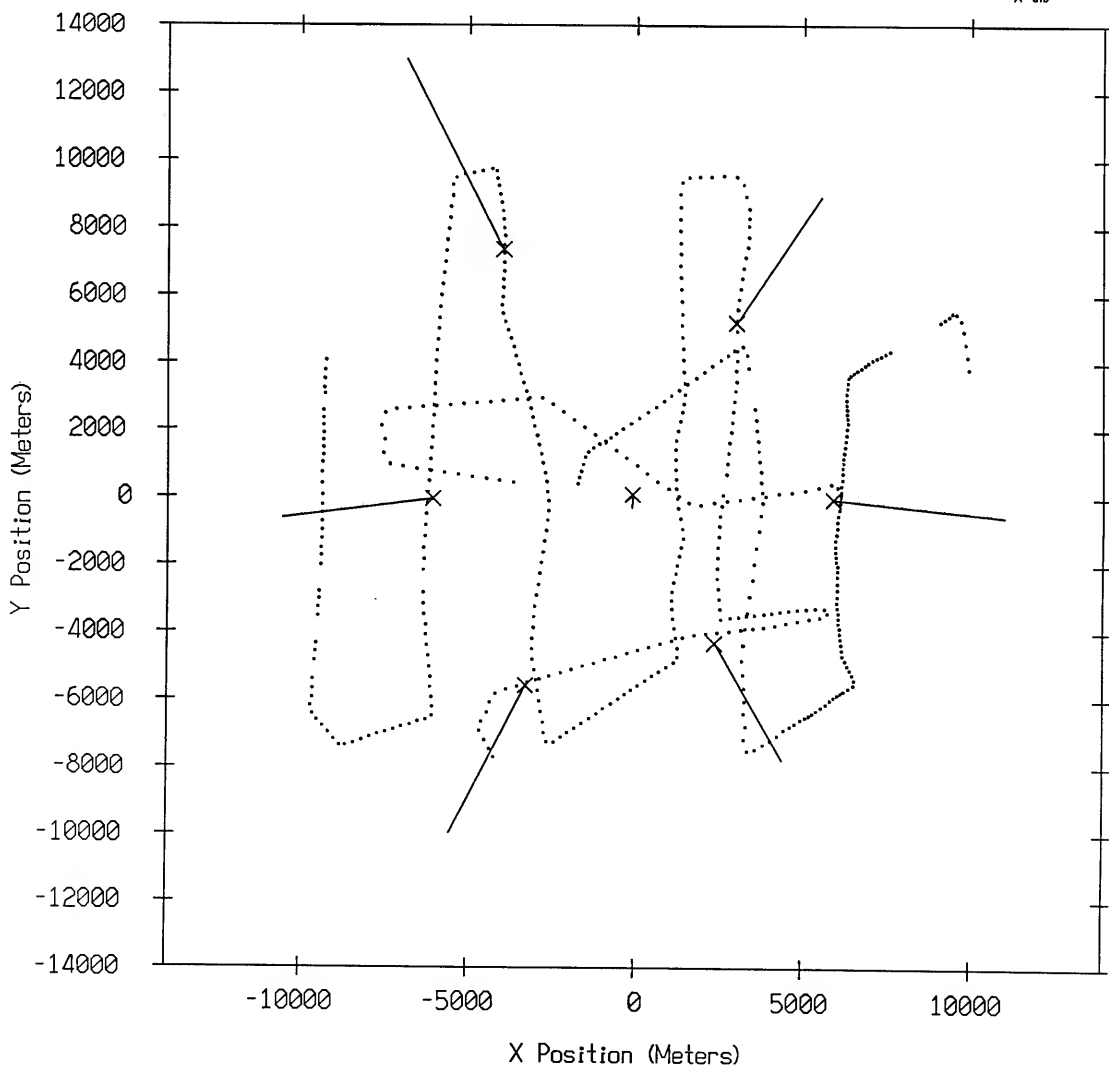
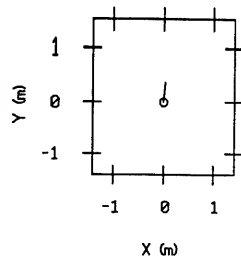
These ray trace corrected positions were obtained by using the Generic Sonar Model (GSM) to predict the differential corrections in the various slant ranges from the various ship positions to the various transponders. Larger corrections are added to more horizontal slant ranges since rays bend more for such slant ranges. Ray trace corrections were implemented for both the transponder survey and the array navigation.

MDA-I 1991

X-Y Directional Movement From Transponder Positions to Ray Traced Transponder Positions

(Xpd positions are not geocentrically correct)

Xpd	-3975.32	7352.17	5164.86	RT Xpd	-3978.23	7357.81	5165.88
Positions	-6069.48	-49.9162	5157.77	Positions	-6073.95	-50.4911	5158.39
	-3278.88	-5578.39	5228.15		-3281.12	-5582.80	5229.26
	2367.83	-4313.45	5180.52		2369.87	-4316.90	5181.68
	5901.99	-44.1004	5192.86		5907.10	-44.6284	5193.78
	3007.15	5204.85	5109.50		3009.66	5208.57	5110.48
	-90.1295	74.8087	5155.62		-90.1668	74.4216	5156.47

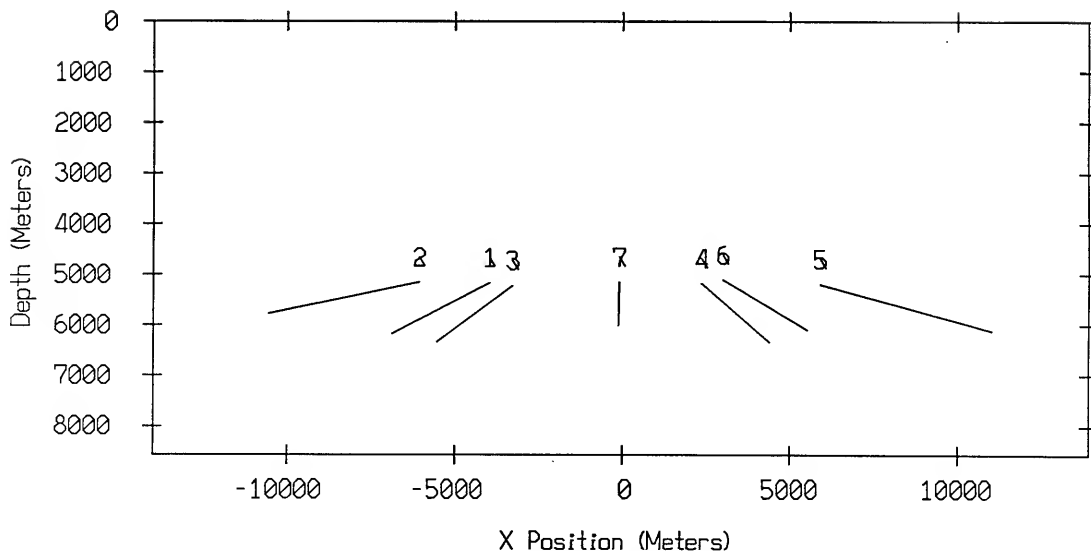
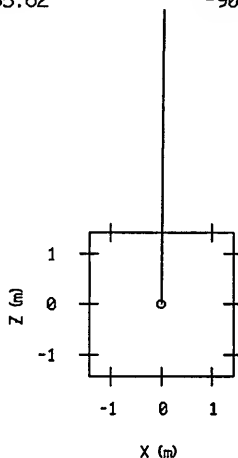


MDA-I 1991

X-Z Directional Movement From Transponder Positions to Ray Traced Transponder Positions

(Xpd positions are not geocentrically correct)

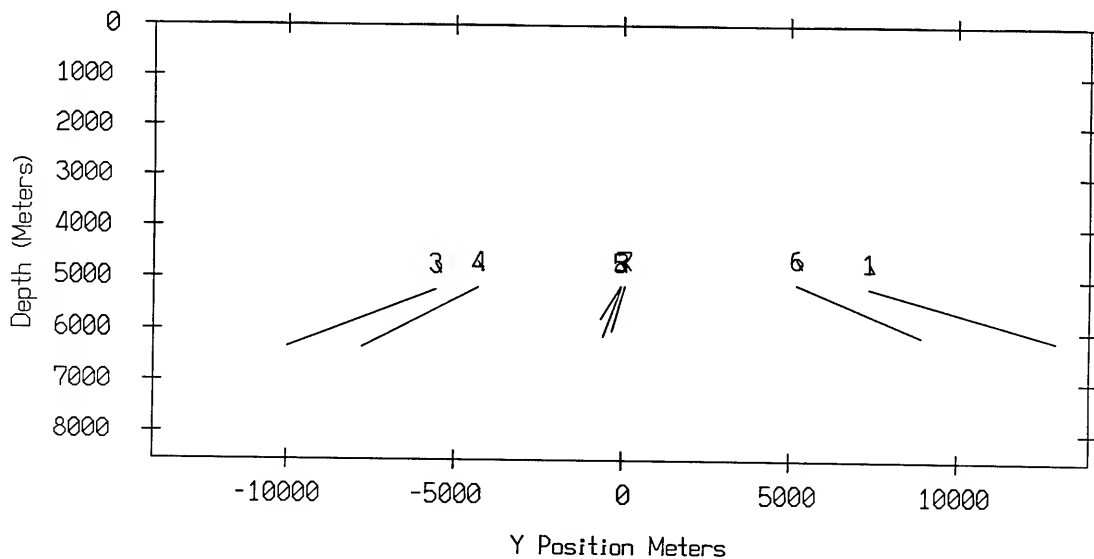
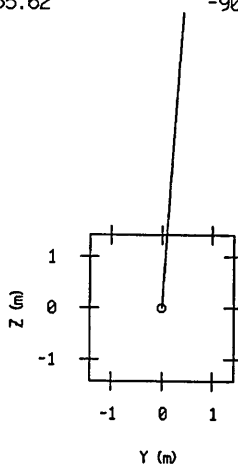
Xpd Positions	-3975.32	7352.17	5164.86	RT Xpd Positions	-3978.23	7357.81	5165.88
	-6069.48	-49.9162	5157.77		-6073.95	-50.4911	5158.39
	-3278.88	-5578.39	5228.15		-3281.12	-5582.80	5229.26
	2367.83	-4313.45	5180.52		2369.87	-4316.90	5181.68
	5901.99	-44.1004	5192.86		5907.10	-44.6284	5193.78
	3007.15	5204.85	5109.50		3009.66	5208.57	5110.48
	-90.1295	74.8087	5155.62		-90.1668	74.4216	5156.47



MDA-I 1991 Y-Z Directional Movement From Transponder Positions to Ray Traced Transponder Positions

(Xpd positions are not geocentrically correct)

Xpd Positions	-3975.32	7352.17	5164.86	RT Xpd Positions	-3978.23	7357.81	5165.88
	-6069.48	-49.9162	5157.77		-6073.95	-50.4911	5158.39
	-3278.88	-5578.39	5228.15		-3281.12	-5582.80	5229.26
	2367.83	-4313.45	5180.52		2369.87	-4316.90	5181.68
	5901.99	-44.1004	5192.86		5907.10	-44.6284	5193.78
	3007.15	5204.85	5109.50		3009.66	5208.57	5110.48
	-90.1295	74.8087	5155.62		-90.1668	74.4216	5156.47



ONR/MPL REPORT DISTRIBUTION

Office of Naval Research (3)
Department of the Navy
Ballston Tower One
High Gain Program
800 North Quincy Street
Arlington, VA 22217-5660
Atten: Dr. Richard Doolittle
Code 321

Administrative Grants Officer (1)
Office of Naval Research
Resident Representative
University of California, San Diego, 0234
8603 La Jolla Shores Drive
San Diego, CA 92093-0234

Commanding Officer (2)
Naval Research Laboratory
Atten: Code 2627
Washington, D.C. 20375-5320

Defense Technical Information Center (4)
Building 5, Cameron Station
Alexandria, VA 22304-6145